

Virtual Power Plant Contributing to Primary Frequency Containment Using Demand Response

- A case study of a commercial building



Viktor Persson

Division of Industrial Electrical Engineering and Automation
Faculty of Engineering, Lund University

MASTER THESIS

Virtual Power Plant Contributing to Primary Frequency
Containment Using Demand Response

- A case study of a commercial building

Author

Viktor Persson

Supervisors

Jörgen Svensson, IEA
Johanna Dahlberg, Siemens AB

Examiner

Olof Samuelsson, IEA

FACULTY OF ENGINEERING LTH

DIVISION OF INDUSTRIAL ELECTRICAL ENGINEERING AND AUTOMATION IEA

September 2019

Acknowledgements

I would like to give my sincere appreciation to my supervisor Jörgen Svensson who has given me the input and knowledge needed to perform this master thesis. I am grateful for your visionary thoughts of the current and the future power system and for inspiring me to continue working within this visionary field. I am hopeful that you will continue to inspire and to teach more student as you have done with me during my studies.

Johanna Dahlberg, my supervisor at the collaborating company Siemens AB, thank you for your continuous support and care of me during my ongoing hardship in this thesis. You have provided me with guidance at the company and the determination needed for performing this task. I hope you have learnt as much of virtual power plants and step responses as I have, after reading this extensive report. And thank you for putting up with me and my intermittent journal updates.

I would also like to extend my appreciation to Daniel Iggström and Pontus Svensson for your knowledge of the case study, the head-start you gave me in this thesis and for our time at the office. Thank you Annah Håkansson for being a mentor at Siemens and introducing me to the company. And lastly, a great thank you to all the interns and colleagues who have helped me throughout my thesis work as Siemens AB.

Summary

The Swedish power grid is experiencing an ever-growing challenge to efficiently balance the grid. An increasing share of intermittent generation, decreased system inertia, continued electrification and more distributed energy resources result in an increasing need for flexibility. Smart grid technologies have, amongst other applications, shown to be a possible solution to this increased need for flexibility.

The virtual power plant, one of many smart grid technologies, uses a heterogenous portfolio of aggregated distributed energy resources, combines their respective characteristics efficiently, in order to create a single operating profile which can be used to offer services to the grid operator, such as system balancing. However, since their potential is relatively unknown, as with any smart grid technology, it is important to determine their prerequisites to offer balancing services to the system operator.

In this thesis the potential for a virtual power plant to contribute to the balancing of the Swedish power grid is analyzed. The analysis is based on a case study of a commercial building which is the basis for the implemented virtual power plant. The virtual power plant, and the energy resources provided by the commercial building, are modeled in MATLAB and Simulink. The energy resources included are air handling units and chillers in a large scale heating, ventilation and air-conditioning system. The models are implemented by performing system identification or system estimation methods. Moreover, an energy storage system is modeled in order to compensate for the activation and deactivation sequences of the chillers in the proposed control scheme.

A control system of the virtual power plant is proposed in order to efficiently control the assets and to participate on the primary frequency containment market FCR-N. The control system uses a regulation controller, implemented with filter to regulate the load of the assets. Furthermore, a scheduling unit is implemented, which together with a load corridor, schedules and places bids with the corresponding available capacity of the assets, on FCR-N. The scheduling also activates the assets and the regulation controller whenever frequency containment is scheduled.

The performance of the virtual power plant is verified by simulating a prequalifying test for the balancing market, which is developed by the Swedish system operator and transmission system operator Svenska Kraftnät. The results of the prequalifying test proved that the air handling units were viable assets in regard to their responsiveness. The chiller also proved to be viable but given the proposed control system and the compensation provided by the energy storage system.

Moreover, a simulation of the virtual power plant performing primary frequency containment based on historical data was simulated. This highlighted how problematic it is to quantify the performance of balancing resources. But despite this, the results indicated that the proposed implementation of the virtual power plant, based on the case study, and its control system could perform primary frequency containment and thus, contribute to increased flexibility in the Swedish power system.

Table of contents

- 1. Introduction1**
 - 1.1 Background 1
 - 1.2 Scope of thesis.....4
 - 1.3 Outline.....6
- 2. Theory7**
 - 2.1 Power system.....7
 - 2.2 Power system players9
 - 2.3 Ancillary services12
 - 2.4 Smart grid.....25
 - 2.5 Virtual power plant.....32
 - 2.6 Energy assets39
 - 2.7 HVAC systems.....50
- 3. Case Study.....58**
 - 3.1 Energy footprint59
 - 3.2 Electrical loads61
 - 3.3 Cooling loads.....62
 - 3.4 Ventilation loads67
 - 3.5 Context of case study70
- 4. Method.....73**
 - 4.1 Overview73
 - 4.2 Data collection.....75
 - 4.3 Modeling82
 - 4.4 Simulation112
- 5. Results117**
 - 5.1 Prequalifying test.....117
 - 5.2 Frequency containment127
 - 5.3 Results summary139
- 6. Discussion.....141**
 - 6.1 Reliability141
 - 6.2 Results144

7. Conclusion	153
8. Future work.....	155
8.1 Thesis expansion.....	155
8.2 Thesis outlook.....	158
Bibliography	160
Appendices.....	165
Appendix A – Air handling unit specifications	165

Abbreviations

aFRR – Automatic frequency restoration reserve
AHU – Air handling unit
BEMS – Building energy management system
BESS - Battery energy storage system
BMS – Building management System
BRP – Balance responsible party
BSP – Balance service provider
C-rate – Charge rate
DEMS – Distributed energy management system
DER – Distributed energy resource
DERMS – Distributed energy resource management system
DoD – Depth of discharge
DR – Demand response
DRR – Demand response resource
DSO – Distribution system operator
EMS – Energy management system
ESS – Energy storage system
EV – Electric vehicle
FCR – Frequency containment reserve
FCR-D - Frequency containment reserve disturbed operation
FCR-N - Frequency containment reserve normal operation
FFR – Fast frequency reserve
HVAC – Heating ventilation and air conditioning
mFRR – Manual frequency restoration reserve
MG – Microgrid
PV – Photovoltaic
RES – Renewable energy sources
RR – Restoration reserve
SG – Smart Grid
SoC – State of charge
SoH – State of health
SvK – Svenska Kraftnät
TSO – Transmission system operator
V2G – Vehicle to grid
VAV – Variable air vent
VFD – Variable frequency drive

1. Introduction

In this chapter an introduction to the overall thesis will be presented. Firstly, the background of the subject and the corresponding problem discussion, lifting challenges and possibilities of the power system, is presented. Secondly, based on the background, a scope of the thesis is defined. In order to specify the scope further, a question formulation is defined with key questions to be answered. Lastly, the scope of the thesis is further defined by the delimitations which are presented.

1.1 Background

With the establishment of national treaties such as the Swedish Energy Agreement [1] and international treaties such as the European Parliament's General Energy Policy Framework [2], it has been made clear that comprehensive changes of the energy system are required. Related to these agreements, explicit goals and plans such as Sweden's National Energy and Climate Plan [3], have been set in order to drive the change forward. Achieving these goals is a challenge itself but is further increased when considering changing future trends in the power system.

The International Energy Agency has predicted that the European electricity demand will continue to increase until 2040. Furthermore, it is predicted that a majority part of the investments in new power generation will be in renewable technologies [4]. Considering the stochastic nature of renewable energy sources, this will introduce new challenges to the energy system regarding the intermittency of generation. Moreover, intermittent generation will also introduce larger forecasting errors thus increasing the need of generation or load-shedding reserves [5]. The challenge of intermittent power is possibly further increased by the electrification of vehicles. It is predicted that the global fleet of electric cars will have increased by 280 million cars globally by 2040 [4], possibly creating even larger variations in peak loads.

Considering the Swedish power grid, increased generation intermittency will require even larger grid flexibility in order to maintain an acceptable level of stability. This introduces new challenges since the grid flexibility is expected to decrease as an affect if considerably reduced system inertia, due to the shutdown of several large synchronous generators in nuclear power plants. Furthermore, also taking the placement of balancing resources and transmission grid bottlenecks into consideration, the Swedish transmission system operator Svenska Kraftnät, has forecasted the possible occurrence of about 400 hours of power shortage annually in southern Sweden in year 2040. This is, if no considerable action is taken to increase load flexibility, increase energy storage or reduce generation intermittency [5].

The Swedish transmission system operator has also noted an increasing need of vertical integration between itself and underlying distribution system operators. This is due to an increasing decentralization of generating resources, increasing share of microgeneration and larger amounts of consumption flexibility. This results in larger amounts of power flow changing from the typical top-down approach of power systems to the power flows in lower grid topologies. This change will require new operation scenarios to be handled by distribution system operators where they will in ever larger degree have to accomplish regional system balancing by overcoming local bottlenecks and capacity limitations in distribution networks by controlling local power flows [5].

Amongst all the challenges created by climate goals, changing consumption patterns and power delivery, new possibilities arise. Swedish Smart Grid has projected that the inclusion of smart grid technologies in the power system can increase integration of renewable and decentralized generation, reduce overall energy consumption, increase flexibility and include prosumers into the power system to a greater degree [6]. Smart grid technologies could prove to be an integral part of future energy supply, solving large portions of aforementioned challenges. The development of such technologies does however require work within nine fields of technology, identified by the International Energy Agency. These fields include integration of renewable and decentralized generation, applications for improved power transmission, management of distribution networks, real-time grid monitoring, storage and charging infrastructure for electric vehicles, integration of information and communication technology and more [7]. Solving

problems within one of these nine fields is key to driving the smart grid technology forwards and consequently contributing to reaching overlying climate goals.

Today in southern Sweden there are only a few cases of fully implemented smart grid technologies [8]. The area is still being researched and the associated legislation is still under development. Players of the energy market are beginning to realize the potential of smart grids but are still uncertain of the technicalities of implementing smart grids; how to utilize energy resources in conjunction to perform ancillary services and what market roles that will be relevant. Some local projects have been performed, exploring the potential of smart grid solutions such as aggregated load shedding, vehicle-to-grid storage and frequency containment with a server's uninterruptable power supply. Whilst showing promising results for the future of Swedish smart grids, they have also proved that there are many improvements to be made and a lot to be learnt.

One technology which has the possibility of being a key factor in the development of smart grids is the virtual power plant. The virtual power plant is a heterogeneous system of aggregated distributed energy resources that efficiently combines the characteristics of connected distributed energy resources to create a single operating profile capable of offering services to the system operator. Services that could include power grid frequency containment, energy trading, peak load management and asset management [9]. In aggregated form the distributed energy resources, of which often are intermittent renewable energy sources, can have the same visibility, controllability and market functionality as a conventional power plant [9]. **Fel! Bokmärket är inte definierat.**

However, due to the fact that the virtual power plant is still a relatively unproven concept, as with any smart grid technology, it is necessary to verify its performance in regard to its impact on the challenges in the power system. It is therefore necessary to measure its ability to contribute to an increased flexibility by performing frequency containment. Consequently, it is relevant to perform a case study of a virtual power plant in order to illuminate some of the potential challenges of implementing a virtual power plant contributing to the Swedish frequency containment reserve.

1.2 Scope of thesis

The scope of the thesis is to perform a case study of a virtual power plant in order to determine its ability to contribute to increased flexibility in the Swedish power system. The virtual power plant will be studied by implementing a control system which will be modeled and simulated in MATLAB and Simulink. The model will be based on a case study of a commercial building where the assets of the virtual power plant are mainly determined by the already existing resources at the site. Furthermore, the model and the control system will be implemented with the aim of contributing to increased flexibility by performing primary frequency containment on Swedish balancing markets. Some adjustments will be made to the model of the control system, the resources at the site of the case study and the included assets, in order to enhance the virtual power plants ability to perform primary frequency containment. The virtual power plants ability to perform frequency containment will be problematized and discussed further to illuminate the possibilities of using commercial buildings as a basis for virtual power plants in order to increase power system flexibility.

The thesis is performed in collaboration with Siemens AB, which has provided information and knowledge of the case study's commercial building and the resources to perform this thesis. Consequently, the scope of the thesis will be further defined by the interests of Siemens AB.

1.2.1 Question formulation

In order to further define the scope of the thesis a question formulation is presented below. The questions are formulated in order to answer relevant topics in academia and to contribute to the overall work at the collaborating company Siemens.

- What are the prerequisites for a virtual power plant utilizing the commercial building of the case study to perform primary frequency containment?
 - Can the virtual power plant qualify as a balancing resource?
 - How well does the virtual power plant perform frequency containment?
- How well are the assets of the commercial building suited for frequency containment in regard to their sheddability, controllability and responsiveness?
- How can the control system of the virtual power plant be implemented in order to efficiently provide increased flexibility to the Swedish power system?

1.2.2 Delimitations

In order to efficiently answer the question formulation and to keep the thesis within the correct scope, some delimitations have been defined. These are presented throughout the report where the most relevant delimitations are presented below.

- The demand response models will neglect each respective resource's endurance and repeatability when performing frequency containment.
- Price components of bids on balancing markets will be excluded when considering contribution to frequency containment.
- Data used in the models are solely based on completely accurate load forecasts. Eventual forecast errors will be neglected.

1.3 Outline

2. Theory - *In this chapter the required theory for this thesis is presented. First, an overview of the power system of today will be given. Then the expectations of the smart grid and some smart grid technologies are presented. This is further expanded on by focusing on the virtual power plant and its related energy assets. Moreover, the function of heating, ventilation and air-conditioning is defined. Lastly, the players and the markets of the power system are presented.*

3. Case Study - *In this chapter the case study subject is presented. A short background is given to get a basic understanding of the site. Then overall data for the case study is presented of which some of the data will act as a basis for understanding and some will be used in the following chapter. Additionally, available information of the assets available at the case study are presented. Lastly, the context of the case study and how it is related to the scope of the thesis will be discussed.*

4. Method - *In this chapter the method for the thesis will be presented in order to achieve an understanding for how the results were attained. The overlying processes of data collection, modeling and simulation will be presented in detail with references to the already presented theory. The workflow process in this thesis has a large influence on the results. Consequently, some conclusions are drawn in the method chapter but will also be presented further on.*

5. Results - *In this chapter the overall results of the thesis will be presented. This is done by first presenting the results of the simulations performed of the prequalifying test and secondly by presenting the results of the simulations performed of the frequency containment tests. The results are analyzed for each simulation and are further summarized at the end.*

6. Discussion - *In this chapter the results of the thesis will be discussed. Initially, the reliability of the sources, methods and results will be highlighted in order to understand their impact. Further, the results from the prequalifying tests and the frequency containment simulations are analyzed. Lastly, appropriate future work on the subject will be suggested, both to improve the methods and results in this thesis, but also future work in order to contribute to new understanding in the field.*

7. Conclusion – *In this chapter the conclusions of this thesis are presented. By summarizing the results and the main points of the discussion, the general outcome of the thesis method is settled. Furthermore, by answering the question formulation the scope of this thesis will be covered.*

8. Future Work - *In this chapter different subjects for future work suggested in order to forward the work on the thesis topic. These are chosen to achieve a more nuanced and complete study in the area. Following this, some ending remarks with an outlook on the future of virtual power plants, demand response and frequency containment is presented.*

2. Theory

In this chapter the required theory for this thesis is presented. First, an overview of the power system of today will be given with the relevant players and markets. Then the expectations of the smart grid and some smart grid technologies are presented. This is further expanded on by focusing on the virtual power plant and its related energy assets. Moreover, the function of heating, ventilation and air-conditioning, an energy resource of the case study, is defined.

2.1 Power system

The power system of today is going through significant changes where it is transforming from a centralized, and a typically hierarchically structured power system, to a distributed and nonhierarchical power system. Traditionally the grid has been structured in such a way that large generating plants transfer power to the transmission grid which transmits power to distribution networks that in turn distributes the power to end consumers [10], as shown in *Figure 1*. Highest in this hierarchy are the generation plants, whose power is explicitly determined by the need of the end consumers, and lowest in the hierarchy are all consumers which consist of commercial, industrial and residential loads. This way, the supply chain is designed in a one-way and a top-down manner. As a consequence of the transformation from the centralized grid to the decentralized grid, an increased complexity in the number and type of resources as well as the number of actors has been presented [10].

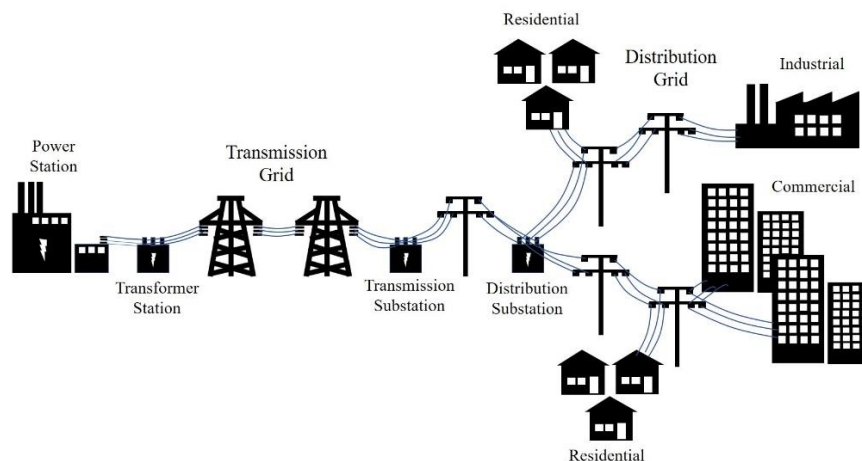


Figure 1: Illustration of the centralized grid with power flow from left to right.

The centralized grid is also experiencing a growth of renewable energy sources (RESs), which mainly consists of wind power. This growth is expected to continue and to replace the centralized, aging and costly nuclear power plants, consequently increasing imbalances due to intermittency and decreased rotating inertia. Furthermore, additional intermittent generation is expected to increase in the form of photovoltaics (PV), distributed amongst real estate, rather than in centralized grid-connected plants. In recent years, this development of intermittent generation has resulted in an increased need for balancing power, where the number of annually accepted bids on balancing markets has more than doubled in 10 years. This change is expected to continue to increase due to a sustained expansion of RESs. Additionally, hydropower which has been the traditional balancing resource making up more than 90 % of all balancing resources, has experienced a limited expansion due to already exploited waterways, which increases the challenges of balancing the power system in the future [11].

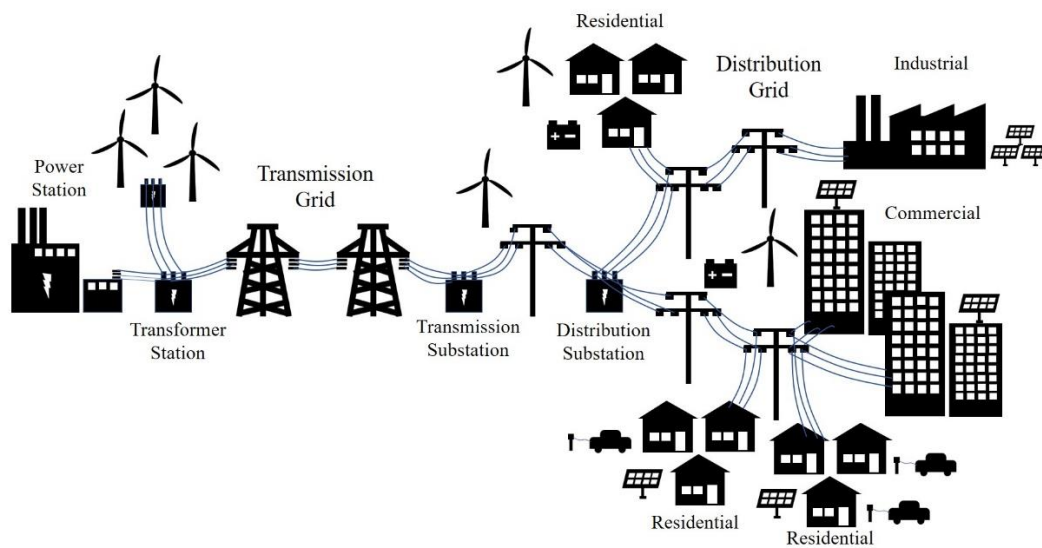


Figure 2: Illustration of the decentralized power system.

Beyond having changed generation patterns due to an increased share of intermittent generation, even consumption is continuing to change. An increased and continued urbanization increases load on specific parts of the grid centered around larger cities. Additionally, the decentralized grid as shown in *Figure 2*, contains new types of loads in the shape of electric vehicles (EVs) and server centers, creating larger peak demand whilst increasing consumption overall. These factors combined with the fact that reinforcements

of the power grid, typically take a long time, result in temporary power shortages, which further increase the need for balancing. [12]

However, since the current balancing resources already are highly utilized and the need for balancing power will continue to increase, an interest for new balancing resources has arisen. The possibility of using energy storage and demand response (DR) to perform balancing has become more and more interesting. However, integrating consumption resources, which mostly are represented by smaller consumers or by commercial and industrial real estate, requires new platforms for aggregation in order to achieve higher levels of power. This is said to require new types of infrastructure, regulations and players, which together can contribute to the activation of consumption resources, or rather DR, on balancing markets. This would contribute to an increased participation on balancing markets, whilst also delivering balancing resources to areas where it earlier was not available. [12]

2.2 Power system players

In order to support the transition to a distributed grid it is important to have a clear and appropriate definition of the respective responsibilities and mandates of the players operating in the Swedish power system. The Swedish transmission system operator (TSO) has outlined some of the problems of the current distribution of roles in the power system and the possible required changes, in order to guarantee a long-lasting reliable supply of power. These changes include the need of player who is solely responsible for power reliability, instead of having the role distributed amongst many players as it is currently. Secondly, the changes also include the establishment of formal requirements or obligations for power generation instead of solely market-driven generation. Lastly, the changes include a review and an expansion of the current role of the distribution system operator (DSO) to also include a subsystem responsibility [13]. However, to fully understand these changes and their impact on the power system, and to that sense how it will impact the implementation of virtual power plants (VPPs), it is important to present the existing power system roles and their respective responsibilities and mandates. However, some of the roles will not be presented individually, but only in relation to the other players.

2.2.1 Transmission system operator

What could be considered to be the main responsible player in a power grid is the TSO. According to the Swedish TSO Svenska Kraftnät (SvK), the TSO is responsible for ensuring that the transmission of power is secure, environmentally friendly and cost efficient. This is ensured by in the short term constantly monitoring the power system, and in the long term, by building new power lines to meet the demand of tomorrow. [14]

TSOs are responsible for maintaining and developing the transmission grids which deliver power from energy sources such as wind power, nuclear and hydropower to the distribution grids. Furthermore, the TSO is the player which is responsible for ensuring a balance between generation and consumption [15]. However, TSOs are not responsible for ensuring that there is a sufficient amount of generation. Instead, this responsibility falls under the roll of balance responsible parties (BRPs) which are financially responsible for having a balance between imported or generated power and exported or consumed power, during a given timeframe [16] [17]. This is done by forecasting consumption and generation and adjusting the net power by trading on energy markets. The imbalance that cannot be adjusted for, is compensated by the TSO which the BRP is charged for [18].

The imbalance is adjusted for by the TSO, by providing balancing markets where balance service providers (BSPs) contribute to grid balancing by providing balancing services. Balancing services include the provision of balancing energy or the provision of balancing power. The provision of balancing services occurs in agreement with the TSO where the BSP places a bid on the corresponding market with the corresponding capacity of power, which is then accepted or declined by the TSO, during a given time frame. If the bid is accepted for that given timeframe, the BSP is then legally responsible to deliver the required capacity during that time. The BSP can deliver the capacity in terms of providing demand response, energy storage or generation, which has to be qualified in beforehand through a prequalification process [19] [20].

Beyond being the primary player responsible for balancing the power grid, the TSO also provides utilizes so-called ancillary services which include frequency containment (FC), voltage regulation and the provision of rotating inertia. With these ancillary services, the TSO manages to ensure the reliability of power [21]. Despite being important components when ensuring the reliability of power, only the provision of balancing services and FC services will be presented further in this thesis.

2.2.2 Distribution system operator

The distribution system operator is generally responsible for mid and lower voltage level networks. This includes the transmission of power from higher voltage level networks and smaller generation sources to lower-level distribution networks or directly to connected prosumers. The responsibility of the DSO is to operate and to ensure the maintenance and development of regional and local distribution grids to ensure a long-term ability to meet the demands for the distribution of electricity [22]. However, today in the Swedish power system, the DSO does not have a responsibility for stability or balancing, meaning that it is solely entrusted upon the TSO. Moreover, this relation is expected to change, where the DSO will take a more active part in system responsibility. This will be done by increasing its collaboration with the TSO and by allowing for, what typically would have been services for the transmission grid, in the regional and local grids as well [13].

2.2.3 Aggregator

Today, the roll of the aggregator is vague. Except for the fact that they are vital for the establishment of VPPs, their roll and their associated legislation is yet to be determined. The role of the aggregator is consequently a topic for discussion where the regulations defining the relation between the BRP and the aggregator is of the largest importance.

However, what is defined is that the aggregator is a player which aggregates or connects many smaller DERs into a larger entity. The larger entity will, together with its larger capacity, make the assets available to what would have been previously inaccessible markets [23]. For instance, the aggregator could combine many smaller demand response

resources (DRRs) in order to offer bids on FC markets, thus opening new revenue streams for DRRs whilst increasing competition on balancing markets. However, the power of the DRRs will change due to participation on balancing markets, which in turn will affect the BRP's ability to forecast their power balance. Consequently, the aggregator could increase the costs for BRPs if their responsibilities and mandates are not clearly defined. [24]

Alternative aggregator business models have been examined in order to develop legislation that encourages the role of the aggregator, whilst still proving a market with fair playing rules for other players. These models can be divided into two parts where one half will not affect the existing roles of the power market but could restrict the penetration of aggregators. The other half of the possible business models could affect the existing players negatively but instead are built on compensation models in order to compensate the BRPs for the caused imbalances. These models have different implications on the role of the aggregator but mainly only are a question of how the role of the BRP is implemented and how the players are compensated for the caused imbalance [25]. Despite this, the aggregation of DRRs for participation on balancing markets could result in the release of hydropower which could improve power reliability. Furthermore, aggregated DRRs could also result in increased availability and competition in dominated power reserve markets, especially in areas where reserves otherwise have not been available [11].

2.3 Ancillary services

Ancillary services are implemented in order to ensure stable and balanced operation of the power system and are utilized by VPPs in order to create value streams while contributing to the power grid balance. The necessity for ancillary services is caused by the occurrence of imbalancing causes which can be categorized after the categories presented in *Table 1*, with their corresponding characteristics and the compensating ancillary service [11]. The compensating services will be covered further on.

Categories	Characteristics	Compensating service
Forecasting errors	Slow	mFRR, aFRR
Stochastic causes	Fast	FCR-N
Disruptive events	Fast	FCR-D
Technical limitations	Medium-fast	FCR-N, aFRR
Market limitations	Medium-slow	Generation adjustment
Strategic causes	Slow	aFRR, mFRR
Special regulation	Slow	mFRR

Table 1: Summary of categories for imbalancing causes and their corresponding characteristic and compensating service. [11]

Forecasting errors are caused by determining generation and consumption of electricity incorrectly. This error is expected to increase as an effect of more intermittent generation and is compensated by the manually or automatically activated frequency restoration reserve (aFRR, mFRR). Stochastic causes include smaller and more random occurrences in the power system and are also expected to increase due to more intermittent generation. Stochastic causes are compensated by the frequency containment reserve for normal operations (FCR-N). When the power system is affected by a larger disturbance such as the loss of a large HVDC connection or a generating facility, the frequency containment reserve for disturbed operation is activated (FCR-D). Technical limitations include causes such as limiting power line transfer capacities, whereas market limitations include causes such as market time basis limitations. For instance, does a time-basis of 1 hour create larger imbalances than one of 15 min. Other causes include, the failure of following planned operation as well as imbalances caused by the special regulation by the system responsible player. [11]

Beyond the services presented above, there are other services which also could be considered ancillary services. These include voltage regulation and the provision of rotating inertia, but do not currently have any associated markets simply due to the fact that they are either indirectly provided by generating sources or provisioned by the system operator. The ancillary services have varying requirements in order to efficiently respond to different causes of imbalance [11]. The speed of each service and its corresponding market is presented in *Table 2*.

	Rotating Inertia	FFR	FCR		aFRR	mFRR	RR
			FCR-N	FCR-D			
Input	-	Frequency	Frequency	Frequency	Control room	Control room	Control room
Output	Power	Power	Power	Power	Energy	Energy	Energy
Product	-	Power	Power & energy	Power	Energy	Energy	Energy
Activation time	< 1 s	~ 1-2 s	~ 1-3 min	~ 5-30 s	< 120 s	12-15 min	> 15 min



 Activation time

Table 2: Balancing markets in Swedish power system with corresponding characteristics. [11]

The inputs of each market describe how the reserve is controlled. Today, the markets are controlled by either a central control room which activates the reserve, or by individual measurements of the power grid frequency. The output of each market is what the reserve delivers in order to contribute to balancing the grid where the outputs are evenly split between power and energy. The product of each market is what the reserve is compensated for. In the case of power, the reserve is compensated the provision of control capacity, irrespectively if the reserve is activated or not. In the case of an energy-product the reserve is only compensated if it is activated, where its compensation is determined by the utilization of primary control. The activation time is simply how fast the reserve has to respond to a signal change. Rotating inertia is not truly a market since reserves providing inertia will not be compensated. However, the indirect contribution of rotating inertia in larger generating facilities despite this, is an integral component in power system balancing. Moreover, FFR (fast frequency reserve) and RR (restoration reserve) are also not markets today but are planned for a future implementation. FFR is designed to respond to very fast changes in the frequency signal whereas RR is designed to operate as a slower tertiary reserve that operates to restore FRR. [11]

Of the existing markets, there are also varying degrees of required capacity in order to participate. Beyond this, and having requirements of activation time, there are also further requirements for each market, which together regulate and determine which assets that are suited for participation. The minimum capacity, i.e. the smallest bid size, for each market is presented in *Table 3* with their respective role in power regulation. [26]

	FCR-N	FCR-D	aFRR	mFRR
Reserve	Primary	Primary	Secondary	Tertiary
Min. capacity	100 kW	100 kW	5 000 kW	10 000 kW

Table 3: Requirements for balancing markets and their respective role. [26]

2.3.1 Primary regulation

Primary regulation in the Nordic power system is supplied by the markets FCR-N and FCR-D. Since the market FCR-D only is activated during disturbed operation, i.e. when the frequency falls below 49.9 Hz, and that the principle of primary regulation is the same for both FCR-N and FCR-D, only the primary regulation during normal operation will be covered. However, it is important to note that one key difference between FCR-N and FCR-D is that FCR-N requires a symmetrical product meaning that the FCR has to be able to regulate up and down where as FCR-D is only in one direction. [26]

Primary regulation is employed in order to maintain the power grid frequency within reasonable limits, by balancing power generation and consumption. As presented earlier, limits that are considered to be normal operation are 50 ± 0.1 Hz. Outside these limits, the operation is considered to be disturbed and measures are taken in order to restore the system to normal operation. It is important to keep the power grid system within limits in order to avoid harm to equipment connected to the grid. This harm can be caused by harmonic vibrations in turbines, heating of generators and transformers and disturbance of other loads. Consequently, primary regulation has been employed to ensure a stable operation by acting as an automatic proportional controller that regulates the power grid frequency. [27]

2.3.2 Frequency filtering

Primary frequency regulation, also called FCR [28], is currently the fastest deployed form of FC where the reserve acts on changes which occur at the time scale of seconds to a few minutes. However, since the power grid frequency changes faster than the FCR can respond, some type of signal processing is required in order to perform FC efficiently by choosing which frequency changes to respond to. Due to the stochastic nature of load

change in the power grid, and thereby also the grid frequency, the grid frequency includes many higher frequency components. These components are mostly of small amplitude in comparison to the lower grid frequency components, meaning that the higher frequency components have a limited impact on the grid balance. Moreover, the high frequency components also are mostly out of phase, meaning that any correction made to compensate for these components will be out of phase as well, thus increasing the imbalance. Consequently, it is necessary to remove the higher frequency components by the means of signal processing, in order to improve the overall regulating performance. [28]

Typically, in primary frequency regulation, a dead band is applied in order to remove small changes. The dead band is applied on the grid frequency signal and is configured to remove any deviation from 50 Hz that is smaller than a certain value. However, this processing method has proven to be poor since it has a low impact on the actual number of removed signal changes. A better method, which is said to widely outperform the normal dead band, is to apply a floating dead band that follows the lower frequency components in the power grid frequency instead of being static at 50 Hz, and then removes any deviation from that floating point. A typical configuration of the dead band is ± 0.01 % from the reference frequency. [28]

Another applied technique is a linear filter, typically a low-pass filter in order to maintain the vital lower frequency components and to remove the disturbing higher frequency components. The cutoff frequency (f_{cutoff}) of the linear filter is described by (1), where (τ_c) is the time constant of the filter system.

$$f_{cutoff} = \frac{1}{2\pi\tau_c} \quad (1)$$

The linear filter is said to have a limited impact on the reduction of higher frequency components which consequently will lead to higher costs in terms of wear and tear. However, the linear filter does retain a higher quality of the initial frequency signal which will improve the overall regulating performance. Moreover, since the filter is a frequency-dependent system, it is important to ensure that no instabilities occur. The filters preferably are implemented as first-order filters, to ease the operation of PI-controllers in

regulating applications. The risk of causing instabilities with low-order filters is lower than what it would have been for a higher order filter. [28] [29]

Beyond the mentioned techniques of filtering, there are other methods such as moving average or weighted moving average which could be suitable as frequency filtering techniques. Moreover, when choosing which filtering technique to implement, the sampling rate of the frequency signal has to be considered. However, since a rate of 1 s is shown to be acceptable whilst still being a reasonable rate for measurement systems, this will not be considered further, given that a rate of 1 s or faster is implemented. [28]

2.3.3 Bidding process

In order to perform primary frequency regulation, the available capacity for regulation has to be known. The procurement of resources for the FCR-N market occurs one or two days ahead the day of operation at 16:00 and 20:00 respectively. In order for a resource to participate in the procurement process, it has to place its bids for the day of operation before 15:00 for D-2 and before 18:00 for D-1, containing information of the capacity, the grid area where the capacity is delivered, and the price of capacity [30]. Since this is a requirement for participating on FCR-N, it is important to correctly determine the available capacity of the resource for the hour of operation before the bids have to be placed.

In order to determine the available capacity for FCR-N ($P_{capacity}$), the symmetrical power product has to be determined, i.e. the capacity to regulate power both up and down. This symmetrical power can be calculated by (2) where the smallest of the capacities to regulate up or down is chosen, given that the capacities are larger than zero. Furthermore, this value is rounded down to the nearest multiple of 100 kW, the minimum bid size for FCR-N. [31]

$$P_{capacity} = \max(\min(\Delta P_{\max_up}, \Delta P_{\max_down}), 0) \quad (2)$$

The capacity to regulate up and down is determined by the ability to increase or lower the power level of the resource. This implies that upper and lower limiting factors, i.e. boundaries, as well as the power reference level will determine the capacities available. By calculating the boundaries that are static, forecasting the ones that are dynamic and forecasting the power reference level, for any given operation hour, a load corridor can be determined [32]. From the resulting load corridor, the capacity for FCR-N can be determined. The term load corridor implies that a consumption resource is considered. However, the same methodology and reasoning applies for dispatchable generation resources as well. The load corridor as illustrated in *Figure 3*, can be applied for individual resources which are aggregated into a larger system, such as a VPP, giving a comprehensive way to determine the available capacity for the entire VPP portfolio. Furthermore, the load corridors can be applied in such a way that the assets can be prioritized depending on their contributing capacity. Thus, the VPP can optimize the dispatch of assets further. [32]

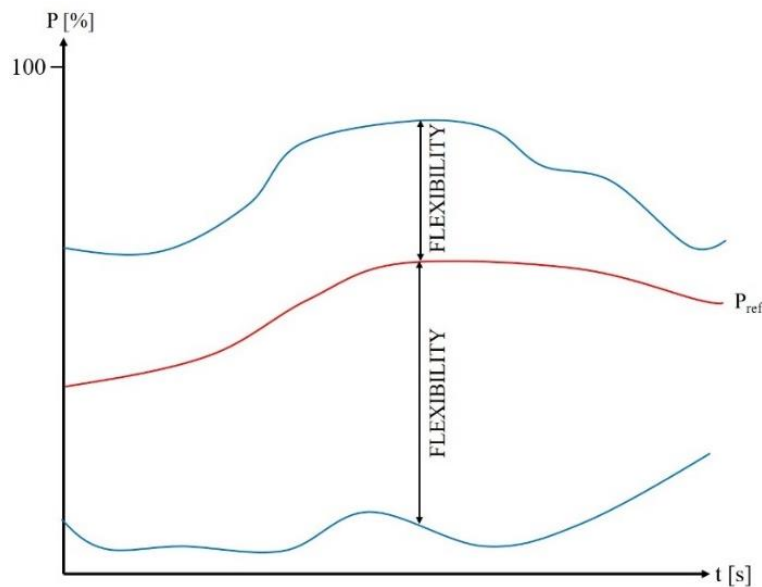


Figure 3: Illustration of load corridor with dynamic upper and lower boundaries.

The total capacity of all assets which are to participate on FCR-N, as determined by the load corridor, is placed as a bid for the corresponding hour of operation. All bids are then ordered by the system operator, responsible for FCR-N, from the lowest price to the highest. The bids are then accepted in increasing order until a sufficient capacity for the specific grid area is attained. Consequently, the price of the offered capacity, which is cost-based, has a large impact for a resource's ability to perform FC. However, if a bid is accepted and if the bid is not cancelled following this, the party placing the bid is responsible for delivering the required capacity during the given hour of operation. Given this, SvK has defined how the power regulation is to be determined.

SvK applies a linear relationship between the power grid frequency and the regulating power. This is presented in *Figure 4* where the acceptable power is presented in blue, corresponding to a deviation of $\pm 10\%$, and an example of stepwise activation of resources is presented in red. Full activation of the resources, corresponding to $\pm 100\%$, is determined by the bid during the given hour of operation. 100% activation corresponds to the full bid capacity being activated [31]. This relationship, together with the signal processing procedures presented earlier, are the integral parts of a regulation controller performing primary FC, presented as linear power in Figure 5.

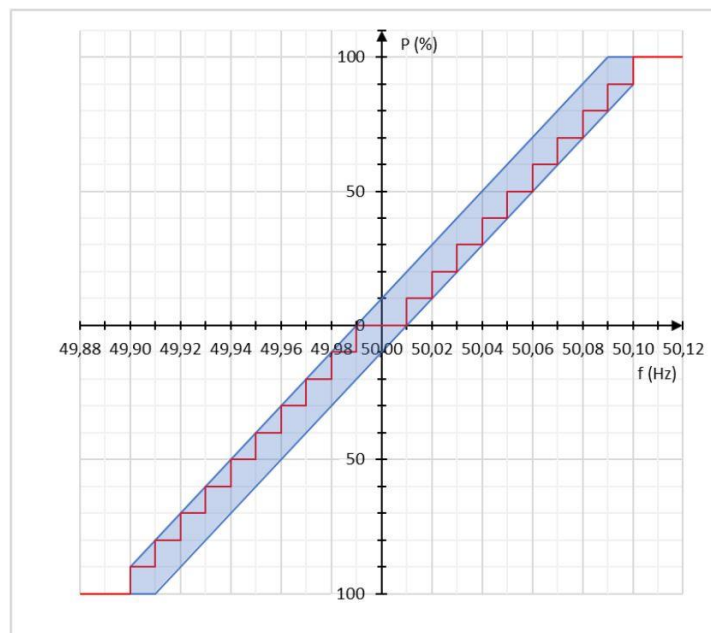


Figure 4: Linear regulation as determined by SvK with acceptable bound marked in blue and an example of stepwise operation is in red. [31]

2.3.4 Regulating power

The bidding process has to take the available capacity for any given hour, into consideration when placing a bid on FCR-N. This capacity is determined by upper- and lower boundaries, and the power reference level during that hour. The power reference level (P_{ref}) is simply the net power of the balancing asset at the beginning of an hour, during which balancing is to be performed. This power reference level is held during the entire hour and is then to be used as a reference when calculating the power delivered to FCR-N. Any deviation from this power reference level is considered balancing power (ΔP), and is supposed to correspond to the resulting power given by the power grid frequency and the linear relationship shown in *Figure 4*. A schematic presentation of the total power (P_{tot}) calculation is presented in *Figure 5*.

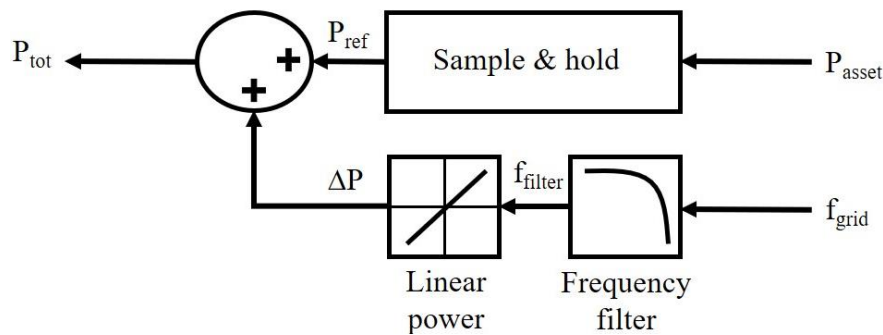


Figure 5: A schematic describing how the asset power during frequency containment is calculated.

The input signals of the calculation are the power grid frequency (f_{grid}) and the asset power. The frequency passes through a filter, as presented in (1), and is then passed into the linear power relation as presented in *Figure 4*. From this, the balancing power is calculated, based on the value of the current filtered frequency signal (f_{filter}), or rather the regulation signal, and the capacity placed in the FCR-N bid for the corresponding hour. The balancing power is then added with the power reference signal, which is a constant value based on the sampled asset power at the beginning of the hour. If the forecast value of the power reference level was correct, this value should correspond to the forecasted value used earlier, in order to determine the regulating capacity when placing the bid. The output signal of the calculation is the total power of the asset, when participating on FCR-N. An illustration of the power reference level (P_{ref}) and the balancing power (ΔP), as shown in *Figure 5*, are presented for three consecutive hours of FCR-N participation in *Figure 6*.

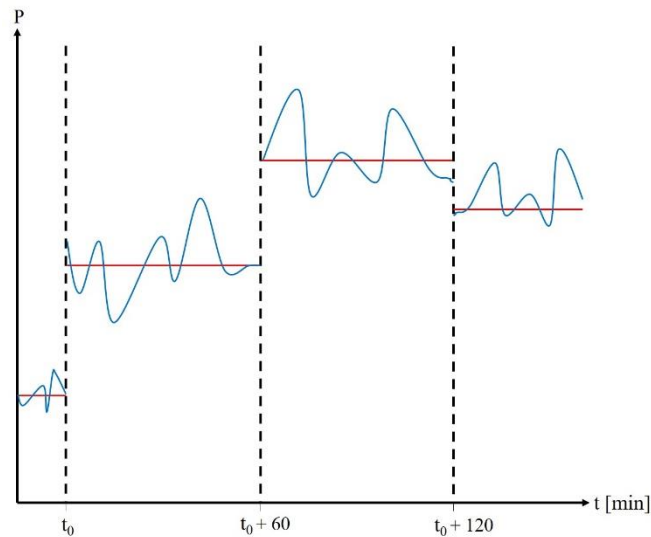


Figure 6: Illustration of power reference level and balancing power during three consecutive hours of FCR-N participation.

In order to further clarify the function of how the calculation of asset power when performing frequency, an example is given. Two days ahead of the specific hour where frequency containment is planned to be performed, the capacity which is to be bid has to be determined. By forecasting the typical power of the asset, the reference power level is determined by choosing the forecasted value for the start of the specific hour which is 1 000 kW. From this level, the capacity to increase or decrease the power during the entire hour is determined as 100 kW and is placed as a bid on FCR-N. Two days later, the power reference level will, if the forecast is completely correct, correspond to the actual power of the asset (P_{asset}). When the hour starts, the power of the asset is held as a constant power reference level (P_{ref}) of 1 000 kW. At the beginning of the hour the filtered grid frequency ($f_{filtered}$) is 50.05 Hz. With the linear power relationship, the balancing power (ΔP) is determined as + 50 % of the bid capacity. The resulting total power at that time is 1 050 kW and is requested from the asset. During the rest of the hour, the balancing power, i.e. the deviation from 1 000 kW is determined by the linear relation between filter grid frequency and the bid capacity.

2.6.5 Asset prequalifying

In order for an asset to participate on FRC-N the asset has to be qualified by SvK as a balancing resource. This qualification is achieved by passing a prequalifying test which is developed by SvK and which is performed by the balancing responsible service provider, i.e. the player which operates the balancing resource. The prequalifying test is

developed in order to fully evaluate the performance of the balancing resource and to ensure that the resource can operate efficiently when performing FC. The main characteristics that are to be verified in the test is the responsiveness and the endurance of the asset. [33]

The responsiveness is determined by the time constant and the time delay of the system, where an increasing time constant and time delay of the system corresponds to lower responsiveness. The time delay is a simple measurement of how long it takes for the asset to respond to a change in the input signal. The time constant however, describes how quickly the system can respond to the change once it has been noticed [34]. An illustration of this is shown in *Figure 7*, where a step change signal has been sent as input and the output is shown in blue.

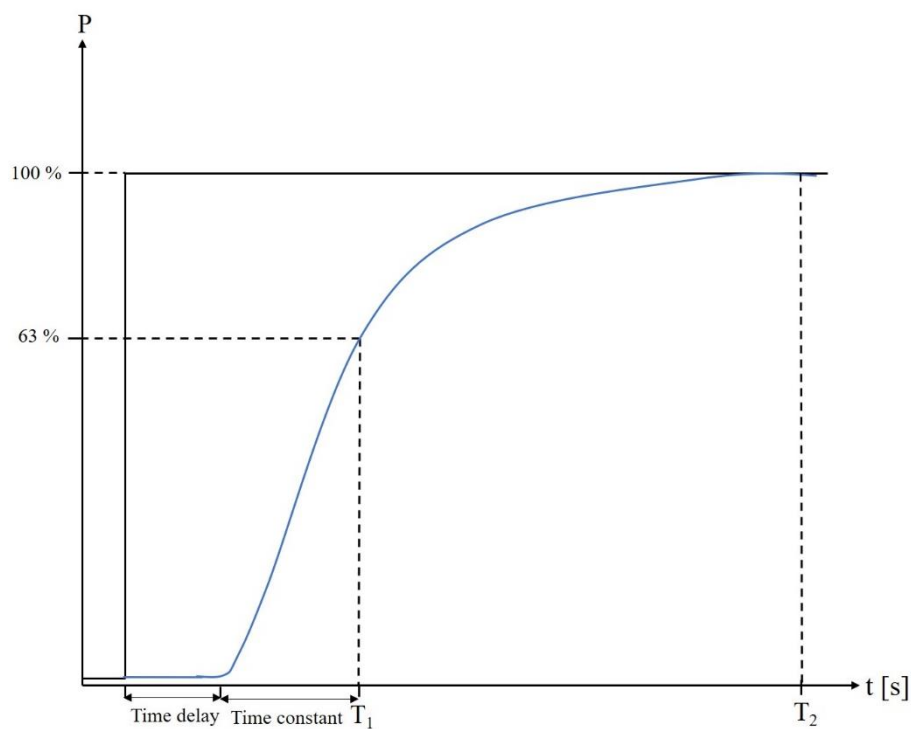


Figure 7: An illustration of a step response and the system time delay and time constant.

In order to determine the responsiveness of the system, the prequalifying test is implemented as a series of step changes with varying amplitude. Furthermore, the step changes alternate direction in order to verify that the resource is symmetrical. The required responsiveness of the resource is determined by the minimum requirements of FCR-N where the resource has to be able to activate 63 % of the bid within $T_1 = 60$ s and 100 % within $T_2 = 180$ s [31] [33]. Comparing this with the step response presented above, it would correspond to a maximum total time delay and time constant of 60 s. Between the time points of 60 s and 180 s, the required power is not explicitly defined. However, it is apparent that before 60 s there is no requirement of power, between 60 s and 180 s at least 63 % of the bid has to be activated and the time after 180 s, 100 % of the bid has to be activated as a stationary value. The signage of the activated power is solely determined by the input signal, where the activated power is in the bound of $\pm 0 - 100$ %. The minimum requirements of responsiveness, determined by a step change, are presented in *Table 4*.

Time	< 60 s	60 - 180 s	> 180 s
Required power	0 %	63 %	100 %

Table 4: Minimum requirements of responsiveness for FCR-N. After 180 s the resource must have reached a stationary value.

The time presented in the minimum requirements is measured from when the input signal is sent, or rather when the step change occurs [34]. The power corresponds to the maximum capacity for which the resource will be allowed to bid on FCR-N. In order to verify the endurance of a resource, the prequalifying signal is held for a period of at least 1 hour after each step change. This is done in order to ensure that the capacity being tested can be delivered for an entire consecutive hour, which is the longest period of time which the resource can be required to be activated on FCR-N. Furthermore, since the input signal of the test is supposed to simulate the actual power grid frequency, the signal is implemented as a series of step changes, where the lowest and highest values of the steps, correspond to the active frequency bounds of FCR-N, i.e. 49.9 Hz and 50.1 Hz respectively [33]. Given this, the input signal of the prequalifying test is presented in *Figure 8*.

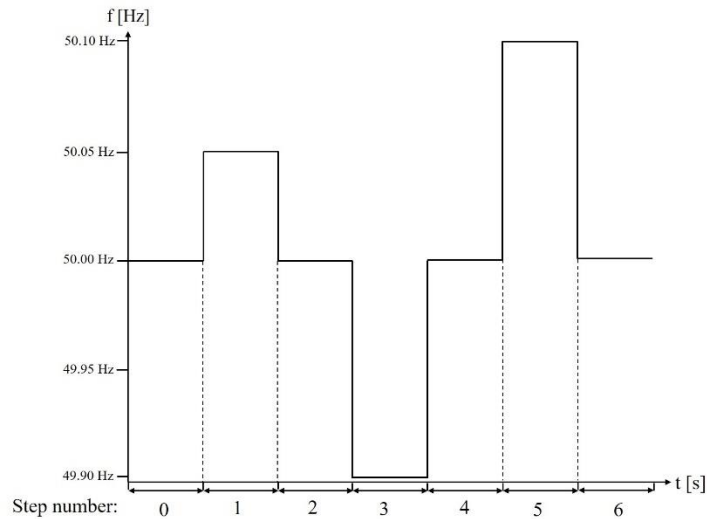


Figure 8: The prequalifying test input signal consisting of a sequence of frequency (f_{grid}) step changes. The number of each step refers to the flank at the beginning on the step and the constant value after the flank. [33]

The prequalifying test consists of six steps where the first step of the sequence, denoted as step 0, is not included in the assessment of the results. During this step, the resource is allowed to stabilize and reach stationary operation before commencing with step number one. During each step change, the resource has to respond fast enough to pass the minimum requirements presented earlier. Once it has reached a stationary value, it has to be maintained within $\pm 10\%$ of the correct value. At the end of each step, the deviation from the correct value is measured and is used to determine the endurance of the resource. [33]

2.4 Smart grid

2.4.1 Expectations

The smart grid (SG), also called the twenty-first-century grid, is a concept that includes a complex system of technologies and systems, hardware and software, communication and controls that together will provide a high level of visibility and control to producers and consumers in the power systems. Expectations set on the SG is to be affordable, clean, reliable and capable of supporting an evolving economy and society. These rather high expectations have a strong influence in shaping the future power system. [35]

Affordability translates to expectations of efficiency, both in terms of energy efficiency and operational efficiency [35], implicating a power grid with low losses in generation, transmission and consumption. Furthermore, operational efficiency implies the need to automate business processes and field operations. The automation of business processes and field operations include the digitalization of the power grid, increasing the amount of sensors and connected devices to improve visibility and increase control. Furthermore, to keep costs low, it has been apparent that the constant reinforcement of the power grid is both costly and slow in regard to the ever-growing demand of electricity. Thus, DR programs are expected to be a larger component in the future grid. The use of DR can shift the need from over-dimensioning the power grid in order to accommodate for redundancy and peak loads to cost-efficiently maximizing the available grid capacity. [36]

Expecting the SG to be clean suggests an increased share of RESs and a decrease of fossil-fuel based energy resources. The impact of RESs on the power grid is largely dependent on which types of resources that are considered to be clean but also which amount of each resource that is integrated into the power grid. Considering an increased share of PV or wind power the intermittency of power delivery would increase due to the stochastic nature of the RES. However, if the increased share of RES mostly consists of hydropower the effect would be the opposite. Hydropower is known to be an efficient balancing resource with an ability to increase the amount dispatchable generation whilst also increasing system stability with larger inertia. But considering factors possibly limiting the expansion of hydropower, such as environmental protection, physical restrictions in

rivers and capacity limitations in transmission networks, it is suggestive that hydropower will not be the sole RES in the upcoming expansion [11].

Furthermore, somewhat related to the cleanliness of the SG, is the use of EVs. EVs can have, depending on whether it is a Plug-in electric hybrid vehicle or an EV, a power requirement in the scale of a typical home. Considering this, the desire of a clean grid also increases peak load where urban areas are especially affected, having a larger amount of chargers connected in a densely populated area. This creates the need to create smarter infrastructure capable of optimizing loads and thus reducing their impact, possibly by utilizing connected vehicle's batteries as an aggregated energy storage system (ESS). [35]

The existing twentieth-century grid is built upon the expectation to deliver power of reasonable quality and reliability to any consumer or load at any time. This high standard has become to be expected as more and more technologies are developed around this standard, thus increasing the technological dependency of highly reliable power of high quality. Moving into the era of the SG, this technological dependency remains, thus requiring an increasingly intelligent transmission and distribution system [35]. However, since grid reinforcements are both expensive and take time, the need for an alternate way to increase reliability whilst maintaining high power quality is needed. By making reliability a market-driven service it is possible to introduce new SG technologies such as virtual power plants, microgrids and distributed energy management systems, by partly formulating their business models after the income generated by the increased power reliability that they deliver. [35]

One expectation of the SG, which most likely will prove to be vital to its development, is the expectation that the grid will continue to support our economy and society. To date, most small consumers have simply connected to the grid without any regard to the size of their consumption or the capacity of the grid. And for most cases a single consumer will not have to take the capacity of the grid into consideration. However, collectively a large amount of consumers will together make up a considerable load on the local grid and with consumption-patterns solely based on their daily behavior, this implies an inefficient way to utilize grid capacity [35]. This effect becomes more and more relevant for the future grid when considering the continuous urbanization where large amount of the population graphically concentrates itself to cities where the grid is already utilized

near to its maximum capacity. Further, taking the time it takes to reinforce the grid into consideration, it has become evident that in some cases, the grid reinforcements can't be made fast enough to respond to the ever-growing demand of power [37]. If this problem is not addressed correctly it can lead to costly losses in terms of a restricted economy where industries and companies seeking to expand into urban areas with high loads, are prohibited to do so, simply because the grid capacity is not capable of servicing the addition of their operation [38]. Thus, it is important that the SG offers solutions to more efficiently utilize the already available grid capacity and to support the further expansion of industries and commercial businesses.

2.4.2 Technologies

By presenting the expectations set on the SG and thus, also its constituting technologies, it is possible to formulate applications designed to solve some of the problems presented so far. The formulated SG applications are goals or end-uses of technologies designed in order to solve problems of the twenty-first-century-grid whilst meeting the expectations set on SG technologies, as presented in the previous chapter.

[39] presents technologies related to SGs. These include DR, grid design and architecture, energy management, energy storage, faults and transients, information and communication technology and modeling, smart homes and buildings, and more. [39] also presents future research areas within forecasting methods, self-healing grids, power flow optimization, EV battery techniques, methods for large-scale RES integration, cloud-based control and management, and lastly, new and improved battery systems. Each area itself implies several use-cases and possible implementations but nonetheless gives an overall view of some SG technologies. It is also important to note that these technologies can be compiled into larger systems comprising of several areas.

Microgrid

An example of a system comprising of several SG technologies is the microgrid (MG). The MG is defined by the U.S Department of Energy as “a group of interconnected loads and distributed energy resources (DERs) within clearly defined electrical boundaries that acts as a single controllable entity with respect to the grid. A MG can connect and disconnect from the grid in order to enable it to operate in both grid-connected or island mode” [40]. They also consider the MG as a key building block for SGs and have therefore established the MG as a key focus area for the development of SG-technologies and their possible implementations. It is predicted that the deployment of MGs will accelerate the integration of information and communication technology. Furthermore, the two main goals of investing in this technology is to guarantee a “plug-and-play” electric grid and to fully integrate DR and consumer participation into electric markets and grid operations. [40]

It is clear that the MG is a broad technical concept that potentially encompasses many key SG technologies. However, with regard to the definition of a MG it is evident that a MG itself does not have to be complicated. The definition suggests that it must be able to perform voltage and frequency regulation when in island mode and that it in some way it must have a system responsible for control of the connected DERs. Additionally, the definition does not specify a capacity necessary for the system to attain in order to be defined as a MG. Thus, a system meeting the aforementioned requirements, as long as it encompasses a clearly defined grid in terms of electrical boundaries, can be defined as a microgrid for any size. Also, the definition does not specify a necessary voltage level, suggesting that the MG can be connected to the low voltage distribution network or directly to the high voltage transmission grid. With this rather unclear definition it is important to compare it to definitions of other SG systems to illuminate the differences. An illustration of a microgrid is presented in *Figure 9*.

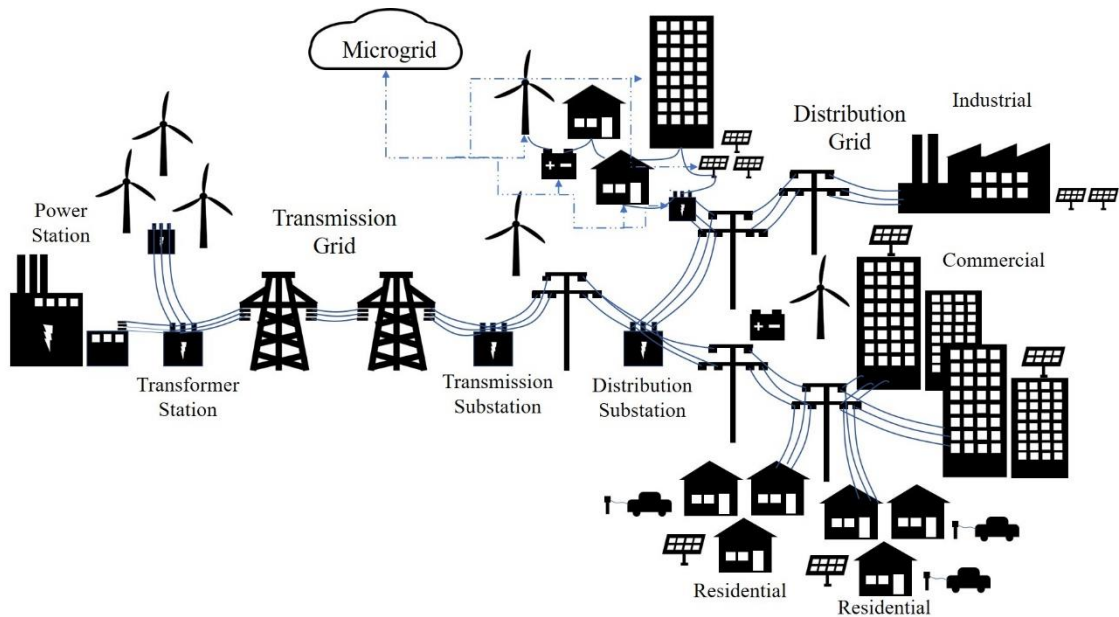


Figure 9: An illustration of a microgrid consisting of wind power, PV, ESS, residential and commercial.

Virtual power plant

The virtual power plant (VPP) is another SG concept which is gaining focus. The VPP does not have a clear definition and is in some cases closely defined to the MG. However, most definitions do have in common that the VPP is a heterogenous entity of aggregated DERs. These are in turn combined in order to participate in energy markets and to deliver services to the system operator. Furthermore, the VPP can be split into two types called the Technical VPP (TVPP) and the Commercial VPP (CVPP). The TVPP consists of DERs concentrated to the same geographical area and delivers services to the local distribution system operator (DSO) and the ability to perform ancillary services to the transmission system operator (TSO). Also, the TVPP has proven to have an enormous technological potential with the possibility for DSOs to optimize network operation by performing tasks such as continuous condition monitoring, asset management, fault location, facilitated maintenance and portfolio optimization with statistical analysis. The CVPP is differentiated from the TVPP in the sense that the CVPP is not as dedicated to the use of the DSO as the TVPP. Instead the CVPP utilizes the aggregated capacity of DERs to visualize portfolio assets to energy markets [41] [42]. The TVPP is similar to the MG in the sense that both are restricted to a certain area. Regardless if the system is restricted to a geographical area or a part of network with clear electrical boundaries, the implication is for the TVPP and the MG is the same. Both the MG and the TVPP contain some type of control to utilize energy resources and both are relatively independent of

what voltage-level and what system operator they interact with and are thus similar in some sense. They do however differ in the sense that a MG is required to have the ability to island and the TVPP does not. An illustration of the VPP is presented in *Figure 10*.

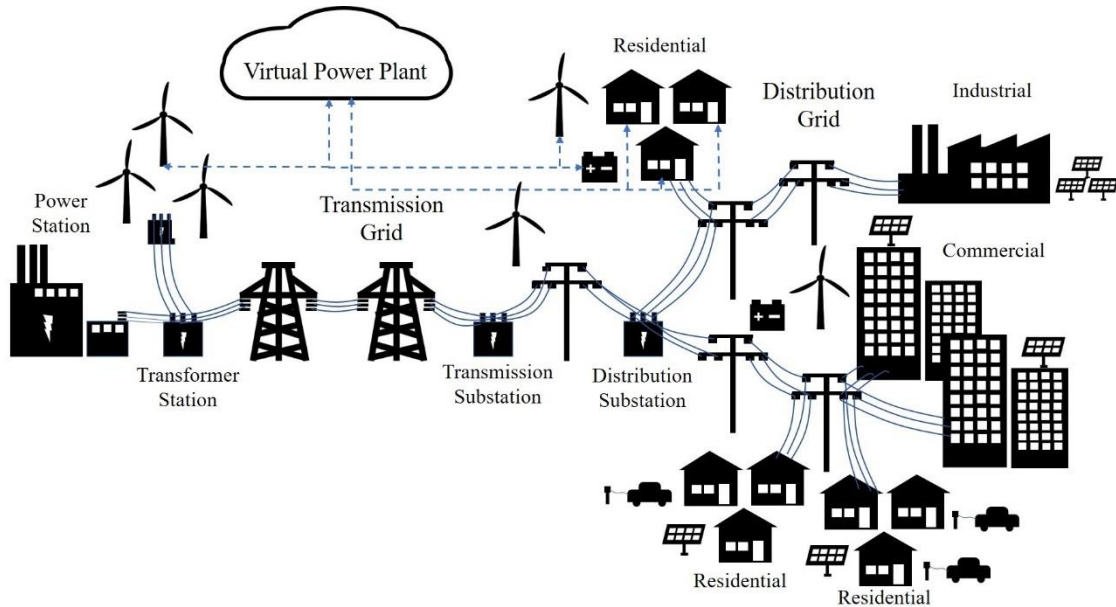


Figure 10: Illustration of a virtual power plant with wind power, PV, ESS and residential connected.

Distributed energy resource management system

The distributed energy management system (DEMS) or the distributed energy resource management system (DERMS) as it also is called, is another SG solution which is closely related to the VPP [9]. The DERMS is introduced as a solution to better integrate DER assets with the power grid. Due to the fact that most DERs are connected at lower voltage levels to the distribution network, the DERMS is mostly aimed towards delivering services to the local DSO. These services have been mentioned earlier in the context of other SG technologies and include asset monitoring and control, scheduling and dispatch, active and reactive power import and export, voltage control, constraint management, forecasting, resource evaluation and optimal DR dispatch [42]. In this DSO-centered solution, it is apparent that the DERMS is similar to the TVPP. A supplier of VPPs even states that depending on your point of view, the VPP is similar or even identical to the DERMS [9]. They do however consider that there are some key differences when regarding each technology's application. They consider the DERMS to be a solution aimed at DSOs, helping system operators control voltage levels in the distribution network, optimize power flows in the within the grid and to manage local loads. The VPP

is instead aimed at commercial customers in order to deliver frequency stabilization, perform energy trading, manage portfolio assets and to manage peak load or demand. Just as with MGs and VPPs there are no specific requirements regarding aggregated capacity. It is however differentiated in the sense that it is mostly aimed towards delivering services to the DSO whereas the VPP can, depending on whether it is a TVPP or a CVPP, deliver services to both the DSO and the TSO. The microgrid however, does not imply delivering any services to the DSO or the TSO and is thus mainly focused at independent operation of a certain part of the grid. Nevertheless, it does not mean that a microgrid is not capable of delivering services in order to gain revenue from extra value streams during grid-connected operation.

Considering the fact that the case study does not imply that the system must be able to operate in island mode or that the system shall deliver services in line with a DERMS, it is concluded that a VPP will be the system in focus for implementation in the thesis's case study. Thus, only the concept of a VPP will be further expanded on in this chapter. This does not however, mean that the definition of a VPP is completely in line with the type of solution of interest for the case study, thus the specific differences will also be expanded on in the following subchapter.

2.5 Virtual power plant

2.5.1 Definition

In order to fully understand the concept of a VPP it is important to establish a common definition for this thesis. Considering the fact that the definition for the VPP is generally not well defined [41], some accepted definitions will be presented in order to discuss their differences and disadvantages. [41] discusses the definition of the VPP based on a literature review. The references presented defines the VPP with descriptions of aggregated resources, resources with varying operating patterns and availability, different connecting points to the distribution network, multi-technology and multi-site heterogenous entity. These descriptions emphasize the mix of energy resources that make up the VPP and that the resources in some way are dispersed in the distribution network. This concept is further agreed upon in [42] where it is stated that a VPP is a heterogenous aggregated mix of DERs. However, it builds upon the concept and includes a measure of necessary capacity where it states that a VPP should be able to influence the system at the scale of the aggregated output. Further, it also presents different types of DERs where it suggests that both dispatchable and non-dispatchable power plants should be included in the VPP, in order to increase reliability and to overcome the stochastic nature of RESs. Additionally, it includes the fact that heterogeneity not only suggests a mix of generating units, but also loads and ESSs. Thus, DERs included in the VPP concept could be either loads, generating units or ESSs.

Another well accepted definition of the VPP is by the project called flexible electricity network to integrate the expected energy evolution (FENIX). The definition from FENIX also includes the descriptors of aggregation, diverse DERs, a single operating profile and network impact. Furthermore, it also includes the notation that a VPP should be able to make contracts in the wholesale market and to offer services to the system operator, thus being in line with previous definitions. The FENIX project continues to discuss how the VPP can be defined as a TVPP or a CVPP, as mentioned earlier. It also presents the fact that DERs could be included into both a TVPP and a CVPP simultaneously. [44]

Technical virtual power plant

The FENIX project further defines the TVPP as consisting of DERs concentrated to the same geographic location. Further it states that the TVPP has real-time influence of the local distribution network thus being able to deliver services to the DSO. To do this it requires detailed information on the operation of the local network, supplied by the DSO, further integrating the use of the TVPP with the DSO. The TVPP is also capable of delivering system balancing and ancillary services to the TSO [44]. [41] presents the possibility of the TVPP being integrated into an active distribution network, where the DSO itself would be the operator of the TVPP. It would then be used to deliver ancillary services in order to optimize operation of the distribution network. Furthermore, it is also stated that the application of TVPPs in active distribution network, could potentially be used to deliver ancillary services to other system operators. It is also discussed how a hierarchical or parallel structure of the active distribution network could apply to the integration of TVPPs. For instance, TVPPs could be connected in parallel in lower voltage levels of the distribution network and then be aggregated to an overlying TVPP of higher hierarchical order at a higher voltage level [41]. This type of system architecture will be discussed in more detail further on.

Commercial virtual power plant

The purpose of the CVPP is not as suited for the DSO as the TVPP. The purpose of the CVPP is to create an aggregated profile of DERs in order to represent their cost and operating characteristics. Additionally, FENIX states that the CVPP does not take the distribution network into consideration when aggregating DERs. The CVPP can deliver functions that include trading in energy markets, balancing of trading portfolios, and other services to the system operator by bidding processes. As a difference from the TVPP, the operator would not typically be the DSO, instead the operator would be an aggregator or a balancing responsible party with energy market access [41] [44]. The use of a CVPP enables smaller DERs to participate in energy markets where they otherwise would not have sufficient capacity to be considered relevant. Additionally, aggregation of DERs contributes to a larger portfolio diversity further increasing the flexibility and possibility to efficiently participate in energy markets. Furthermore, CVPPs do not have to be constrained to certain system boundaries set by distribution networks as TVPP are. Since

the energy markets do not necessarily take placement into consideration, when validating the delivery of bids, it is possible for DERs included in the portfolio of a certain CVPP to be distributed amongst different distribution and transmission grids, as long as, they still remain within the market boundaries. Thus, one geographical region could contain more than one CVPP operating [45]. Another aspect which is important to the operation of a CVPP is the optimization of its operations, this will however be discussed further in the application of the VPP controller.

2.5.2 VPP Energy management system

The VPP energy management system (EMS) is the central component of the power plants operations. It is the logic unit that organizes the use of the VPP's assets by sending commands and receiving operational data by bidirectional communication. It is capable of controlling all possible energy resources, from generation units and loads to ESS, even taking non-dispatchable resources into consideration. The EMS acts on the basis of a control objective. The objective differs depending on the application of the VPP, how it is implemented and possibly also by who the operator is. The objective of the EMS could for instance be minimizing costs, minimizing environmental impact, maximizing revenue and increasing grid stability. However, there are potentially several more objectives and the EMS is not necessarily confined to only one objective. A EMS could potentially strive towards fulfilling several objectives or a balance in-between [41] [42]. Logically, the objectives of a TVPP and a CVPP would differ due to their probable differences in who the operator is and what the application is.

Depending on what the control objective is, the strategy and the means used to fulfill that objective will differ. For instance, if the objective is to maximize VPP profit, the EMS will utilize the necessary value streams and apply a predetermined strategy in order to maximize the total profit from the value streams available. The way that this is done is partially determined by what the strategy is, but also how the EMS is implemented. For instance, the EMS could be implemented as manual control where all calculations and decision-making are done by an operator. The most common control scheme, however, is to apply autonomous control of the virtual power plant. [42]

Autonomous control schemes must take the constraints that affect the VPP's operations into consideration. The constraints can for instance be economical, technical, environmental or regulatory. Due to these constraints, the control scheme must be regarded as an optimization problem which determines appropriate actions for the VPP, in order to not violate the system constraints [46]. The optimization problem is based on the control objective. From the control objective an objective function is formulated. If for instance, the objective is to minimize virtual power plant costs, the function will describe the costs for the entire system. By using mathematical optimization techniques, the function can be evaluated by the optimized scheduling unit inside the EMS, with the goal of minimizing the function's output. The result of the optimization problem is a set of input parameter values which minimizes the cost function and that correspond to actual operating parameters such as battery SoC, generating power and shedded loads. This way, the optimal input parameters can be forwarded to the VPP's assets as control values thus operating the VPP efficiently in regard to its control objective. However, depending on which optimization method that is used, the accuracy and thus, the uncertainty of the optimization solution will vary. Further uncertainties are introduced by other sources such as the stochastic generation of RES. These uncertainties have to be considered by the VPP controller when dispatching its connected DERs in order to ensure VPP stability. [46]

VPP stability can partly be ensured by increasing portfolio diversity or by increasing the share of dispatchable DERS but also by considering uncertainties in the VPP EMS. CVPPs have the possibility of using trading models based on stochastic programming in order to place bids in day-ahead and balancing markets which maximizes profit in regard uncertainty parameters in the VPP [47]. CVPP EMSs can be improved further by considering market price uncertainties. By simulating the action of market performers during a given time frame, it is possible to evaluate the economic behavior of the performers and thus predict future market variations [42]. Further improvements can be made to take to asset participation uncertainties into consideration. This can be done by implementing a distributed optimization algorithm which optimizes the dispatch of DERs by taking their possible loss into consideration, thus making the VPP more resilient to a decrease in number of connected assets [48]. Moreover, asset participation can be optimized further by taking the assets' short- and long-term firm capacity provision periods into consideration. This improves the connected assets participation and enables them to contribute to power markets more efficiently [49]. Many more

uncertainties can be considered when implementing a VPP EMS which possibly can optimize VPP operation in order to fulfill the objective efficiently. However, these optimization techniques will not be discussed further in this thesis and are subject to future studies and improvements. An illustration of the VPP with its possible components is illustrated in *Figure 11*.

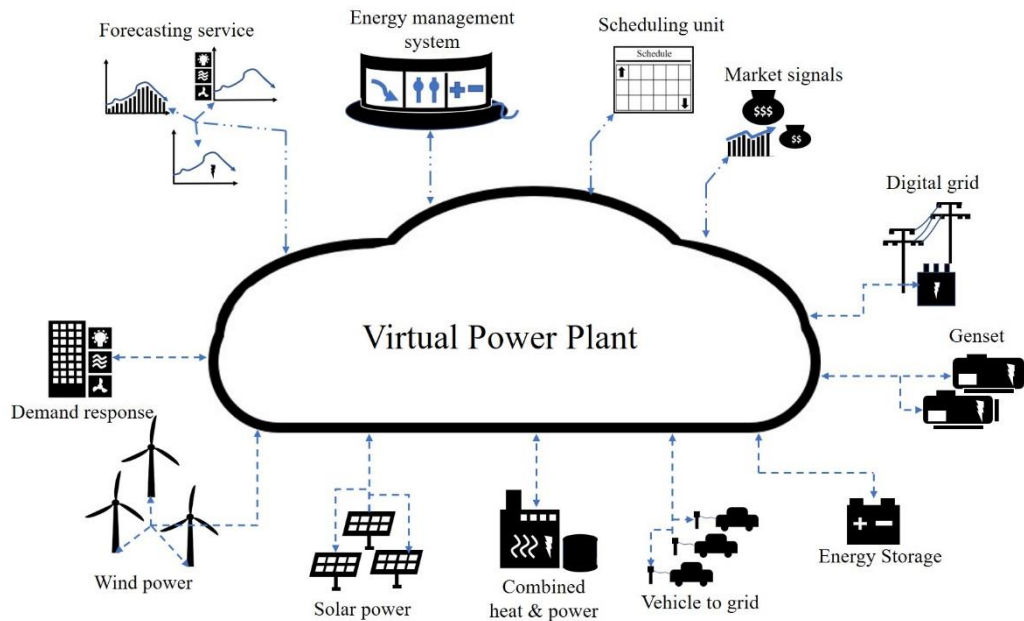


Figure 11: Illustration of a virtual power plant with some of the possible components.

2.5.3 Control architecture

With the ongoing change from a centralized and hierarchical power system to a distributed parallel system, the VPP control architecture gains relevance as it has to be compatible with the existing grid but also the upcoming distributed grid. The typical top-down approach of the power grid, and the definition for the VPP suggests that the control architecture for the VPP should be centralized where all assets hierarchically are placed under the VPP EMS. This central control architecture uses one central EMS which receives operational data from assets and returns commands based on the optimal operation of the VPP in regard to its objective and its connected assets [50]. This type of control architecture is hierarchical in the sense that the EMS is a master and the assets are slaves. A centralized control architecture is presented in *Figure 12*.

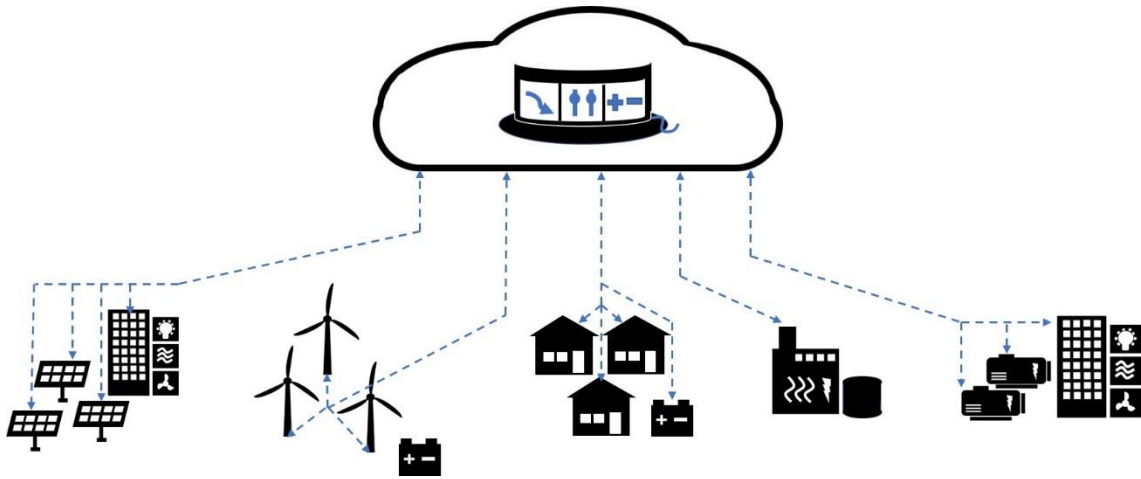


Figure 12: Illustration of a centralized VPP.

In a pilot study performed by Svenska Kraftnät (SvK) and the Swedish electrical company Fortum, where a DR-program utilizing household water heaters were aggregated to a central EMS, it was shown that this type of architecture performed adequately in regard to the market requirements. It was however shown that reliability and varying time delays in ICT is a possible obstacle to consider [51]. Further obstacles in a central control topology have been presented where resiliency to network losses is a large possible problem and has to be taken into consideration when designing a VPP EMS. If the control architecture is centralized the loss of a single communication channel could hinder the operation of the VPP, thus requiring redundant EMSs in order to guarantee resiliency. [52]

In order to avoid the limitations of typical centralized control architectures, distributed control architectures have been suggested. A fully distributed control architecture uses one controller connected to each asset and in some non-fully distributed applications the architecture even applies a central controller that is connected to all distributed controllers. A fully distributed system without a central controller is built on communication between neighboring assets. Each asset is connected to several other assets in which in turn are connected to another set of assets. Each set of assets makes up a neighborhood and is thus unique from every asset's perspective. Since all controllers, or in this context EMSs, are built upon the same logic their optimized operation shall consequently result in the same action despite each asset representing a different type of DER. This however only applies if the neighboring assets to a specific assets contains all assets connected to the VPP control architecture. In reality, this is not the case since many

of the connected assets are hidden from each other since they do not have any direct means of communication. This results in that certain measures have to be taken in order to guarantee that each EMS converges to the same solution or to the same optimal solution to the VPP objective. This type of fully distributed control architecture is viable as long as the information exchange between assets is sufficient. Furthermore, it is said that it will allow for an increased plug-and-play manner. [52] An illustration of a fully distributed control architecture is presented in *Figure 13*.

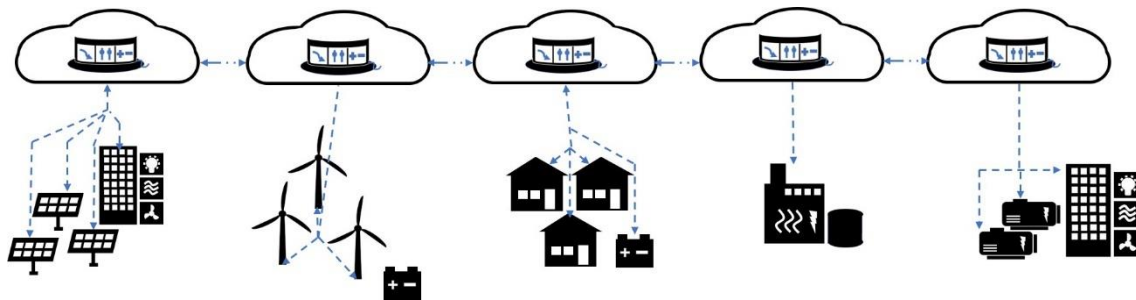


Figure 13: Illustration of decentralized VPP.

As mentioned, distributed control architectures do not have to be fully distributed. Many architectures apply a hierarchical approach with a high number of assets and overlying controllers in different levels. A hierarchical architecture typically has three levels which are based on the required responsiveness to perform services and the required communication channels. The lowest hierarchical order with the fastest response is first level control. First level control is tasked with operations related to device management and DER operation. This could for instance be to maintain voltage setpoints, operate maximum power point tracking of PV arrays and respond to dynamic system changes. In between the lowest and the highest hierarchical order is the secondary control level. In the secondary control level is the controller responsible for enterprise operations. This is often referred to as an EMS since its function partly overlaps the functionalities of the VPP EMS presented in the chapter above. This controller can be in charge of long-term voltage and frequency control, forecasting models and cost-optimized scheduling of primary controllers whilst outputting setpoints to the first level controllers based on prior responsibilities. Usually the secondary level controllers also contain human to machine interfaces to enable operators to interact with VPP operations. The highest hierarchical order is the third level controller. The third level controller is the slowest controller and acts on market changes to control an aggregated group of secondary controllers. It is the

central component of the distributed system and is responsible for market interactions built on long-term forecast-based decision-making. [53] [54] An illustration of the hierarchical VPP architecture is shown in *Figure 14*, without the primary control layer presented, as it is distributed amongst the assets.

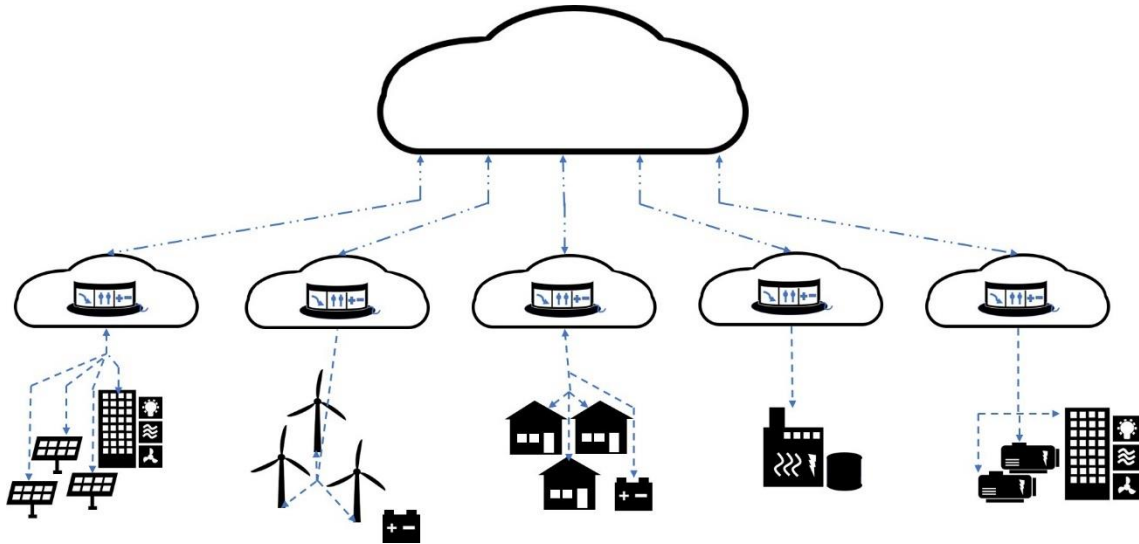


Figure 14: An illustration of a hierarchical VPP without the primary level control layer illustrated as it is distributed amongst the connected assets..

2.6 Energy assets

In [42] the VPP is presented having three main assets: generating resources, energy storage units and loads. However, it can be argued that without other components such as the power grid, ICT and the EMS, implementing a VPP would not be possible. Nevertheless, the available energy assets are a prerequisite for what components and which strategies are implemented in a VPP and will thus be presented first. [41]

2.6.1 Generating assets

When considering the application of a VPP it is important to note that it is aimed at integrating a larger share of renewable and thus intermittent resources into the energy mix. Furthermore, the included resources are not only RES but also DERs. The fact that the energy resources also are distributed imply that they typically are smaller scale and connected to lower voltage levels in the grid. Consequently, mostly smaller generating assets are included into the generation portfolio. The term small however, is always

relative to the size of other generating sources and the overall size of the VPP generating portfolio [42]. Generating assets can be categorized between domestic- and public generators. Domestic generators refer to those which serve an individual consumer, thus a prosumer, for residential, commercial or industrial parts. Public generators do not belong to an individual consumer and instead focus on delivering power to the grid. [41]

Generating assets can further be categorized as dispatchable power plants or intermittent generating units. Dispatchable power plants refer to typical generating units, which traditionally have been fossil based, such as gas turbines and diesel generators, but also their more environmentally friendly counterparts such as biogas turbines, biodiesel generators and hydropower plants [55] [42]. However, dispatchable power plants also refer to the less traditional generating units such as fuel cells and combined heat and power units [41]. If it is possible to determine for a generating unit when to generate power, it is considered to be dispatchable, otherwise it is non-dispatchable [41] [42]. Non-dispatchable generating assets, also called intermittent generating units, typically are wind power plants or PV. Due to recent increases and an expected continued increased installation of wind power plants and PV, these intermittent generating units are becoming more and more relevant and will perhaps make up even larger shares in VPP portfolios. An overview of some typical generating assets included into VPP portfolios is presented in *Figure 15*.

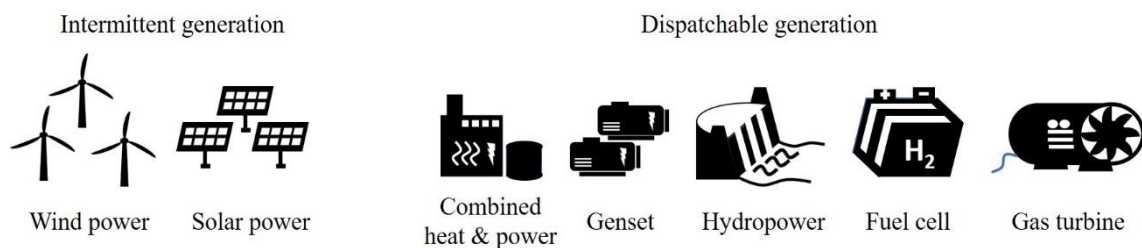


Figure 15: Illustration of common generating assets for VPPs.

The VPP portfolio of generating assets should strive to be as renewable as possible. It is however important to consider the stochastic nature of RES since they typically are very hard to predict. When including this type of non-dispatchable resource in the portfolio it is important to compensate by including dispatchable backup units such as small-scale hydro power plants or ESSs. This way, it is possible to include more RESs whilst decreasing the risk of intermittency by maintaining an acceptable degree of

dispatchability. CHP plants are attractive to use in VPPs since they are dispatchable. Furthermore, they can be combined with district heating, which allows for two energy sources to be controlled by the VPP. Moreover, the fact that they are dispatchable enables them to reduce financial risks by removing the imbalance between predicted and actual generated power, caused by intermittent solar, when liable of bids on day-ahead markets [42]. In this fashion, it is important to have a diversity of generating assets in order to decrease risks, by efficiently combining each assets characteristics, in order to even out their respective limitations.

2.6.2 Energy storage systems

Energy storage systems provide the opportunity to transfer electric energy from one time-point to another. The most important purpose is to utilize the stored energy in the future at a time of greater need. ESSs are taken into consideration in the application of RES in order to balance demand with generation [42]. Several ESS technologies exist and vary in regard to in which state energy is stored. Energy storage technologies include pumped hydro, compressed air, flywheel, superconductive magnetic, capacitive, electrochemical, fuel cells with hydrogen and many variations thereof [56]. EVs have also been proposed to offer energy storage solutions in a vehicle-to-grid (V2G) configuration, where charger-connected vehicle's internal batteries are utilized in the same way as a typical electrochemical storage systems [42]. However, not all ESS technologies are suitable for the application of VPPs. It is important to consider what existing ESSs that are available for the inclusion into a VPP portfolio but also, what ESS technologies that should complement the existing assets.

Performance evaluation

When studying different ESS technologies there are some technical properties to consider in order to determine what technology that is appropriate. Firstly, and perhaps one of the most crucial properties to study is the energy density. Energy density is a measurement of the amount of stored energy in comparison to the ESS's physical volume or in its weight. When regarding mobile ESS, the weight is relevant since it most likely will affect the performance of the overall application. However, in stationary applications, the energy to weight density is not as relevant and thus, only the ESS energy to volume

density is considered. When studying this property, electrochemical storage types prove to be efficient since they boast relatively high energy density. Furthermore, of the different types of electrochemical batteries, lithium-ion and sodium-sulfur, typically have the highest energy density [56] [57]. In some applications, the specific density is not as relevant as the capacity. This applies when the application is stationary and is not confined to a certain area.

Secondly, and closely related to energy density, is power density and specific power. Power density refers to a measurement of power capability in comparison to the ESS's volume. In turn, specific power instead is comparison of power capability and the ESS's weight. Capacitors and supercapacitors, superconductive magnetic and flywheel storage technologies have the highest power density ratings. However, it is important to point out that several other ESS technologies are not considered in weight or volume density ratings since their values vary largely depending on the specific implementation. For instance, could pumped hydro have a very large power capacity whilst not requiring a large reservoir and thus, have a high power density. However, if the pumped hydro were to have a very large reservoir, the result would be the opposite. [56]

Thirdly, another property to consider is the storage's system autonomy. This property is a measurement of the appropriate timescale at which the ESS will operate most efficiently. The level of autonomy varies from the scale of milliseconds to several months, where capacitors offer some of the fastest storage types and fuel cells with hydrogen storage offer some of the longest. Furthermore, autonomy is often compared to the power capacity of the battery in order to determine the appropriate application for the ESS. This is due to the fact that, despite some technologies being capable of responding to very quick changes with a high power output, it might lead to increased capacity degradation. For this reason, some technologies are combined to create hybrid storage types, where the benefits of short-term and long-term storage can be combined. [56]

Lastly, it is also very important to consider the economic viability of ESS solutions. Thus, parameters such as efficiency, lifetime and overall costs are crucial. Battery energy storage systems (BESSs) prove to have very good round-trip efficiencies but do however, have relatively limited lifetimes. Other technologies such as pumped hydro, flywheels and superconductive magnetic energy storage have proven to have much longer lifetimes

and can thus endure a larger number of charge- and discharge cycles. When considering the costs of an ESS, not only the capital costs of the storage should be considered, but also costs regarding its lifetime, efficiency and surrounding infrastructure, such as power electronics. [57] Common energy storage systems are presented in *Figure 16*.

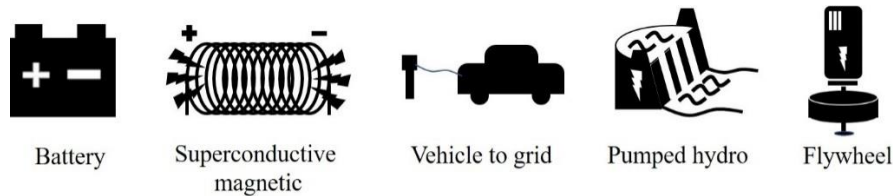


Figure 16: An illustration of common energy storage system for VPPs.

In conclusion, parameters describing energy density, power density, autonomy and costs are the most relevant parameters to evaluate when considering what ESS technology to include into the portfolio. However, this process is not always as straight-forward as it can seem as it is further complicated by factors such as geographical placement, existing portfolio resources and VPP control objectives.

Battery dynamics

The properties of BESSs are attractive to VPP applications since they have good energy to volume density, decent power density and a large autonomy range. This has possibly lead to the increased installation of BESSs in behind-the-meter applications but also, in grid-scale applications [58]. However, due to the high cost of ESSs in general [59], it is important that the dimensions of the BESS are optimized after its application, but also that the operation of the BESS is optimized.

Considering a BESS implemented with Li-ion batteries, there are some effects that have to be taken into consideration when optimizing battery operations. The lifespan of a battery is measured by the number of charge- and discharge cycles with certain charge characteristics and is called cycle life. The cycle life is an estimation for a new battery that has not been used as it is affected by the operations of the battery. The cycle life can also be measured as state of health (SoH) which is a percentage indicating the remaining amount of full life cycles compared to a new battery. [60]

The SoH decreases, i.e. the battery ages, due to calendric and cyclic aging. Calendric aging is the process of decreasing SoH without changing the state of charge (SoC), whilst cyclic aging is the process of decreasing SoH due to changing the SoC. Both calendric and cyclic aging can be reduced by operating the battery efficiently and will thus prolong the cycle life of the battery and therefore, enable operators to optimize the potential revenue of the battery. Calendric aging is affected by the temperature and SoC at which the battery is stored. To achieve optimal cycle life of the battery it is important to keep the battery cool and to keep a SoC near 50 %. The specific values for optimal temperature and SoC however, varies largely depending on the specific battery chemistry in focus. The same factors also affect the cyclic aging of batteries. Moreover, the cyclic aging is also affected by factors such as, depth of discharge (DoD), charge rate (C-rate), discharge rate and consequently also the number of cycles [56]. Therefore, when operating it is important to keep the battery cool, at a reasonable SoC without charging or discharging too deep whilst not charging or discharging too quickly nor too many times. Quite apparently, there are many considerations when optimizing the operations of a battery, for which reason most of the battery operations are handled by a battery management system. However, when including a BESS into a VPP portfolio, the EMS still needs to consider battery aging affects in the optimized scheduling unit in order to fulfill the control objective efficiently. [59] [61] An illustration of the SoC and DoD is presented in *Figure 17*.

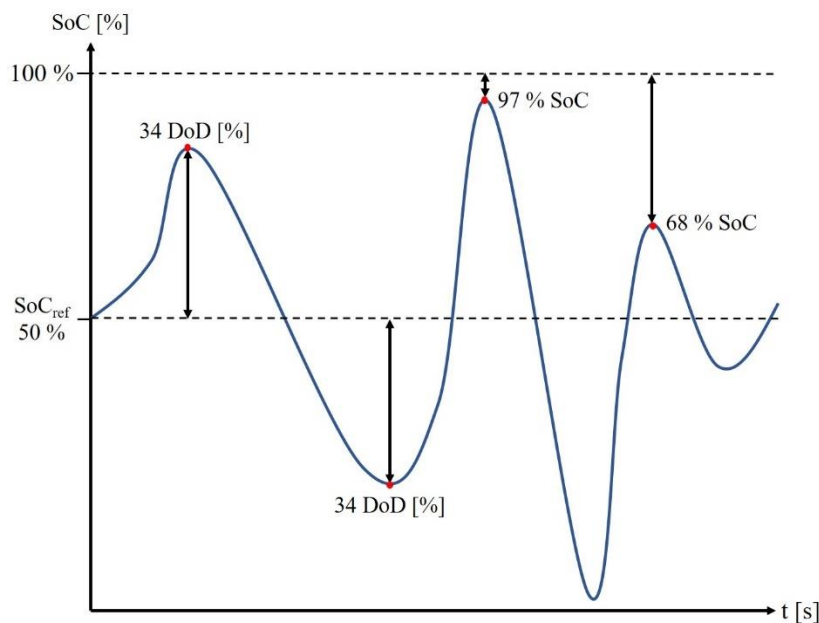


Figure 17: Illustration of the state of charge (SoC) and depth of discharge (DoD). The DoD is measured from the reference SoC of 50 %.

Vehicle to grid

EVs' forecasted increase [4] is predicted to affect the DSOs' operation and management of regional power grids by increasing peak-load and increasing intermittent loads [61]. However, with the inclusion of V2G technologies these effects could possibly be mitigated in the same manner as a typical BESS. It is predicted that V2G could contribute to peak-shaving (sending power back to the grid when demand is high) and valley-filling (receiving power from the grid when demand is low) thus, contributing to more efficient use of grid capacity [62]. Consequently, this can reduce congestion of the distribution grid whilst enabling larger shares of intermittent RESs. V2G would possibly allow consumers to manage their own charging strategy by setting preferences for the ongoing charger connection. By defining how flexible their SoC is, determined by how long their next upcoming trip is, and how flexible their charging time is, determined by how soon their next upcoming trip is, it is possible for the operator of the V2G-solution to either buy back energy via an auctioning process or to charge the EVs in a suitable way. This allows for EV charging where short charging stops in the middle of a long-distance trip will charge quickly and shorter more flexible trips where the charge is already sufficient can offer more flexibility to the grid. Furthermore, the pricing of the V2G capacity will be dynamic, based on a supply and demand relation where the price is influenced by the charging flexibility of connected vehicles [63]. Consequently, it can be argued that V2G stations close to highways will offer less flexibility, since cars usually have longer trips, whereas V2G stations connected to workplaces and shopping centers possibly could offer more. Furthermore, it is also important to note that the use of V2G could increase the cyclic degradation of EV batteries, thus suggesting that car owners should be compensated by the inclusion of a cost component in V2G pricing.

V2G ESSs can possibly also contribute to ancillary services such as frequency regulation. Inclusion in the FC reserve does however, require that the capacity of resources is known [31]. When regarding an EV charger, the amount of vehicles that are connected, their respective storage capacities and their initial SoC, will vary. Consequently, this implies that the capacity of a V2G ESS has to be predicted in advance in order to efficiently deliver ancillary services in day-ahead markets. Each charger station has to be considered individually since its placement will largely affect the parameters which determine the capacity. For instance, if the charger station is placed in the garage of a large office building, the capacity of the ESS suggestively would be large during working hours.

However, if the charger station consisted of aggregated chargers at households, the affect would be the opposite where the capacity instead would be higher during the rest of the day. In order to accurately predict the capacity ahead of time, stochastic programming models can be applied. By using trip-prediction of statistically based user profiles the available capacity of V2G ESS can be increased. Furthermore, studies have also shown that aggregation of chargers to implement V2G ESSs, should focus on charger stations at specific locations in order to gain desired characteristics. For instance, it was shown that chargers connected to the premises of office buildings increased capacity during the day during normal working hours, which perhaps could be beneficial for daytime peak-load reduction. [64]

2.6.3 Electrical loads

Previously, power systems have been designed after the centralized top-down approach where load determined the amount of generation needed. However, since this approach is changing towards a distributed and partly intermittent power generation, load will not continue to determine generation in the same manner as earlier. Instead, to cope with the challenges of this changing system, and to meet the requirements of the 21st century grid as presented earlier, load will have to be determined by the availability of power. The control of loads, or rather demand, is called demand side management. Where demand side management refers to both the efficiency of loads and DR [32]. DR refers to the actions by individual electric customers that reduce or shift their electricity usage in a given time period in response to a price signal, a financial incentive, or a grid reliability trigger [65]. DR in which demand response resources (DRRs) respond to market-based incentives such as varying electric prices and peak load pricing is referred to as implicit DR. If the DRRs instead are offered as resources on markets or DR-programs such as ancillary markets, it is considered to be explicit DR [66] [32]. However, due to the fact that implicit DR has been affected by a low degree of participation and below expected performances, this type of DR has been rather unsuccessful. Since explicit DR in general is not reliant on the incentivized participation of specific DRRs, this type of DR can therefore be used as a resource in ancillary markets, which have higher requirements of accountability [67]. Since ancillary markets are considered to be important value streams for CVPPs, only explicit DR will be considered in this thesis.

Demand response characteristics

Which loads that can be used as DR and what services that can be delivered by DR is determined by each resource's respective characteristics. Each load should to be evaluated by the criterias sheddability, controllability and acceptability. Sheddability refers to the share of a specific load for a given end-use that can be removed when required. Analyzing the sheddability of a load assumes that the required communication, controls and incentives exist in order perform the actual shedding. Controllability, the second criteria to evaluate, refers to the prerequisites in terms of the software and the communication and control equipment, required to perform DR strategies. In the same way as sheddability, controllability is also a measurement of the controllable capacity in relation to the total capacity. A high controllability therefore implies that a large share of the total capacity has sufficient software and equipment to perform a specific DR strategy. Lastly, acceptability refers to the share of the load, associated with equipment or services that can accept the reduced level of service during a DR event. Often acceptability is in direct relation to the size of the incentive to take part in DR. [68]

These three criterias mentioned above are integral when determining the available capacity of a DRR. However, when determining what end-use or what type of DR event the resource is suitable for, further criterias or characteristics have to be taken into consideration. Response time is the measurement of the time it takes for a signal changing operational parameters, from being sent to being received by the operating asset which then responds to the signal. The response time is largely reliant on the system by which the signal is passed. The ramp rate however, another important characteristic to consider, is a measurement of how quickly the asset responds to a changed operational signal and can also be described as responsiveness. In the case of DR, this would be equivalent to how quickly a DRR can increase or decrease its load. Furthermore, it is also important to consider for how long the asset or resource can maintain a level of changed load. This is also called the maximum up-time or endurance. Depending on the asset, some might even require a minimum up-time. The endurance of an asset can be affected by decreased acceptability during a DR event. Closely related to minimum and maximum up-time, is the characteristics of the call frequency which describes how often an asset can respond to DR events. If the DRR for instance has a period where it has to restore its operational values to normal, after responding to a DR event, this would naturally decrease its call

frequency or repeatability [69]. This type of characteristic is oftentimes called rebound affect and refers to an increased power draw after DR participation where the DRR restores operating values to normal.

Demand response resources

Analyzing the characteristics of specific loads allows for the possibility of determining the prerequisites for the resource to respond to DR events. Naturally, the type of load will affect its performance as a DRR. Loads categorized as commercial loads, including end-uses such as heating, cooling, lighting and ventilation which together make up a majority of the total commercial loads, have shown to have very specific characteristics in regard to availability patterns. Their availability is directly related to the operating hours of the commercial building where availability increases during open hours and decreases during closed hours [69]. Regarding controllability, commercial loads have been proven to have rather high controllability due to the use of building management systems (BMSs) allowing for sophisticated control of its internal systems. Furthermore, the use of commercial buildings' heating, ventilation and air conditioning (HVAC) loads as DRRs, could be beneficial in terms of acceptability and sheddability since the high thermal inertia of a building results in lower effects on perceived occupant comfort during DR events. [70]

Residential loads, in the same way as commercial loads, also have an availability largely determined by their load curves. Regarding end-uses of residential buildings, HVAC systems seem to be the main candidate as DRRs [69]. Thus, residential loads could offer high acceptability and sheddability, due to their thermal inertia in buildings. It is however noteworthy that the building performance in residential loads will vary and will consequently affect their performance as a DRR [70]. Regarding controllability, residential buildings do not typically have a BMS nor do they have as advanced control systems as commercial buildings. Additionally, taking the size of residential loads into consideration, they have in comparison to commercial loads, lower controllability due to less control systems in relation to the size of their load. In a study performed by SvK approximately 100 households were aggregated in order to deliver balancing services. It was shown that the water heaters used as DRRs were limited to on/off control and that additional communication and control systems had to be installed at each household in

order to qualify as the loads as DRRs [51]. Thus, controllability of such systems seems to be quite poor. Especially when regarding that the 100 households were not sufficient in order to attain a total capacity of 100 kW.

Industrial loads can be categorized as main process loads, ancillary process loads, or environmental process loads. These refer to the load of main process of the industrial plant, any loads of supporting functions to the main process and any loads created by processes dedicated to maintaining a safe and comfortable working environment, respectively. Each category presents different amounts of flexibility in regard to their electric consumption where main process loads make up the large majority of the industrial flexibility, ancillary process loads almost make up the rest with only a little flexibility supplied by environmental process loads. [71]

In general, industrial loads are said to be less distributed than its corresponding sectors, with high loads in confined areas. Furthermore, industrial loads typically have a high degree of automation contributing to high controllability. This automating comes from the many existing sensors, metering technologies, and existing staff such as plant managers and energy buyers. In order to determine the acceptability and sheddability for industrial loads it is important to study each industrial sector separately as each one has different processes, process steps and thus also different equipment and loads. [71]

Since the analysis of industrial loads is specific for each site where it's specific industrial sector, process and equipment affects its overall performance regarding the criterias mentioned above, these types of loads will not be covered in further detail. Furthermore, since residential loads have proven to be small in capacity in relation to their DRR performance, these will also be left out. However, since commercial loads have proven to be viable DRRs and usually consist of the same physical loads independent of the specific site, these types of loads will be covered in further detail.

2.7 HVAC systems

As previously mentioned, the end uses heating, cooling, ventilation and lighting together make up the majority of the commercial loads. Other end uses include electrical equipment such as elevators, escalators, appliances, office equipment and other electronics. However, since these end uses typically have high sheddability but not controllability, with the exception of some lighting systems with a digital addressable lighting interface, these are often not included as DRRs [72]. The remaining end uses heating, cooling and ventilation, together make up typical HVAC systems, which has been the object of many DR studies with focus on commercial loads. [73] [74] **Fel! Bokmärket är inte definierat.**

2.7.1 System overview

Typical HVAC systems can consist of a hot side and a cold side where each side of the system are designed for heating or cooling the building respectively. Both sides of the system have piping combined with many pumps used to distribute a hot or cold fluid which transports energy throughout the system. In order to cool the fluid, air- or water-cooled chillers are used. These machines are basically large compressors combined with condensers and are the primary components in an HVAC system. They feed cool refrigerant to the rest of the cooling loop and operate to supply constant and sufficient cooling power to the system. The heat absorbed by the chiller from the incoming warm refrigerant is either dissipated from the chiller into the room where they are situated, or it is passed on to external cooling towers which are large air-cooled heat exchangers. Connected to either the hot or the cold side of the HVAC system, or possibly both, are the air handling units (AHUs). They receive heating or cooling power by the connected pipes and use heat exchangers, cooling coils and large fans to dissipate the heating or cooling energy into air-conditioning ducts. In the AHU there usually is one exhaust fan, removing air from the building, and one supply fan, feeding air in to the air ducts. These ducts have either constant air volume or variable air volume, regulated by connected AHUs and diffusers, in order to distribute hot or cold air to the building. The way AHUs, diffusers and ducts are connected varies largely between buildings. Some complex systems can have several AHUs interconnected by several ducts which in turn deliver air to several rooms or climate zones through different diffusers. Whereas a simpler system

can include one AHU, connected to one duct, supplying one room through one diffuser. Furthermore, depending on whether constant air volume or variable air volume is used, either the pressure or the air flow in the duct is the parameter which is regulated. How much of the heating or cooling energy is delivered into the building, will affect the heating or cooling load on the source. For the hot side of a HVAC system the source could be district heating, heat pumps or other internal sources [75]. An overview of a typical HVAC system is illustrated in *Figure 18*. The illustration is however simplified, it neither shows heating supply for the AHUs nor cold-side pumps for the chillers which would have been included. In practice, the system would be much more complex and interconnected.

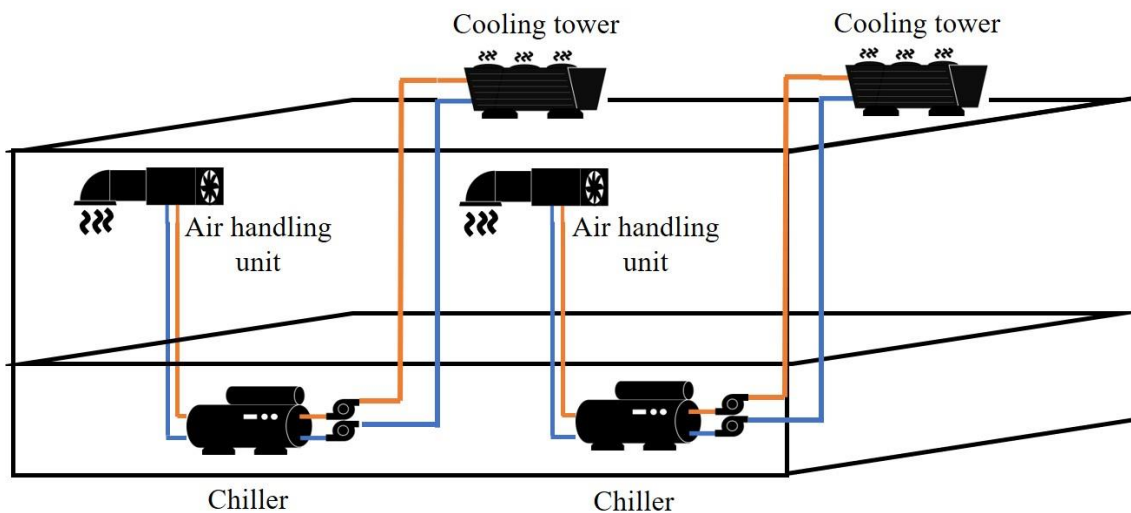


Figure 18: A simple illustration of a HVAC system with cooling towers, chillers and air handling units (AHUs)

2.7.2 Load reduction

When determining the relevant components to include as DRRs it is important to know which overall components in the HVAC system that constitute relevant loads. The main components to consider are chillers, pumps and the fans in AHUs. In [72] cooling towers are neglected since they are argued to have a small load. However, since the main power consuming component of the cooling towers are fans, these could potentially be controlled in the same manner as the fans in AHUs. By predicting the required cooling power of a commercial building and setting a threshold thereafter, it was shown that chillers, pumps and fans could contribute to a power reduction of about 23 %, during a DR event lasting for 2 hours. This was done by dispatching the connected loads in an

optimized way with consideration of the indoor climate, which resulted in achieving an acceptable deviation of zone temperature of less than 3 °C [72]. It can be argued that these DRRs proved to have high acceptability due to the small temperature deviation whilst achieving a high sheddability with regard to the reduction of 23 % of overall power [72]. Despite proving relatively high acceptability and sheddability, and possibly controllability, it does not specify other important aspects of DRR performance such as response time, ramp rate, endurance or call frequency. Being able to perform a reduction of 23 % for 2 hours suggests a relatively high endurance. Furthermore, the increased indoor temperature resulted in a rebound effect where the buildings HVAC system had to increase its load beyond the initial load in order to restore the temperature back to normal. This rebound period lasted for approximately a quarter of the time of the DR event which suggest a rather low call frequency for such large power reductions of this length. However, it is noteworthy to point out that during the rebound period, the stress on the grid was reduced by using simple power limiting of the DRRs. In summary, the study shows how HVAC systems can be a suitable DRR to quickly perform power reductions in order to decrease load on the grid, possibly even in MG implementations where the MG has to reduce loads in order to stabilize operation. [72]

2.7.3 Regulation performance

Beyond using HVAC DR for load reductions, many sources study the use of HVAC for the provision of ancillary services, or more specifically, frequency containment [76] [77] [74] [78]. As for DR load reduction, frequency containment also utilizes the thermal mass of buildings as energy storage to increase DR capacity. Since frequency containment requires rather fast response of both generators and DR, typically in the timescale of seconds to minutes, this sets higher requirements of DRRs and their control systems than what typical load reduction events do. When performing frequency regulation, the DR assets respond to variations in the grid power balance, measured by the power grid frequency, in the same way as typical fast-responding generators, with the exception of that instead of having a net input of power, DR has a net outtake. When the grid frequency indicates that the power balance is too high, i.e. too much power is fed into the grid, the DR assets regulate the frequency by increasing their load. If the balance is too low, the DR assets instead reduce their load. The grid frequency is a direct measurement of the net

power in synchronous area of the grid and is measured individually by all balancing assets [78].

In order to efficiently track regulating signals, it is important to take relevant control system and DRR performance into consideration. Given that a HVAC-based DRR has an acceptable degree of sheddability, controllability and acceptability, it is also important to consider its ramp rate, endurance and call frequency. When performing frequency containment, high frequency variations of the regulation signal will result in high frequency variations in load of the DRRs, i.e. fans, chillers and pumps. Since the thermal dynamics of buildings are constituted by low-pass characteristics, these high-frequency changes impart only a little impact on the indoor climate [78]. Thus, it is expected that after a period of performing frequency containment that the indoor climate will not have been impacted in a notable way. Therefore, as a difference from long-term load reduction, frequency containment will not suffer from a lower call frequency due to a prolonged rebound period. This also implies, that since the indoor climate will not be affected in a notable way, that the endurance of frequency regulation should be maintained rather high. However, the specific physical constraints of HVAC components that affect endurance and call frequency should be evaluated further to ensure sufficient performance.

In order to ensure sufficient frequency containment performance, the ramp rate of HVAC DRRs should be high enough to respond to high-frequency changes in the regulation control signal. The ramp rate of fans and thus, AHUs and cooling towers whose main power consumers are fans, has been proven to have a sufficient ramp rate in order to efficiently track regulation signals. The possibility of using chillers in order to perform primary frequency regulation has been discussed but has been neglected in many cases due to a perceived poor ramp rate since they typically have time constants larger than 200 seconds [73]. However, it is important to point out that the time constant of chiller systems is largely affected by its proprietary internal control logic and could possibly be optimized to improve its ramp rate. This could be done by implementing lower-level control of the chiller's compressor, which constitutes the main load of the chiller. By employing compressor speed control with a variable frequency drive (VFD) it has been shown that the chiller is able to respond to step changes in approximately 40 seconds or less, a large improvement of the typical chiller control logic in regard to its overall ramp rate [79] [80] [81]. This implies that chillers might not only be viable as slower secondary frequency

regulation resources as shown in some sources [76] [77], but also could prove to be viable for faster primary frequency regulation. Furthermore, [79] states that the availability of the pumps, circulating refrigerant and water to the chiller, are affected by its operation regimes. Depending on whether the pumps are variable flow or constant flow, they may or may not be available for frequency regulation. However, since the pumps can respond to the cooling load changes set by the chiller with sufficient ramp rate [79], it is arguable that they also can perform primary frequency regulation.

Consequently, chillers, AHUs, pumps and cooling towers could potentially perform primary frequency regulation, as for instance on FCR-N, given some specific criterias of controllability. However, as stated earlier, the overall controllability of commercial loads, also include overlying systems such as BMSs. Therefore, the specific control systems that are relevant when performing ancillary services should be discussed in further detail.

2.7.4 Control systems

As mentioned previously, the internal proprietary control logic of the chiller has been shown to introduce large delays in chiller control making it typically less suitable for fast responding ancillary services [79]. In the same way, it has been shown that other control systems such as the BMS could largely affect DR performance of building loads. An important part of the BMSs effect on DR performance is the control method used in order to regulate the power of internal DRRs. [77] discusses three different control methods for regulating the power of AHU fans through the use of the BMS. The different control methods utilize the control of parameters in varying levels of the BMS, ranging from low-level control to high-level control, each presenting varying advantages and disadvantages.

Fan speed offset method

The lowest level of control is the fan speed offset method. This is based on adding a fan speed offset (Δf) signal to the existing fan speed signal (f_{fan}) in order to increase or decrease the fan speed and thus its power consumption, given by the fan affinity law below, derived from [77], where (P_{ref}) is the measured power at the speed (f_{ref}).

$$P_{fan} = P_{ref} \left(\frac{f_{fan} + \Delta f}{f_{ref}} \right)^3 \quad (3)$$

This law is based on the use of variable speed fans complemented with VFDs where the total frequency output signal of the VFD is changed by varying the parameter Δf . This method is the most direct way to regulate the power use of the fans. It is possible to implement it both as an open- and a closed-loop system. The closed-loop system uses a feed-back loop to ensure correct load, whereas the open loop system uses a physical model of the AHU to accurately estimate the controlled systems load without any measurement of the actual load. In both cases some type of system identification is required. Either it can be determined by an experimentally measured system transfer function describing the load characteristics of the AHU, or it can be determined by a trained predictive model of the same system characteristics. The advantages of using the fan speed offset method is that the control chain is closely coupled with the controlled system thus increasing responsiveness by simply excluding systems that otherwise would include delay. The excluded systems can for instance be variable air valves with mechanical inertia or overlying BMSs with delays in its control logic. Furthermore, since the fan offset method is closely coupled with the controlled system, i.e. the AHU, it allows for simpler system identification for the same reason as earlier, where the system to be identified is limited by the exclusion of other systems. However, this control method has proven to have some disadvantages. Firstly, it can require retrofits to already existing hardware in order to host the required control systems, thus increasing costs and complexity of the overall system. Secondly, the fan speed offset method can sometimes be counteracted by downstream control systems, regulating parameters such as air flow or duct pressure by the fan speed setpoint and thus changing the AHU load. Lastly, this method lacks the ability to customize its control after the specific comfort of occupants in the building or conditioned spaces that are sensitive to variability. [77]

Supply pressure/mass flow offset method

The supply pressure (Q_{fan}) or mass flow (H_{fan}) offset method is similar to the fan speed offset method in many aspects. But instead of interacting with the AHU directly by adding an offset signal to the fan speed signal, this is instead done via the BMS where the supply pressure- or the mass flow set point signal is changed. This change of pressure, or mass flow, is done by changing the speed of the fan until the new pressure or mass flow set-point is reached, which translates into a changed load of the AHU. The affinity laws below show the corresponding relation between pressure, mass flow and fan speed respectively, and the relation between pressure, mass flow and power.

$$H_{fan} = H_{ref} \left(\frac{f_{fan} + \Delta f}{f_{ref}} \right)^2 \quad (4)$$

$$Q_{fan} = Q_{ref} \left(\frac{f_{fan} + \Delta f}{f_{ref}} \right) \quad (5)$$

$$P_{fan} = H_{fan} Q_{fan} \quad (6)$$

As seen by the equations above, by changing the set-point for pressure or mass flow, the AHU load will change as a result of the changed fan speed required in order to meet the new set-point. This method does however require the inclusion of the BMS into the control chain since it is the system responsible for the regulation of pressure and mass flow. Consequently, the supply pressure or mass flow offset method will possibly have higher latency than the fan speed offset method and will also prove to have higher complexity due to the inclusion of physical inertia of air flow in the air ducts and the pressure, or mass flow, controller's internal logic. Despite the drawback of being slightly slower than the previous method, the supply pressure or mass flow offset method does have the advantage of not being affected by downstream control systems. [77]

Thermostat set-point offset method

The thermostat set-point offset method is the highest level of control of the three control methods. It affects overall HVAC control by changing the temperature set-point of the whole building or some of the internal climate zones. The change of temperature set-point translates into an increased pressure or mass air flow by the AHUs, and by what is known from earlier, this consequently will increase the overall load of the building. This control method has both been implemented and simulated in open-loop form. The advantage of this method is that it is the least susceptible to conflicts with other control systems, since its rather high hierarchy in the BMS. Furthermore, it is easy to dispatch since it only requires minor changes in the BMS software to accommodate the control method. Additionally, since it is directly integrated into the BMS, and due to the fact that only temperature bounds are changed, the thermostat set-point offset method will easily guarantee the correct degree of comfort. However, since the method also includes the control-logic of the entire BMS and underlying systems such as VAVs and AHUs, the control method experiences significant delays. This is further worsened by the fact that such an expansive system is easily subject to many disturbances, decreasing its overall reliability. [77]

3. Case Study

In this chapter the case study subject is presented. A short background is given to get a basic understanding of the site. Then overall data for the case study is presented of which some of the data will act as a basis for understanding and some will be used in the following chapter. Additionally, available information of the assets available at the case study are presented. Lastly, the context of the case study and how it is related to the scope of the thesis will be discussed.

In order to fully answer the question formulation in this thesis a case study is used to examine the implementation of a small-scale VPP. The case study is based on a retail area called Våla in southern Sweden. The retail area is selected as a case subject due to its ambitions in corporate social responsibility and due to its portfolio of energy resources, making it an interesting case for the implementation of a VPP. Våla has expressed ambitions of zero net emissions and has in the last five years reduced its electricity consumption with almost 40 %. Furthermore, the retail area is actively working with waste plans, accessibility adaptation and offers its tenants to take part in an approved suppliers' program where the suppliers have gone through an extensive control of social sustainability. Våla sees sustainability as an obvious part of its operations where it is a prerequisite for its success by utilizing resources efficiently and thus reducing environmental impact [80]. In this thesis, the case study will be based on the main building in Våla retail area called Våla Centrum, shown in *Figure 19*.



Figure 19: An overview of Våla Centrum.

3.1 Energy footprint

Being a shopping centre with 11.3 million calculated annual visitors and a host of around 200 tenants, it is reasonable that the overall energy footprint of Våla is large. The total electrical use for year 2018 was about 12.7 GWh, according to their annual energy statistics report. The annual electrical load varies throughout the year which is presented for 2018 in *Figure 20*. Here it is shown that the load of the building mostly remains above 500 kW, indicating a constant load during the entire day. Further, the peak load for Våla during 2018 was about 3.5 MW, occurring during the summer-half of the year. This is significantly larger than the average peak load during the winter-half of the year which is slightly higher than 2.5 MW. These trends are also confirmed in *Figure 21* where both the monthly peak and average load for 2018 is presented. It is however important to note that these values are measured from the point of connection to the grid and consequently includes the generation from the roof-mounted PV. Due to this, it can be expected that the consumption during summertime, when PV generation is higher, would be greater than what it seems like when viewing the figures below.

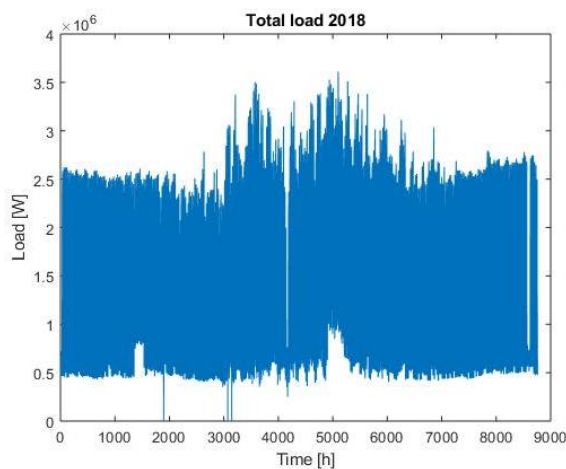


Figure 20: Total load of Våla for 2018 starting from Jan 1st 00:00.

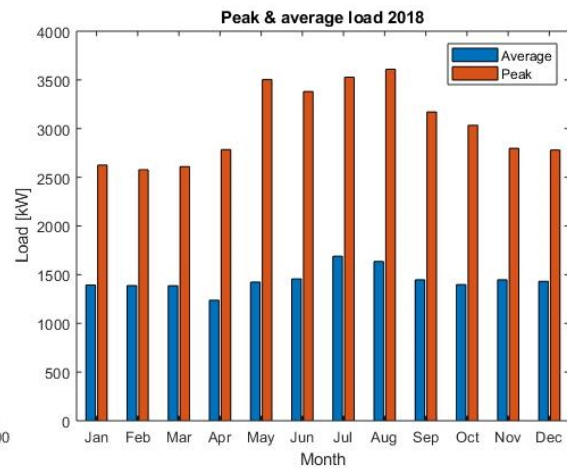


Figure 21: Monthly average and peak load of Våla

When studying monthly variations in *Figure 22* it is clear how the average energy and power consumption varies from day-to-day, where weekends are slightly lower due to shorter open hours. The same pattern is recognized for all months during 2018, thus only one month for 2018 is presented. Some outliers occur, such as reduced energy and power consumption during holidays, when Våla is closed. Furthermore, when studying Våla's footprint in even smaller timescale in *Figure 23*, even daily variations can be exposed,

witnessing about Väla's daily load profile and opening hours. However, as mentioned, it is important to note that all figures of the total load at Väla actually represent the net load. This differs from the total load in the sense that the net load includes any on-site generation. In the case of Väla, it happens to include the claimed to be largest roof-mounted PV installation in Sweden with a rated power of 1.1 MW_p, which can be seen in *Figure 19*. However, the PV panels will be excluded in this thesis for reasons that will be presented later.

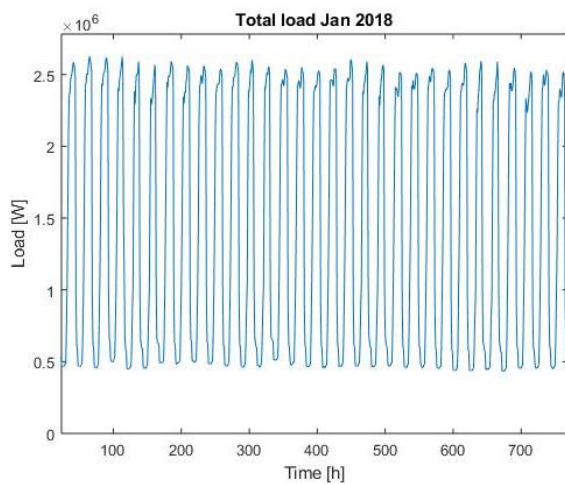


Figure 22: Total load of Väla during January 2018

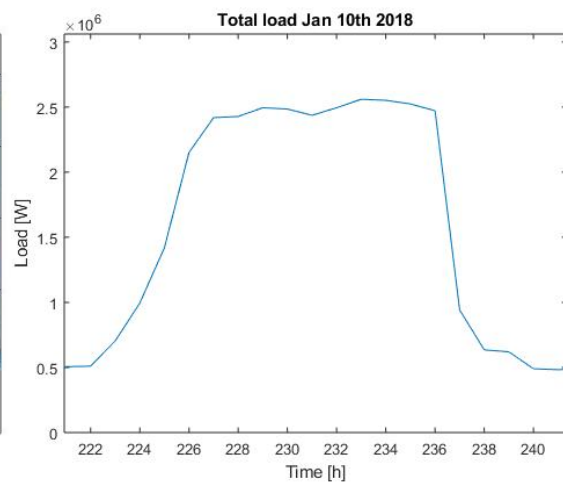


Figure 23: Total load of Väla during January 10th 2018

The amount and the rate at which the energy is consumed, are not the only interesting parameters to study in the shopping centre's footprint. Even how the energy is used and to what purpose can help in order to draw conclusions regarding the energy characteristics of Väla. For 2014 an energy audit was made. In *Figure 24* it is shown that 2014 had an overall higher consumption of electricity than 2018, where the electric consumption 2014 was about 14.3 GWh and the corresponding value for 2018 was 12.7 GWh, possibly due to the recent improvements of energy efficiency. Moreover, the power supplied to cooling increases to a larger net energy, perhaps indicating the use of chillers with a coefficient of performance higher than one. Furthermore, air conditioning consists of cooling-, heat- and electrical energy, together making up one of the largest end uses at Väla. Lastly, it is apparent that the electricity consumed by tenants is also one of the largest end uses, and despite this is not measured in greater detail due to regulations in the tenants' contracts which prohibits disclosure of their consumption.

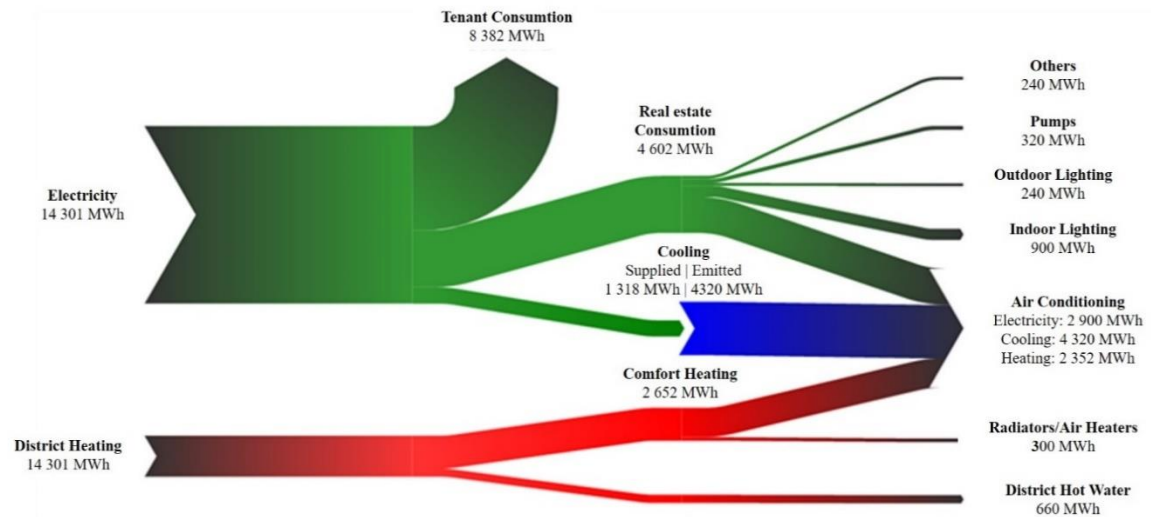


Figure 24: Sankey diagram of energy end-uses at Väla for 2014.

3.2 Electrical loads

Väla contains a wide variety of tenants operating their business on the premises. The tenants range from restaurants and grocery stores to clothing and electronics stores. Each tenant operating on the premise has specific requirements regarding power use, lighting, indoor climate and operating times. These requirements are regulated through tenant-specific contracts which are agreed upon with the operational management team of Väla and the specific tenant in focus. Both parties are upon agreement obliged to follow the terms in the contract. From the operational management team's point of view this translates into delivering a reliable supply of electricity and pleasant indoor climate, which varies between each tenant. Consequently, as a result of their specific needs and the wide range of businesses on the premises, the control of variables defined in the tenants' contracts is almost surgical. Regarding climate control, a tenant could for instance, be wall-to-wall with another tenant despite having different climate requirements and their climate zones being physically interconnected allowing energy to flow between zones.

Väla Centrum has many separate climate zones. Each climate zone uses at least one AHU which is interconnected with the cooling and heating system. The heating system is supplied by district heating. This means that it does not constitute an electrical load and will therefore be a delimitation in this thesis. The cooling and the ventilation system, however, consists of several electrical loads. These loads include AHUs, chillers, air

coolers, cooling towers, circulation pumps and other components used for measurement and control in the HVAC-system. It is expected that each one of these loads has varying rated power and characteristics. Thus, each load must be presented in further detail in order to be modeled with enough accuracy.

Other electrical loads at Väla, except those which are categorized as electricity consumed by tenants, consist of indoor- and outdoor lighting, pumps and other end uses. Despite being a large end use of energy, the loads consisting of tenant electricity use is hard to affect since it is regulated in their contracts and is often directly related to their specific businesses. Furthermore, the measurement of such end-use is often classified in order to protect the tenants' integrity. Consequently, only cooling and ventilation loads will be regarded in this thesis since they constitute the main candidate for DRRs.

3.3 Cooling loads

Cooling loads refer to all components that are devoted to providing cooling power the HVAC system at Väla. These components could include the central chiller converting electrical energy to cooling energy as well as downstream system such as pumps, pipes, refrigerant and more. However, not all cooling components constitute loads relevant for demand response applications. Therefore, only the ones relevant for this application will be presented further.

3.3.1 Chillers

The central components of the cooling system at Väla are five chillers. Two of these chillers are of the brand and model Trane RTHD D2, denoted as VKA01 and VKA02, and the three others are Carrier 30HXC 310, denoted as VKA03 to VKA05. The five chillers are all connected to the same cooling system, supplying the main building at Väla with refrigerant. The chillers operate based on the momentary cooling load in the building. Their rated cooling capacity and their rated load are specified in *Table 5*.

	Trane RTHD D2	Carrier 30HXC 310
Notation	VKA01 – VKA02	VKA03 – VKA04
Cooling Capacity	1138 kW	994 kW
Electrical load	209 kW	265 kW

Table 5: Chiller specifications of rated cooling capacity and load at Väla. The system includes two Trane models and three Carrier models.

The combined rated load of the five chillers is 1213 kW. The chillers are operated in a sequential manner where a chiller is activated one after another in response to an increasing cooling load, which is indicated by an increase in refrigerant temperature. The activation of a second chiller occurs when the first one is running on full capacity. When the second chiller is operating on full capacity, the third one will activate if the cooling load requires. In the same manner, all the chillers will continue activate in order to supply sufficient cooling power. Naturally, the deactivation process occurs in the same way but in the opposite direction. The order in which the chillers are activated is varied in order to ensure equal wear of all machines to avoid premature failure of one machine that is cycled harder due to extensive starting and stopping sequences.

The chillers are currently operated by their proprietary internal control logic which only has been configured to accommodate the prerequisites at the shopping centre. This control logic is not well suited for DR applications since it is not developed for high controllability, but rather high efficiency. However, the manufacturers of the chillers have stated that by installing VFDs to the chiller's compressors and reviewing the control logic, the controllability can be improved greatly implying that the chillers possibly could be suited as DRRs. Without VFD the idle power level during operation of the machines would correspond to 40 % and 30 % of the rated power respectively for the Trane and Carrier chillers. However, when installing VFDs, these limits can be decreased by decreasing the output of the VFD from 50 Hz to 30 Hz. This frequency change decreases the lowest compressor speed from 3000 rpm to 1800 rpm which corresponds to a 40 % decrease of idle power level for the Trane models. When regarding the Carrier chillers, the corresponding values are unknown but have been assumed to apply to the Carrier chillers as well. With VFDs, the idle power level of the machine during active operation

would correspond to approximately 24 % and 18 % of the rated power respectively for the Trane and Carrier models, based on the assumption that the relative power decrease is the same for both machines. The idle power levels for the chillers are presented below.

	Trane RTHD D2		Carrier 30HXC 310	
Idle power without VFD	40 %	83.6 kW	30 %	80.7 kW
Idle power with VFD	24 %	50.16 kW	18 %	48.42 kW

Table 6: Minimum load during active operation of chillers with and without VFD and reviewed control logic.

From idle power to the rated power of the Carrier models have a stepwise increase of load. Each step is 10 % of the power between idle and the rated power, corresponding to about 22 kW, increasing with a total of 10 steps to reach rated power. When active, the Trane models at idle power have the VFD set at 30 Hz corresponding to a compressor speed of 1800 rpm. In order to increase cooling power from this point a sliding valve is used. When the valve is in full operation the VFD will start to increase the compressor speed instead until the output signal has reached 50 Hz and the chiller is running at full capacity. During this process the relation between load and VFD output signal is linear. The operation schemes for both the Trane and Carrier machines, with VFDs equipped and with reviewed control logic, are presented below.

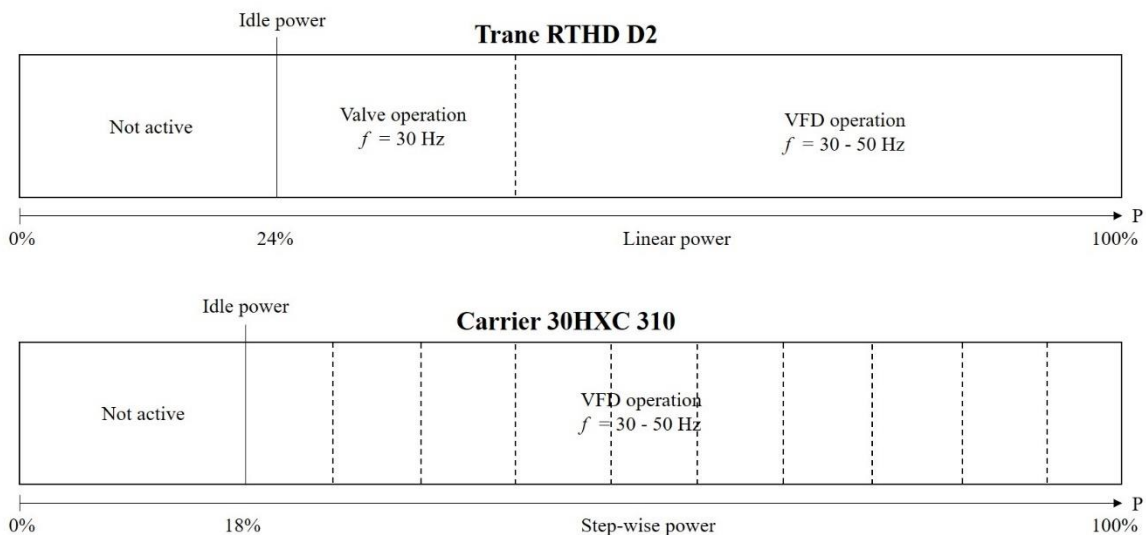


Figure 25: Operation scheme of chillers equipped with VFDs, with VFD from zero to full load operation.

Apart from considering the operation scheme during active operation, it is also important to consider how the starting and stopping sequences of both machines are configured. However, since both the starting and stopping sequences of the Carrier machines are unknown, these have been assumed to be the same as the Trane sequences. Some parameters have been adjusted accordingly to fit the characteristics of the Carrier chillers. As with the operation scheme, the starting sequence also varies depending on whether a VFD is equipped or not. With a VFD, the starting sequence takes between 30 s and 180 s. During this time the VFD will operate the compressor at 3000 rpm which corresponds to an output signal from the VFD of 50 Hz. While the compressor is running at 3000 rpm, without any external load and drawing a constant amount of power corresponding to 60 % of idle power, the chiller runs a check-up that takes 30 s to ensure that the machine has sufficient oil lubrication. If the check-up fails, it repeats the process up to a total and maximum of six times which in total would take 180 s. If it fails consecutively six times, the machine will simply turn off and send out an error. How many times the machine usually runs this sequence is largely affected by the surrounding temperature and the oil temperature. Thus, the chillers oftentimes take longer to start during the colder months of the years. When the starting sequence is complete, and the check-up says it is well lubricated, the chiller proceeds by running according to the normal operation scheme.

The stopping sequence takes in total 80 s and is divided into three separate steps. The first step takes 40 s and during this time the machine prepares to shut down by lowering the load. This is done by decreasing the VFD to 30 Hz and closing the sliding valve in case it is a Trane machine. After this step the machine is in its idle power level which corresponds to 24 % and 18 % of the rated power, according to the figure above. Then the machine initiates the next step where it turns off the power to the compressor which powers down from 30 Hz to 0 Hz which occurs almost instantly. After this it takes 20s before it initiates the next step of 20 s where no power is drawn. After all steps are completed, the chiller is turned off.

The chillers activate when the outdoor temperature is 17 °C or above and from then adjust their power after the cooling load. Furthermore, they also follow a predetermined schedule where they are either only turned off or allowed to turn on depending on the cooling load. These times are determined by the opening and closing hours of the shopping centre and are presented below.

	Weekdays	Weekends
Operating hours	07:00 – 20:00	07:00 – 18:00

Table 7: Operating hours for the chillers at Väla during which the chillers are active, given that the outdoor temperature is 17 °C or above.

3.3.2 Pumps

Except for the chillers, there are other components such as pumps and cooling towers that together constitute the cooling loads at Väla. These components are however, in comparison with the rated power of the chillers, rather small. Each chiller has two pumps each; one on the warm side and one on the cool side. These are rated at 12.6 kW each for the Trane models and 15 kW each for the Carrier models. In total the rated power of all the chiller pumps is 138.64 kW, making their combined capacity small, even in comparison with the power of only one chiller. Today the pumps supplying the Trane models are only run in on/off mode, meaning that they have low controllability since they only can supply a constant pressure. The pumps supplying the other models however, are both variable speed and variable pressure, thus offering higher controllability. It is however noteworthy that the on/off controlled pumps will be changed in the near future to variable speed pumps. All pumps are configured to supply the chillers with constant pressure. Consequently, a higher load on the chillers leads to an increased load on the pumps who have to maintain the same pressure despite the increased flow.

3.3.3 Cooling towers

The cooling towers, which operate to supply constant water temperature to the warm side of the chillers, only has one considerable electrical load. Since, they in simplification only consist of large fans and radiators, which are passive, the fans make up the main load of the cooling towers. In total there are five cooling towers with 12 fans each. Each fan is rated at 1.64 kW which all together make up 98.4 kW of rated power. Since all fans are equipped with VFDs they make up a load with high controllability. Despite having a small rated power, even in comparison with the pumps, they do offer a controllable load, which

in the same way as the pumps, can be regulated to follow the chiller load. Increased chiller load leads to higher supply water temperatures which in turn, has to be counteracted by the cooling towers, which speed up their fans, thus decreasing the supply water temperature.

3.4 Ventilation loads

A central part of the HVAC system is the ventilation. The ventilation is connected both to the heating and the cooling system, supplying the building with hot or cool air in order to regulate the indoor temperature and to maintain sufficient air quality. The main component of the ventilation system is the AHU. In total there are 35 AHUs at Väla which all are dimensioned after the need of the respective climate zone that they serve. Due to this they vary a lot in size, anywhere from a single kW of power up to the largest rated power of a single AHU of 67 kW. Further, each AHU consists of one supply air fan and one exhaust air fan which together make up the total load of the AHU. The rated power of the supply and exhaust air fan in an AHU is almost equal, with a slight bias towards the supply air fan, in order to ensure a positive pressure in the supplied climate zone. Most of the AHUs at Väla use a heat recovery system in order to increase the energy efficiency of the building. This heat recovery system does not however constitute a sizable electrical load and will thus not differentiate the AHU from other units without heat recovery. Consequently, the load of each AHU is only related to their rated power and their respective degree of utilization. This varies largely between AHUs in the building and will not be presented in this thesis due to extensive amounts of data. The rated power of each AHU is presented in

Appendix A – Air handling unit specifications together with their respective scheduled active hours. Their scheduled active hours are based on which climate zone they feed and what the need is for that zone. At times outside their respective scheduled hours, their load is zero since the AHUs are turned off.

The load of each AHU cannot be determined solely from the rated power and their active hours since their actual load is determined by the speed of the fan, as shown in (3). Thus, the speed of each supply and exhaust fan has to be known for each AHU in order to derive their total load. Since the speed of a fan is determined by the ventilation need of its respective climate zone and the fans rated power, due to the fact that it typically

determines its mass air flow, the rotational speed of the fan also has to be known in order to determine the total fan load, if not the load is explicitly known. Since the power is not explicitly known, the rotational speed is shown instead, for 14 supply air fans, for an arbitrarily chosen week during the year, in *Figure 26*.

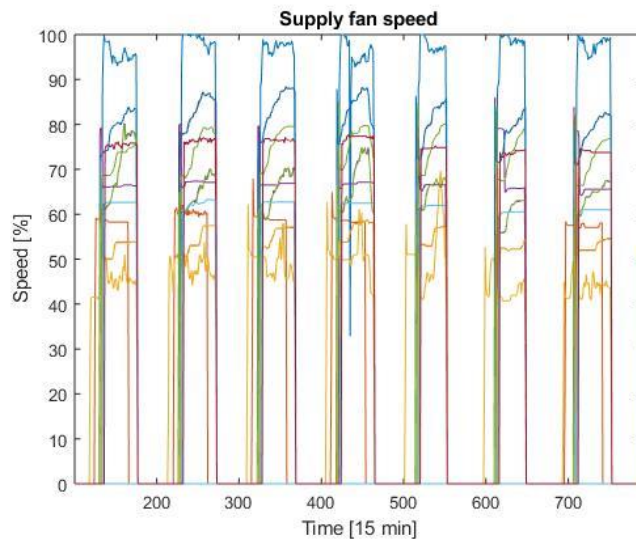


Figure 26: Rotational speed of arbitrarily chosen supply air fans.

The fans presented in the figure are chosen since they are the only fans with accessible speed data. They do however nonetheless present differences in their respective speed and active hours. For instance, it can be seen that the supply air fan of the AHU represented by the blue line mostly operates at a speed near its maximum value. Additionally, the AHU represented by the yellow line presents different operating hours where it consecutively activates earlier each day, perhaps in order to supply a tenant who starts its business earlier than others. It is also important to note that the speed presented in the figure above is not simply a measurement between standstill and full speed. Instead, it represents the relative speed between the minimum and maximum value, where minimum is rated at 20 Hz and the maximum speed is rated at 50 Hz. Consequently, a measurement of 0 % would correspond to a value of 20 Hz, 100 % to 50 Hz and 50 % to 35 Hz. Given the fan affinity law, the power of each AHU can then be derived from this data. Furthermore, the measurements of fan speed are currently not based on a feed-back signal but are instead based on the output signal from the VFDs connected to the fans. This means that the actual speed is unknown but considering that the difference between

the actual fan speed and the speed output from the respective VFD typically is small, this error is thus negligible.

3.5 Context of case study

In order to fulfill the scope of the thesis it is important to present what will constitute the VPP that will be modeled and why the implementation can be considered to be a VPP. Furthermore, due to the large number of possible implementations of VPPs it is also important to highlight how the implemented system in this thesis could differ from a fully implemented VPP.

Väla offers available energy resources in terms DR and PV. With the use of theoretical BESS, the resulting portfolio of assets would be heterogenous since it would consist of two or more types of assets. This fact is further strengthened when considering that the DRRs are of different types. Beyond having a mixed portfolio of assets, the DERs at Väla, despite being relatively constrained to a small area, are still being aggregated in a sense. When considering the HVAC system, not as a single unit but rather, a mix of varying loads, it is apparent that the system cannot be controlled as a single entity. Instead each AHU and chiller make up a DRR which in the presence of a BMS is being aggregated into a larger entity. In this sense, despite being constrained to a small area, the assets of the VPP would still be considered to be aggregated. Beyond this, the VPP will also dispatch the assets to perform FC. Consequently, since the VPP participates on FCR-N, a market which otherwise would not be available for the assets, it is obvious how the implemented system would satisfy the definition of a VPP, as presented earlier. The cooling towers and the chillers' pumps are not included in the portfolio sine their capacity is determined to be negligible whilst their control is not completely familiar.

Since the VPP only includes three types of assets which are aggregated over a confined area using existing ICT and is only participating on one market, the implementation of the VPP in this thesis could at least, be considered as small. Due to this, it is important to note that the implementation which will be proposed in this thesis, does not necessarily constitute the best possible implementation of the VPP. In practice, the VPP could be expanded to participate on more markets, include more DERs of varying types and aggregate more commercial buildings into a larger, more heterogenous portfolio. In order to highlight the difference between the VPP implemented in this thesis and a possible further expansion of the VPP, an illustration is presented in *Figure 27*.

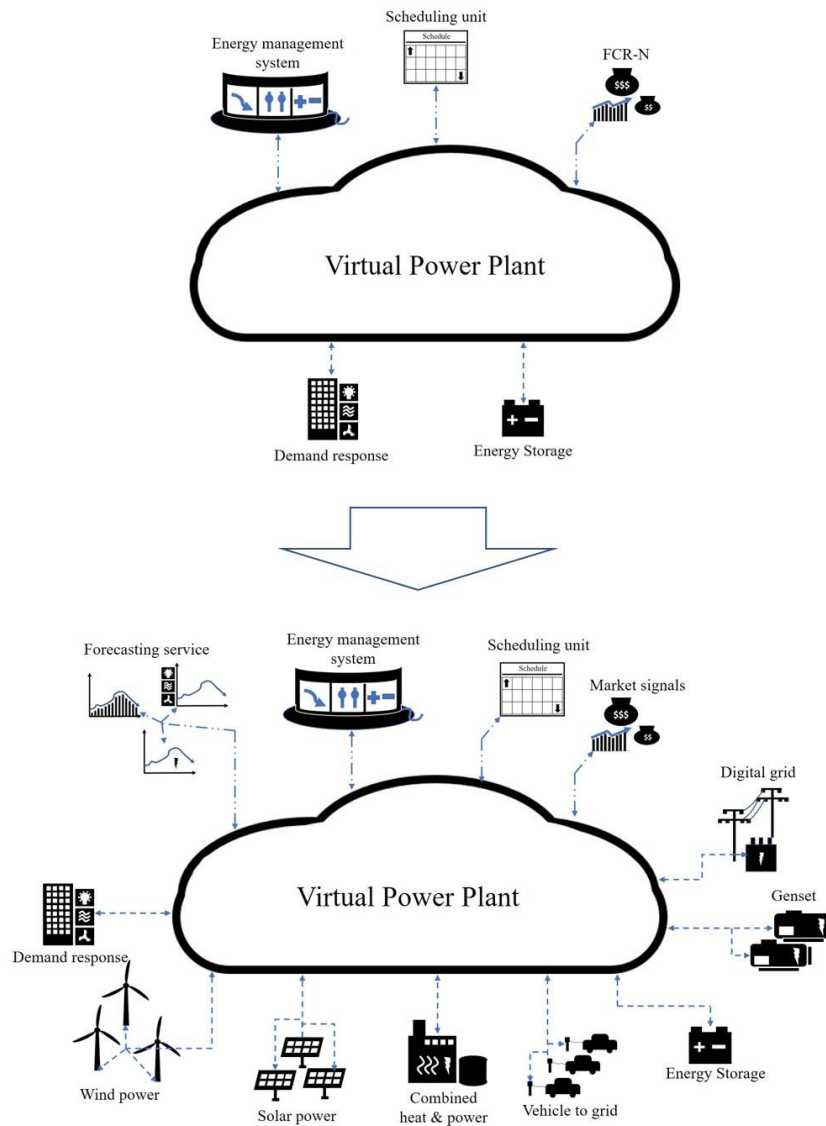


Figure 27: An illustration of the VPP implemented in this thesis and a possible future implementation.

In Figure 27 the upper VPP illustration is a representation of the model of Väla Centrum implemented in this thesis. The VPP only uses two assets which are the ESS and the HVAC system. These two assets are used together with a simple VPP EMS and scheduling unit to perform primary FC on FCR-N. However, to highlight the possibilities of the VPP, the lower illustration is also presented, giving a context to the simple implementation in this thesis. The VPP could include more assets such as wind power, PV, CHPs, V2G and more. With these potential assets the system could, together with forecasts, optimal dispatch of assets and an optimal implementation of the scheduling unit, perform more services and generate new revenue streams for the owner by performing load management, energy trading, secondary FC and more.

4. Method

In this chapter the method for the thesis will be presented in order to achieve an understanding for how the results were attained. The overlying processes of data collection, modeling and simulation will be presented in detail with references to the already presented theory. The workflow process in this thesis has a large influence on the results. Consequently, some conclusions are drawn in the method chapter but will also be presented further on.

4.1 Overview

In order to answer the question formulation in this thesis several methodologies were used. Initially, the workflow was based upon a literature survey in order to review the current state of studies to further define the scope and the delimitations of the thesis. The results from this literature survey outlined important components to include and significant factors to take into consideration when executing the following steps. The main methods used in this thesis are:

- Literature survey
- Data collection
- Modeling
- Simulations

Following the literature survey, extensive data collection was performed. The data that was collected was based on several sources. The primary source for data used in the thesis, is a Siemens-provided cloud-based platform called Navigator. This platform continuously collects, computes and logs data which is stored online. By accessing the data available on Navigator, collected from systems at Väla such as the BMS, this could then be formatted for future use in the following methodologies. Secondary data was sourced internally at Siemens from available data sheets of components at Väla and already compiled data from previous work and tests done on the site. These were also compared to and verified against external data supplied by original equipment manufacturers and suppliers of systems at Väla. Additional data was collected from external sources such as SvK who provided data on the power grid.

Following, and partly during the data collection, the data was incorporated into a detailed model of the small-scale VPP. The model was developed gradually component by component in the software Simulink, developed by MathWorks. Simulink is a tool for modelling, simulation and analysis of dynamic systems and was used extensively during the thesis. Parts of the modelling work were also performed in MATLAB, which instead of using a graphical interface as Simulink, is completely code-based. Since MATLAB and Simulink offer interconnectivity it allowed for more effective workflow where modelling best suited a in code-based interface was done in MATLAB, and the modelling best suited in a graphical interface was performed in Simulink.

The model was then used in simulations of the small scale VPP in order to analyze and improve the model. The results of the simulations were compared to the expected values in order to debug and to improve the performance of the model. In many cases the model proved to be too demanding to run on the system, thus requiring large amount of work to improve model efficiency. When the model ran as expected and was not too demanding for the system, the final results were generated and analyzed. In order to attain some of the results, some of the model parameters had to be adjusted gradually by running the simulation several times in an explorative way in order to derive suitable parameter settings. An illustration of the simplified model overview is presented in *Figure 28*. The model contains all components which will be covered in greater detail in *4.3 Modeling*. The entire model will not be presented since it is considered to be too extensive. The core of the model, which offers the most important functionality, will be presented however.

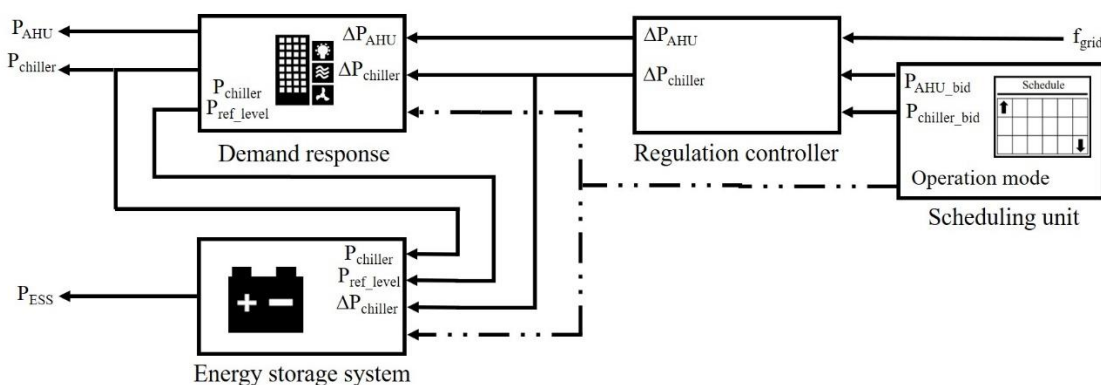


Figure 28: An illustration of a simplified model overview.

The inputs of the system are the power grid frequency signal (f_{grid}) and the simulation time with a resolution of 1 s, which is excluded from the illustration. The outputs are the powers of all DRRs and the ESS. Some signals have been logged for the sake of the results but are not a part of the overall function of the model and have thus also been excluded.

4.2 Data collection

The data used in the model was sourced both from internally available sources, but also from external sources such as SvK. Much of the data did not directly correspond to the required value and thus had to be calculated or extrapolated from other available values. The method used for each data set incorporated into the model is presented further.

4.2.1 AHU load data

The load data for the AHUs at Väla is not explicitly available as a power measurement since there has not been logging performed of the active power of each AHU. The only active power measured is the total load of Väla which consists of all other end uses of electricity, as shown in *Figure 24*. Since the distribution of energy consumption is only known for the entirety of a year and not specifically for any given time-point, it is not possible to derive the load of any given AHU or the entirety of all AHUs at any given time.

Since the simulation was to be run over a longer time-period, it was also important that a long enough dataset was available. This implies that establishing a measurement of the AHUs would not be possible since it would allocate a too large part of the thesis timeframe. Additionally, the measurement of active power of the AHUs would require changes to either existing software or hardware in order to start logging power values. Due to constraints in time and budget for the thesis, this proved to be impossible, especially considering the number of AHUs of which had to be measured.

The parameters available, that were already being logged in Navigator and that could be used to derive AHU load, were the output fan speed signals from the VFDs to the supply and exhaust fans of most AHUs. Using the fan speed and the rated power of a fan it would

be possible, with the use of the fan affinity laws in (3), to derive the load of the fan, and thus the load of the AHU for the time-point for which the output fan speed signal was available. The simulations were to be run for an entire year, where 2018 seemed to be most suitable due to large data availability in comparison with other years. Due to this, the output fan speed signal had to be available and of sufficient quality for the entire year of 2018. Given that as many AHUs load data should be included as possible in order to capture the load characteristics as correctly as possible, this would result in a total of two datasets for each AHU, resulting in a total of 70 datasets describing the fan speed of the AHUs at Väla.

Since it turned that some of the fan signals were not being logged, the entire dataset encompassing all AHUs was not available. Consequently, it had to be restricted to only include the AHUs that were being logged. Furthermore, since the dataset was so large and due to restrictions in Navigator, downloading the data had to be done split in multiple smaller batches which then were compiled after downloading the data. However, when downloading the data in batches, it was shown that due to further limitations in Navigator, that only batches containing 14 fan datasets could be downloaded. The other 21 datasets missing from the batches had to be downloaded individually in order to attain the output fan speed signal for all AHUs. However, since this would have proven to be too immense of a task, it was decided that the AHU load data instead was to be extrapolated from the available dataset from the 14 AHUs in the batch-download. The output fan speed signal of from the batch-download corresponds to the AHUs with their respective rated fan power, presented in *Table 8*.

AHU	FTX-12	FTX-14	FTX-25	FTX-32	FTX-34	FTX-36	FTX-37
Supply fan Rated power	15 kW	2.82 kW	1.85 kW	18 kW	18 kW	18 kW	18 kW
Exhaust fan rated power	11 kW	2.82 kW	1.85 kW	15 kW	15 kW	15 kW	15 kW
AHU	FTX-38	FTX-39	FTX-40	FTX-41	FTX-42	FTX-43	FTX-44
Supply fan rated power	18 kW	30 kW	30 kW	30 kW	30 kW	1.1 kW	0.75 kW
Exhaust fan Rated power	15 kW	22 kW	22 kW	22 kW	22 kW	1.1 kW	0.75 kW

Table 8: AHUs of which data was included in the batch-download with their respective rated power P_{rated} .

The delta fan speed signal (Δf) is a measurement of the VFD output speed measured in percent. 0 % corresponds to the lowest configured speed of 20 Hz and 100 % corresponds to the highest configured speed of 50 Hz. Thus, the output fan speed signal (f_{out}) can be expressed as (7). Given that the fans approximately reach their rated power when (f_{out}) is equal to 50 Hz, the fan power can be expressed as (8), where (P_{rated}) is the rated power of the fan.

$$f_{out} = 20 + 30\Delta f \quad (7)$$

$$P_{fan} = P_{rated} \left(\frac{20 + 30\Delta f}{50} \right)^3 \quad (8)$$

(8) was used in order to derive the fan power for both supply and exhaust air fans for the AHUs in *Table 8* for the entire year of 2018. Since the results from this only represent the load of the given fans, the load had to be extrapolated to fit the total rated power of AHUs at Väla. In order to avoid the exhausting work of downloading the output fan speed signal for all missing AHUs, it was assumed that the average load in relation to the rated power of the 14 AHUs was the same for the missing AHUs. Thus, by normalizing the load of the 14 AHUs with their rated power and multiplying with the rated power of all the AHUs, the total load of all AHUs was achieved, given some necessary assumptions. The total AHU load for 2018 is shown in *Figure 29* with a resolution of 15 minutes, only restricted by the available resolution in Navigator.

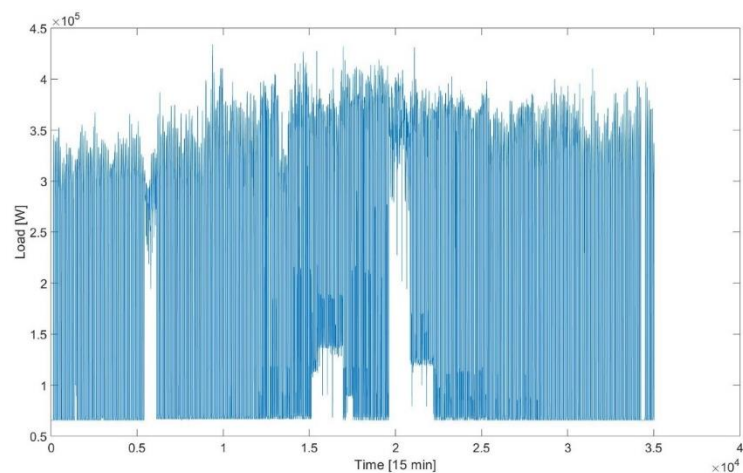


Figure 29: Total load of all AHUs at Väla. The data starts Jan 1st 00:00 and ends Dec 31st 23:59.

It is presented with a resolution of 15 min where the maximum value is about 0.45 MW.

4.2.2 Chiller load data

As a difference from the AHU load data, the chiller data was explicitly available as electricity consumption, measured in MWh in Navigator. The measurements are collected from two transformers connected to VKA01-VKA02 and VKA03-VKA05, as presented in *Table 5*, respectively. When downloading the load data, the datasets from each transformer had to be added together in order to achieve the total electricity consumption of the chillers. In order to attain the power of the chillers, it had to be calculated from the electricity consumption of the chillers. Since the electricity consumption was measured every 15 min the resulting power was converted to MWh/h simply by multiplying each value by four. Consequently, a dataset representing the chiller load data for entire 2018 was achieved. However, it is important to note that since the measurements were measured in MWh and not in kWh, the actual measurements might have been taken every 15 min, but the actual resolution remains poor. When studying the resolution in detail the data seems quantified since the measurements only are available in a resolution of 0.25 MWh. However, since the load of the chillers is known to be inert since it follows the outdoor temperature, the resolution can still be acceptable. This statement is further strengthened when considering how the data is applied in the model, which will be presented later. The chiller load data is presented in *Figure 30*.

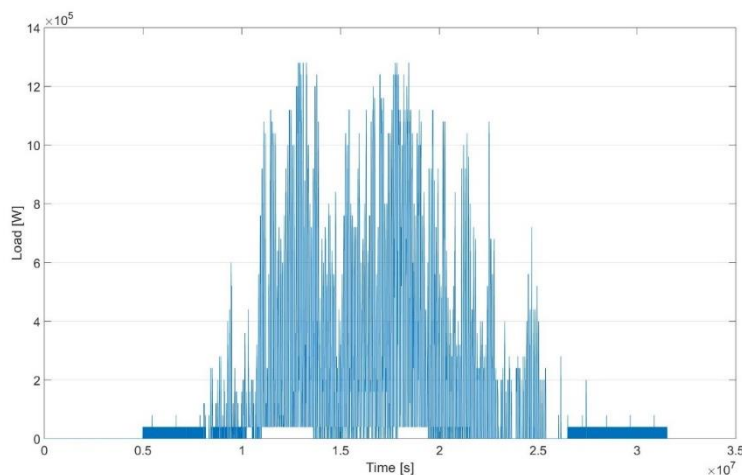


Figure 30: Total chiller load during 2018. The data starts at Jan 1st 00:00 and ends Dec 31st 23. 59. It is presented with a resolution of 15 min where the maximum value is about 1.3 MW.

4.2.3 Power grid frequency data

The power grid data had to be available explicitly in a sufficient resolution. This data is the dataset with the highest requirements considering its application and relevance in FC applications and in the model. Since Sweden, Norway and Finland all are connected to the same synchronous area, the frequency in the grid shall be the same. Due to this, the possible sources of power grid frequency are extended from only Swedish sources to also include Norwegian and Finnish sources. The Swedish TSO SvK who is responsible for the overall power balance of the Swedish power grid, was contacted but did not have the power grid frequency data of sufficient resolution. Instead they referred to the Finnish TSO FinGrid who stored frequency data of the resolution 0.1 s for several years back. This data was available for download month-wise in .csv format. Despite proving to be a very large data set of approximately 8 GB in total, the data was downloaded. In order to improve the usability of the data a down-sampling algorithm was developed in order to reduce the resolution to a more suitable value of 1 s, thus reducing the dataset by a factor of 10. However, this proved to be difficult due to the large amount of computer memory required. It was further worsened by the fact that the dataset was missing several measurement points thus requiring interpolation in order to fill the blanks. Consequently, the dataset remains in a high resolution of 0.1 s. In *Figure 31* and *Figure 32* the frequency data is presented for an arbitrarily chosen week and an arbitrarily chosen 4 minutes in order to visualize a segment of the dataset.

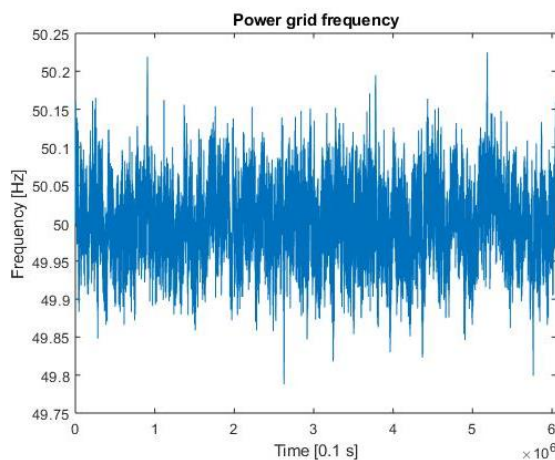


Figure 31: Power grid frequency for arbitrarily chosen week during June 2018 measured in 0.1 s resolution.

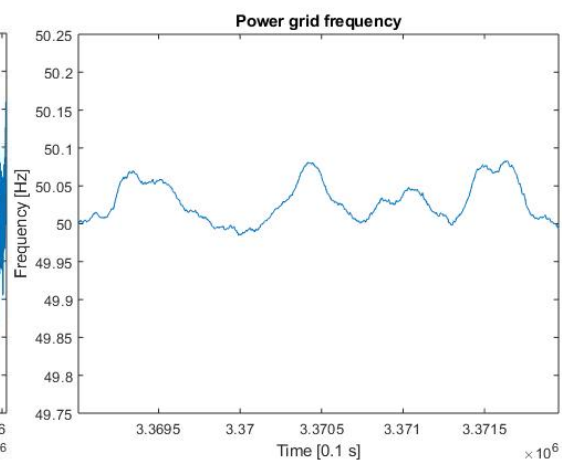


Figure 32: Power grid frequency for an arbitrarily chosen 4 minutes during June 2018 measured in 0.1 s resolution.

4.2.4 System parameters

The last, and perhaps the most extensive part of the data collection process is the process of gathering system parameters for energy resources such as the chillers, AHUs, pumps and more. The entire process has been based on an iterative process where relevant sources and people have been interviewed in order to attain the information needed.

Initially the process started by interviewing relevant people internally at Siemens in order to achieve a comprehensive understanding of the systems at Väla and what sources that are available. It became known that there was previous work performed on Väla where the rated power of the supply and exhaust fans for the AHUs had been collected and compiled. This was done by previous master thesis students who sourced the data from the HVAC systems supplier at Väla. However, there was no information on the specific system characteristics of the fans since no system identification had been performed on the AHUs. Beyond having compiled the rated power of the AHUs, the rated power of the chillers had also been compiled. This information was sourced directly from the HVAC systems supplier at Väla who also supplied concise information on the control logic of the chillers. Again, no system identification had been performed on the chillers. The supplier did however provide with detailed charts of the HVAC system and its components, giving a detailed understanding of electrical loads at Väla.

In order to analyze more electrical loads at Väla than just the HVAC system, deductive questioning was performed internally at Siemens. Loads which were expected to exist at Väla, based on typical load in other commercial buildings, were researched. However, due to the specific contracts and the way that energy end-uses are accounted for at Väla, it became obvious that many loads would not offer any DR capabilities simply because they had little to no acceptability due to their tightly regulated use. Thus, the loads to be analyzed further were constrained to the already known HVAC loads. The only other data that was sourced from already existing sources were the energy reports for 2018, supplied by the same HVAC supplier as earlier.

The remaining data acquisition was from external sources. Since the knowledge of chillers' DR characteristics had proven to be quite limited from the initial literature survey, it was obvious that more data collection had to be done on this subject. By contacting the manufacturers of the chillers at Väla they supplied further insight on the limitations of the proprietary internal control logic of the chillers. This was in line with what is stated in literature. What literature did not present in detail however, was the possibilities of improving the characteristics of chillers. Here the suppliers provided information on possible improvements that could be done on the controllability of the chillers. Measures such as installing VFDs and reviewing the control logic were apparent. Though, they could not supply system characteristics based on system identification tests or simulations since they had not been performed with the mentioned measures, possibly since the application of FC with chillers still is new. However, they did give a qualified estimation of the system characteristics. The estimations from the two chiller manufacturers were compared to each other, compared to a test performed in literature and compared to an estimation from an independent chiller manufacturer, simply to verify the reliability of the estimation. Beyond this, one manufacturer supplied data describing the control logic of its chillers, after the measures to improve controllability has been performed. Since this information was not available for the other chiller model, it was simply assumed to be the same.

Other data collection procedures of system parameters were performed during the thesis work but are less impactful than the ones presented above. Therefore, these will be presented throughout the method chapter. Furthermore, many systems parameters have been defined through reasoning based on factors such as their impact on model performance, estimations of suitable system parameters or are based on simulation results as an outcome of deductive reasoning.

4.3 Modeling

4.3.1 Model overview

The model has been implemented to give an understanding of the active power flows that are related to the operation of the VPP when performing FC. Reactive power flows have been neglected since they are not considered to be a resource of interest on FC markets. Additionally, they do not constitute a limitation in the context of power subscription levels, based on interviews with internal sources at Siemens. Beyond reactive power, internal losses in electric circuits have also been neglected since no information of the internal cable routing at Väla has been accessible.

The model is built on the basis of a few components which represent the energy assets that are included into the VPP portfolio. In this case, the assets are DRRs consisting of existing chillers and AHUs and a theoretical energy storage consisting of a lithium-ion battery. Initially, the aim was to include a third asset into the portfolio consisting of the existing roof-mounted PV-array. However, since the inclusion of PV arrays typically requires complex forecasting models and since PV in general is problematic to schedule since it is very stochastic, the inclusion of PV would only hinder the VPP operation when performing FC. Furthermore, according to the rules for delivering balancing services, set by SvK, submetering is allowed. This enables the possibility of simply defining the system boundaries for the balancing resource in such a way that the PV-array is defined as being outside the scope of the balancing resource. Consequently, it is possible to define the balancing resource to only include the DRRs and the ESS, simplifying the operation of FC. Therefore, the assets included in the model are only the DRRs and the ESS. These models are implemented in Simulink and will be covered individually in greater detail.

Except for including models for the energy assets in the VPP portfolio, the model also includes the necessary models of control systems. These include the regulation controller and the scheduling unit. The regulation controller is responsible for the control of DR assets when performing FC. The entire controller is implemented in Simulink and is activated whenever the scheduling unit has scheduled FC. During any other time, the regulation controller remains passive. As a difference from the regulation controller, the scheduling unit is not only implemented in Simulink, but also in MATLAB. When testing

the model initially, it proved to be very demanding for the computer to run. In order to make the model more effective, the scheduling unit was split into two parts. One part, responsible for the actual scheduling, is run before the simulation starts in Simulink and schedules all operations for the entire simulation time. The second part of the scheduling unit remains in the Simulink model and is run during the simulation. It reads the schedule and sends operating commands to the other components, depending on what the first part of the scheduling unit has scheduled. Splitting the scheduling unit this way resulted in significantly faster simulations without affecting the results.

All other components in the model are only constructed in order to support the simulation and to generate results. These include MATLAB components that load parameters and data into the Simulink model, Simulink blocks that measure and calculate relevant parameters for the results, a Simulink component that runs the SvK balancing resource prequalifying test and lastly, a Simulink component that calculates reference values used in the analysis of the results. In order to achieve a better understanding of how the model is constructed, it will be presented more thoroughly on a component-by-component basis. The components that will be presented are the demands response resources, the ESS, the regulation controller, the scheduling unit and the model for the prequalifying test.

4.3.2 Demand response model

The model of the DRRs consists of two individual models; one for the chillers and one for the AHUs. The basic models of the assets are very much alike with the main difference being their control systems. In *Figure 33* the model for the DRRs is presented where it is clear the model is divided into two parts. Both the AHUs and the chillers have the same types of inputs and outputs. The historical data input is based on their respective loads, presented earlier in *Figure 29* and *Figure 30* respectively, and is linearly interpolated in the historical data blocks. The second input ΔP , is the balancing power input given from the regulation controller as shown in *Figure 6*. The last signal is sent from the scheduling unit and determines the operation mode of the DRRs which can either be normal operation or FC.

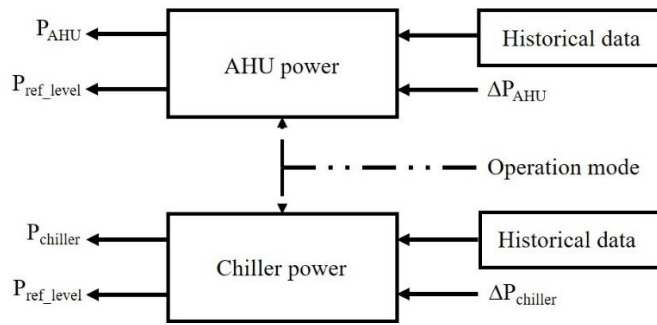


Figure 33: The Simulink model for the DRRs consisting of chillers and AHUs.

The output signals from top to bottom are the actual loads of the AHUs and the chillers which are sent as an output from the simulation. Second is the power reference level, as presented earlier in Figure 6. In Figure 34 an illustration of the AHU power block is presented. The chiller’s block is built on the same logic and will thus not be presented. The power reference level output signal is generated from a sample-and-hold block that samples the historical load at the beginning of every hour when FC is scheduled and then holds it until FC ends. If FC is scheduled for two or more consecutive hours, the block sampling control to the right, forces the sample-and-hold circuit to resample the load each hour. The signal from the sample-and-hold circuit is either passed to the output of the or passed into a prequalifying power throughput. This block allows the signal to pass through if a prequalifying test is not performed, or it blocks the signal and instead outputs a value determined by the prequalification controller.

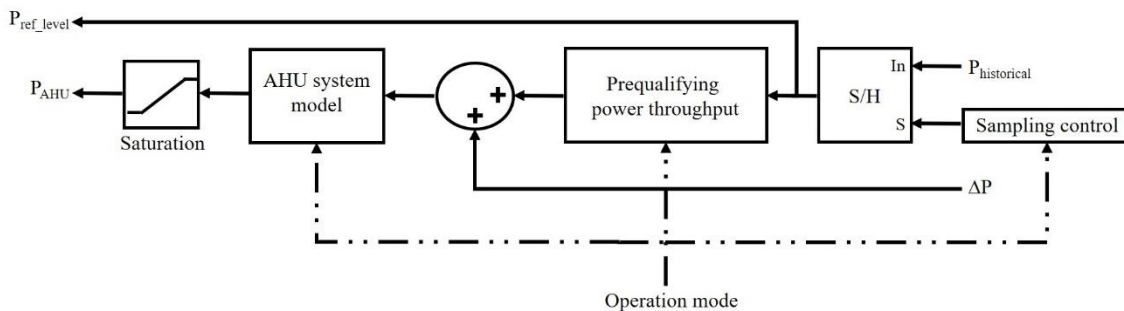


Figure 34: The Simulink model for the AHU. This model is common for the AHU and the chiller.

The signal from the prequalifying power throughput is sent into a sum-block where the balancing power signal from the regulation controller is added to the power reference level signal. The resulting signal is the actual power signal sent to the system model of the AHUs or the chillers, as presented earlier in *Figure 6*, where red represents the signal from the sample-and-hold circuit and blue represents the signal from the regulation controller. The resulting power signal, determined by each assets system characteristics, is passed on if the operation mode signals that FC is being performed. Otherwise, the historical load data is passed straight through. Lastly, the output signal is passed into a saturation-block that limits the signal amplitude to the rated power of the asset. The only blocks at this stage, that differentiate the AHU model in *Figure 34* and the chiller model, are system models. These models vary substantially both in complexity and in how they have been implemented. Consequently, each system model will be covered in much greater detail.

4.3.3 AHU system model

Starting with the simpler of the two models is the system model of the AHU. The model for this is presented in *Figure 35* where the system model is constructed by five blocks. The input regulation signal is passed into an experimentally identified transfer function. The output from the transfer function is then passed into a transport delay and then into a static gain, before being sent to the output signal. Together these blocks correspond to the total transfer function in (9).

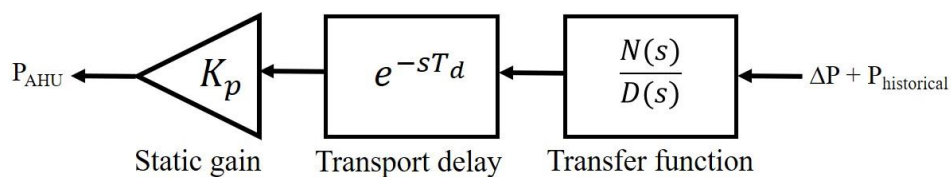


Figure 35: AHU system model in Simulink.

$$H(s) = K_p \frac{N(s)}{D(s)} e^{-sT_d} \quad (9)$$

In order to determine the parameters for the transfer function, a system identification approach was used. The system to be identified is supposed to represent the 35 AHUs at Väla. However, identifying the system characteristics for that many AHUs is a very complex task due to several reasons. Firstly, the number of AHUs that the system identification process has to be performed on, are so many that it simply would take too long time. Secondly, in order to perform system identification on an AHU, physical access to its VFD is required. Since some AHUs are hard to reach and require certain types of access rights at Väla, this work is impossible without planning the process long in beforehand. Thirdly, some AHUs are interconnected via air ducts with other AHUs. This means that when performing system identification tests on one AHU, this could be affected by the other AHUs that are connected to the same air ducts. Lastly, not all AHUs and their relevant operation parameters are known. In many cases, the AHU has been arbitrarily configured in such a way that the AHU will be limited in operation. This will hinder the possibility of performing system identification tests which result in an accurate system model.

Due to these hinders, the system model had to be based on tests of a single AHU which proved to provide the prerequisites for performing system identification. The AHU was physically accessible, a service technician from Siemens had the access rights to the AHU, the AHU was not interconnected with any other AHUs and lastly, it was configured in such a way that it allowed for tests to be performed. The consequence of only using one AHU as a basis for the model of the whole system of AHUs is important to take into consideration when verifying the results of the system identification process and will be discussed further.

AHU system identification

The system identification process is built upon the use of a step response test of the AHU. The AHU used in the tests is the largest AHU at Väla denoted as TA 28 with a total of 67 kW of rated power. The test was performed on only the supply fan which has a total rated power of 37 kW. This was done since there was no way to manually perform the test on both the supply and the exhaust fan simultaneously. The test was performed by feeding the VFD with a signal corresponding to the lowest set-point of the VFD output signal of 20 Hz. By instantaneously changing the signal to the highest set-point, corresponding to

a VFD output signal of 50 Hz, i.e. creating a step, and measuring the active power draw change of the supply fan, the step response was measured. In order to ensure that the step response measurement could be used for system identification, the signal was initially held at 20 Hz for 10 s and afterwards at 50 Hz for 40 s. In practice, the signal should have initially been held at 20 Hz for 40 s in order to ease the identification process. However, due to problems while measuring the active power to the supply fan, this time had to be restricted to only 10 s. The resulting measured step response is presented in *Figure 36* where the black curve is the measured step response and the blue curve is the step response of the identified system.

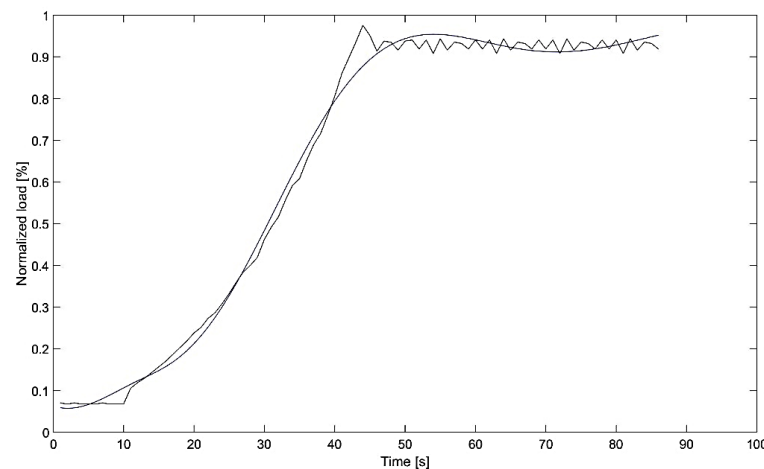


Figure 36: The measured step response of TA 28 and the step response of the identified system, measured in normalized power.

After performing the step response test, the data was compiled and normalized. The power was normalized using the rated power of the supply air fan as a basis and the input signal was already normalized since it is a measurement in percent. Then by inputting the input and output signal of the system, i.e. the normalized power and the normalized input signal, into the system identification tool in MATLAB, the system could be identified. It was done in the tool by inputting the estimated number of zeros and poles of the transfer function and then letting the tool estimate the transfer function based on the parameters defined. This was done iteratively, where the order of the nominator either is one less than the order of the denominator or smaller. By increasing the order of the denominator in steps, and for each step increasing the order of the nominator until a transfer function of sufficient accuracy has been reached, the transfer function for the system model was attained. The transfer function is a third-order system with four poles and zero zeros and is presented in (10). The step response of the system is presented in *Figure 36*.

$$\frac{N(s)}{D(s)} = \frac{8.5148 \cdot 10^{-4}}{s^3 + 0.1226s^2 + 0.02s + 0.0009} \quad (10)$$

When analyzing the characteristics of the step response, it was measured that the system time-constant, i.e. the time it takes to reach 63 % of the step, is approximately 33 s. The time delay of the system cannot be identified using the system identification tool but can be identified by measuring the time it takes for the system output signal to respond to a change to the input signal. By doing this measurement on the step response test data, the time delay (T_d) was estimated to 2 s. The last system parameter to identify in (9) is the static gain. This is adjusted to fit the overall model. Since the input signal of the model is a measurement of power and the output signal of the system is the actual power of the system, it is important that the static gain ensures this relation. When studying the low-frequency gain of the transfer function, i.e. $H(0)$, it is apparent that this is not one as shown in (11), thus meaning that the desired relationship between input and output is not attained. However, by compensating for this error or by adjusting the static gain as in (12), the ultimate system gain can be maintained as 1. Considering the results of the system identification process, the resulting system model is as presented in (13).

$$H(0) = \frac{8.5148 \cdot 10^{-4}}{9 \cdot 10^{-4}} \approx 0.9461 \quad (11)$$

$$K_p = \frac{1}{H(0)} \approx 1.0567 \quad (12)$$

$$H(s) \approx 1.0567 \frac{8.5148 \cdot 10^{-4}}{s^3 + 0.1226s^2 + 0.02s + 0.0009} e^{-2s} \quad (13)$$

By studying the characteristics of the AHU system model, we can achieve further understanding of how the AHU will perform as a DRR on FC markets. One important characteristic to study is the system model's frequency response, i.e. how it reacts to different frequency components in its input signal. The frequency response for the AHU system model is presented in *Figure 37*.

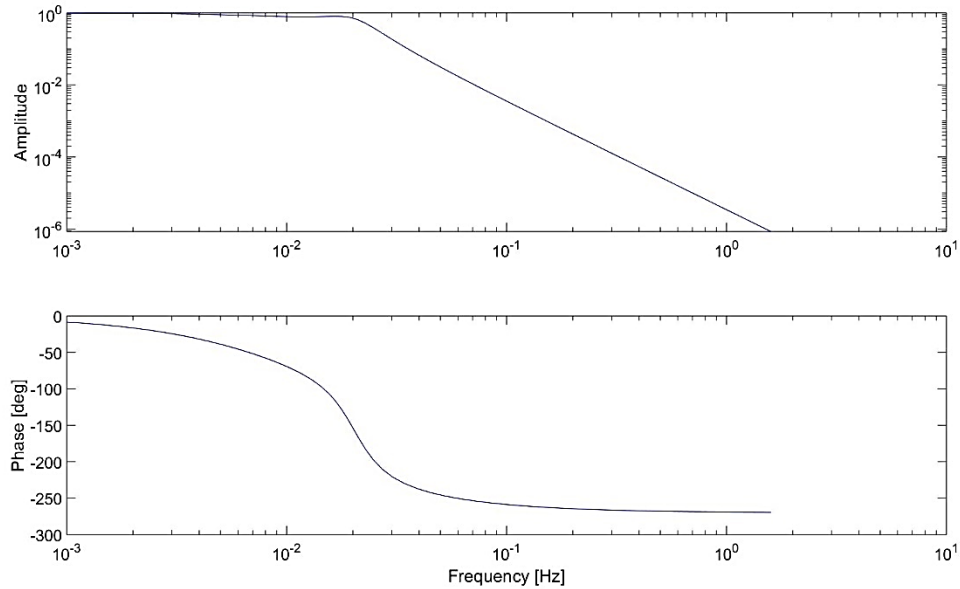


Figure 37: Frequency response of the AHU system model.

It is seen, by studying the universal gain of the system, that the gain remains approximately constant one for frequencies lower than 0.02 Hz. This translates into a linear relationship between input and output for any frequency component in the input signal that changes less often than every 50 s. Any other frequency components higher than 0.02 Hz will be dampened by a decreasing gain. Naturally, the AHU will have low-pass characteristics, filtering the frequency components of the input signal. Furthermore, by studying the phase-shift in relation to the frequency of the input signal, further conclusions can be drawn. The phase delay of a system is defined as in (14).

$$\tau_{\phi} = -\frac{\phi(\omega)}{\omega} \quad (14)$$

Taking the phase delay into consideration whilst studying the phase-shift relative to the input frequency it is apparent that the system also is time-variant, meaning that the delay of the system varies depending on the input frequency. Consequently, some frequency components will be delayed more than others. The effects of this will be discussed further on when considering the combined delay of all systems. However, the equation will not be used as for calculations in this thesis. Rather it will be the basis for greater understanding of the system delay.

4.3.4 Chiller system model

The chiller system model, the more complex model of the two, is mostly based on the internal control logic of the chillers. The control logic that is implemented in the model is not the proprietary integrated control logic of the chillers as it is today, but rather the control logic that is reviewed to accommodate the use of a VFD and to enable the use of DR. Normally when the chillers do not operate as DRRs but instead run in normal operation, they activate sequentially in order to respond to the current cooling need. However, since the chillers with their reviewed control logic, still have a starting sequence that takes up to 180 s, a sequential starting sequence will amplify the impact of the starting sequence. If the machines for instance were to respond to a step in the input signal from zero load to rated power, the sequential activation of the machines would imply that the step would take up to five times the time of a single starting sequence. This would occur simply due to the fact that the machines only would activate once the previous machine is running at full power, which only can occur after the starting sequence has finished. This activation scheme would prove to be too slow in comparison to the demands set by SvK for their primary regulation market FCR-N.

A simplified illustration of the chiller system model, as shown in *Figure 34*, is presented in *Figure 38*. The figure only represents the model for one chiller and in reality, the chiller system model contains five separate models each corresponding to one chiller each. Furthermore, since much of the control logic is separated between multiple MATLAB and Simulink blocks, this logic has also been simplified in the figure below. This logic corresponds to the Start/stop sequence control block.

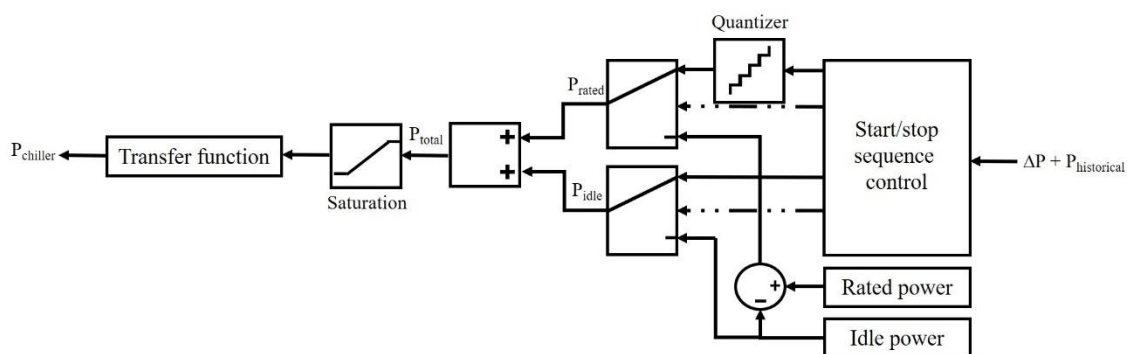


Figure 38: A simplified illustration of one chiller system model.

The chiller system model is split into two parts where one part outputs the idle power of the chiller and the other outputs the power above idle. These are modeled as switches which either pass through the corresponding power value or pass through a power determined by the start/stop sequence control block. This is done whenever the chiller is going through a starting or stopping sequence, or when it is regulating the activation power of another activating chiller. This control logic will not be illustrated but will be presented further on. The quantizer block in *Figure 38* is used to model step-wise power which is used in the chillers VKA03 – VKA05, as presented in *Table 5*. Due to this, the figure corresponds to one of those chillers and in the models for VKA01 – VKA02, as presented in *Table 5*, the quantizer block is removed. The idle power output and the remaining power output from the switches are added together and passed through a saturation block which limits the signal amplitude to the rated power of the machine. The resulting signal is then sent as an input into the chiller transfer function.

Since the chillers today are outfitted with the proprietary integrated control logic, they do not represent the characteristics needed in order to perform adequately as DRRs. Due to this, the system identification process proposed for the AHU cannot be performed on the chillers in order to implement their transfer function accurately. The workaround to this is simply to model the chillers using first-order transfer functions. Defining the static gain of the transfer function, and thus the nominator coefficients is simple. With the same reasoning as for the AHUs, the universal gain should be one, which is why the nominator coefficient and the static gain is defined as one. When defining the denominator, the coefficients have to take the system time-constant into consideration. This is done by setting the first denominator coefficient to the time-constant of the chiller. The second coefficient is set to one in order to maintain the correct universal gain.

Determining the true time-constant of the system is problematic since it cannot be based on experimental results, due to the current control logic. Instead it is based on extrapolated data from literature, where that a step response test was performed, and other sources consisting of chiller original equipment manufacturers that approximated the time-constant to 40 s or less. The assumed chiller time constant of 40 s is slightly higher than the fans' time constant. The time delay for the chillers was assumed to be the same as for the AHUs and was thus defined as 2 s. The resulting system model of each chiller is as presented in (15).

$$H(s) = \frac{1}{40s + 1} e^{-2s} \quad (15)$$

Since there was no system identification process performed on the chillers, only the approximated step response of the system can be achieved. The step response is presented in *Figure 39*. Since the Simulink model for the step response is the same as *Figure 35*, it will not be presented. As shown below, the step response of the system is as what is expected from a first-order system.

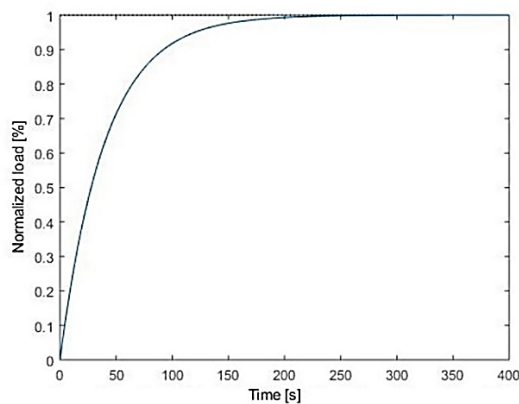


Figure 39: Approximated step response of chiller system model.

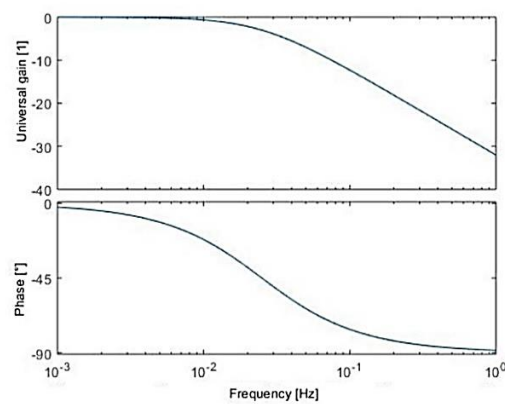


Figure 40: Approximated frequency response of chiller system model.

Further analyzing the frequency step response of the chiller system model which is presented in *Figure 40*, more conclusions can be drawn of its characteristics. It is seen that the chiller, in same way as the AHU, naturally has low-pass characteristics. This is since frequency components of the input signal lower than about 0.01 Hz are passed through with the universal gain of one, whereas any frequencies higher than 0.01 Hz, are gradually dampened more and more for increasing frequencies. Furthermore, the chiller also experiences a phase-shift for higher frequencies, indicating that in the same way as for the AHU, some frequency components will be delayed more than others. However, what is also noticeable is that the chiller has a smaller maximum phase-shift, which is simply due to the fact that the chiller is modeled as a first order system whereas the AHU is modeled as a third order. Consequently, the chillers have a maximum phase shift of -90° and the AHUs have a maximum phase shift of -270° , three times as large. The delay caused by the phase shift will be discussed further later.

Chiller activation scheme

In order to improve the activation times of the chillers, this activation scheme would have to be changed, at least when operating in DR mode. By instead of activating sequentially, the chillers could activate in parallel resulting in a maximum activation time of 180 s, or perhaps even less depending on how long the activation sequence takes. When activating in parallel, the number of required machines required in order to achieve the requested load is calculated. Then the correct number of machines activate or deactivate in order to respond to the required load change.

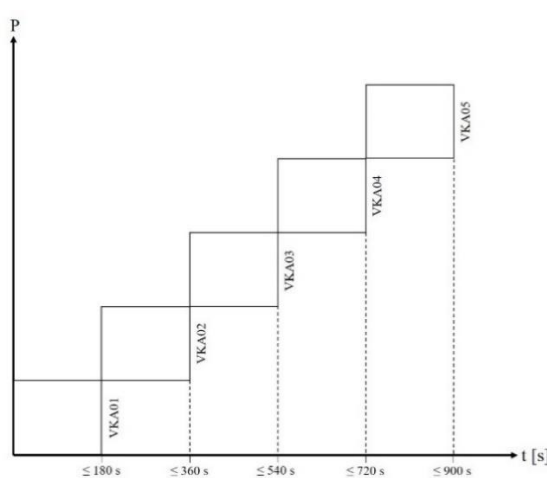


Figure 41: Sequential starting sequence of chillers.

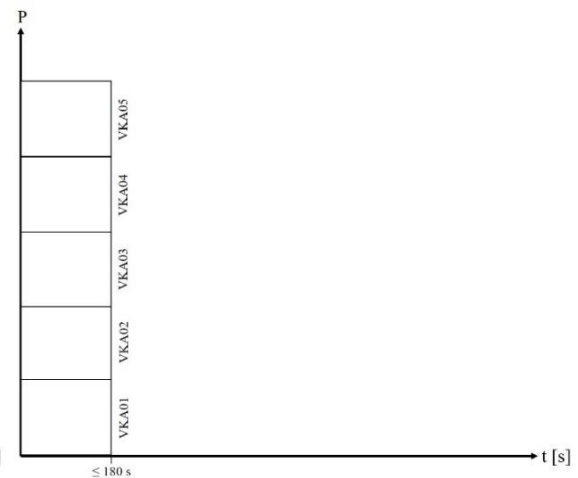


Figure 42: Parallel starting sequence of chillers

In *Figure 41* and *Figure 42* the difference between the two activation sequences is noticeable. It is important to note that both the power and the time in the figures above only include the starting sequences of each machine and does not include the linear or stepwise operation of the chillers after the starting sequence has finished. If it had been included in the figures, the power would be greater, and the activation times for the sequentially activated chillers would be even greater since the time to ramp up compressor speeds would be included as well. With this comparison, it obvious that parallel activation is the obvious choice.

Chiller operation scheme

When considering the operation of chillers once they are already active, they again can be configured as running in either sequential or in parallel. As presented in *Figure 25*, once active, the chiller load can be controlled from the idle power level up to the rated power of the chiller. However, if a power level lower than the idle power of a chiller is requested, the chiller either has to remain at idle power or has to turn off. This causes non-linearities in the control of chillers and has to be taken into consideration when choosing whether to run then in a sequential or parallel manner.



Figure 43: Sequential power of active chillers.

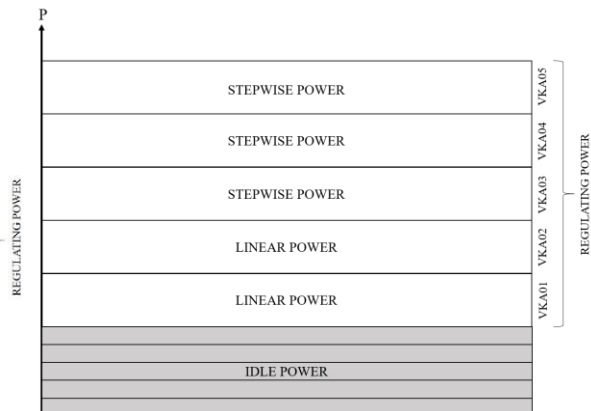


Figure 44: Parallel power of active chillers.

As presented in *Figure 43* and *Figure 44*, the sequential and parallel control of the chillers differs considerably. In parallel, the minimum power level is the combined idle load of all the chillers. The minimum power level is configured in this way since the combined idle load of all the chillers is approximately 246 kW, creating a large gap which could cause too large non-linearities. In sequential control however, the size of the gap is reduced to the idle power level of one chiller which is about 48 kW or 50 kW depending on which chiller that is activated first. This gap is in relation to the gap in parallel operation is quite small, implying that the band available for power regulation is larger, given that the gap size is acceptable. The downside of sequentially controlled chillers though, is that every time the requested power level changes from or to idle power, a chiller has to be activated or deactivated. Consequently, this would introduce new non-linearities in the control of the chillers. However, when considering the size of the power band of each control type it is clear that the sequential band is larger. As a difference from the parallel control, sequential does not lose the capacity of the idle power levels. Thus,

sequential control can achieve up to 246 kW more power available for regulation, given that the non-linearities can either be accepted or compensated for. Although, in parallel control the chillers simultaneously increase or decrease their power in order to adjust the load after the requested power. In this manner parallel control manages to avoid non-linearities that sequential control is subject to since they only operate in the linear or stepwise region.

In summary, a parallel starting sequence of the chillers would be beneficial in regard to the chillers' activation time. Furthermore, by implementing a sequential control of the chillers it is possible to increase the available regulation power, given that the non-linearities caused by intermittent chiller activations can be compensated for. These two strategies have thus been implemented in the chiller system model. Additionally, it is also important to note that despite not being mentioned to the same degree as the activation of chillers, the deactivation is almost as important. However, the effects of choosing either sequential or parallel deactivation are the same as for activation. Thus, it is expected that a parallel deactivation of chillers also is beneficial in regard to deactivation times which is why parallel deactivation also is implemented in the model.

Chiller activation logic

As mentioned earlier, the chillers are activated in parallel and are controlled sequentially. The order that they are activated or controlled in the model is implemented statically such that VKA01 is chiller of highest priority, and then in descending order, the priority decreases until VKA05, which is of the lowest priority. This means that VKA01 will be the first to activate and VKA05 will be the last, depending on the current requested power. In reality, the static order of prioritizing the chillers is not optimal since some chillers will be subject to more wear and tear due to more regular use. Thus, in practice the control scheme should be implemented dynamically, where it always prioritizes the least used chiller. However, in order to keep the model simple, the chillers are prioritized statically, always with the same activation order.

In the system model, each chiller has its own model consisting of separate components. Each chiller model is split into two parts, where one part houses the components to calculate the idle power of the chiller and one part that houses the components which calculate the active power. The active power in this context refers to the power that is

larger than the idle power. The output power from these two components are added together in order to create the total power of the chiller. However, the second part is only active once the requested power is larger than the idle power calculated by the first part. This way, a single chiller can pass from idle power to active power in response to an increased power reference signal. Furthermore, each chiller is equipped with a hysteresis block. The function of this hysteresis block is to ensure that a chiller does not activate or deactivate too often due to a signal that is oscillating around the activation power level, as shown in *Figure 45*.

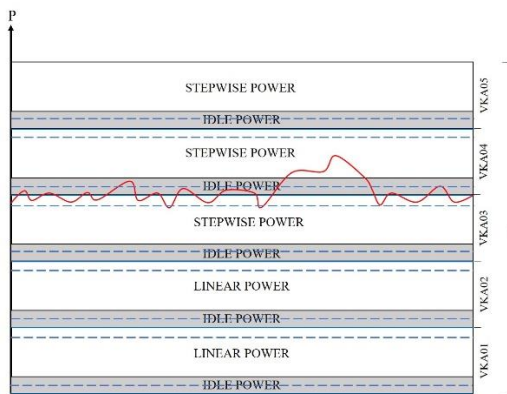


Figure 45: Sequential chiller control with hysteresis control.

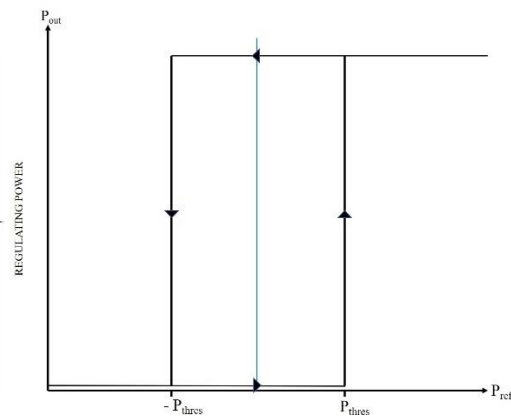


Figure 46: Illustration of hysteresis logic.

The dotted blue lines in *Figure 45* represent the thresholds for the hysteresis blocks whose logic is presented in *Figure 46*. There it is shown how the power reference signal has to be larger than the upper threshold in order for the chiller to activate, and lower than the lower threshold for the chiller to deactivate. The specific value of the threshold is not accurate in the figures above but was determined in simulations by gradually increasing the threshold values until a balance was reached between number of activations and deactivations, and the offset error from the reference signal. The hysteresis threshold value was consequently set to 20 % of the rated power of the chiller for both the VKA01-VKA02 and the VKA03-VKA05 chillers respectively. The denomination of the chillers is presented in *Table 5*.

Beyond having hysteresis blocks in order to control the activation and deactivation of chillers, another control logic had to be implemented in order to efficiently control the chillers. Whenever a large increase in the power reference signal was detected, which resulted in the activation of one chiller, and the increase of load on an already active chiller, the already active chiller did not take the startup power of the first chiller into

consideration. Since a chiller draws a constant power, corresponding to 60 % of its idle power during startup, this power might not be equal to the requested increase of power of the reference signal, simply due to the fact that the activation of a machine causes non-linearities. In order to overcome this problem as much as possible, the already active chiller, which is ramping up in power, is told to regulate the total power of the chillers in order to meet the power reference signal as well as they can. In this manner, when running in sequential operation, any chiller that is already active, that is not currently in a starting or stopping sequence, and that is not running on idle power, will try to regulate the total chiller power as much as possible in order to ensure that the reference power signal is being tracked as well as possible. Consequently, some of the non-linearities of the sequential chiller operation can be avoided simply by controlling the chillers more intelligently.

4.3.5 Energy storage system model

The ESS model consists of three main parts. The first part is the actual ESS, the second part is the control logic used during FC and the last part is the charge controller. The model of the actual energy storage is an already constructed block representing a simple ESS, based on a model of active and reactive power. The model has been modified to only consider active power and disregard reactive power. The model has implemented SOC calculations, limits of charging rates and efficiency calculations. It also includes a simple charging strategy that keeps the SOC within a defined boundary. This feature however, has been disabled in order to accommodate for a customized charging controller. The entire energy storage model is shown in *Figure 47*.

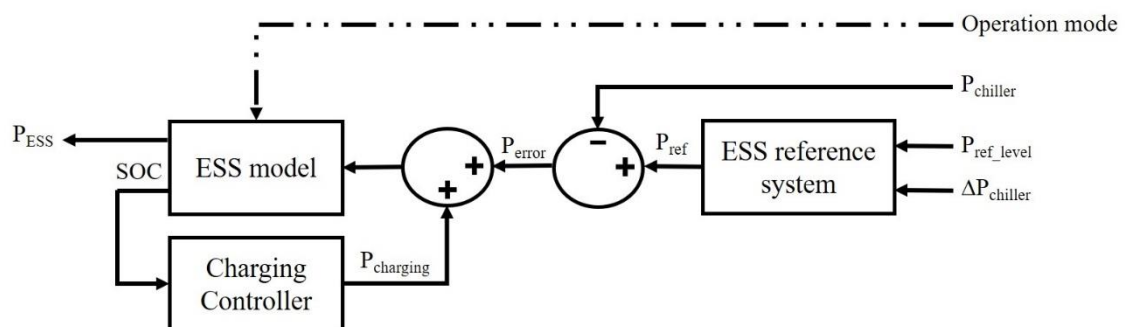


Figure 47: The energy storage model implemented in Simulink.

The ESS is only active when the scheduling unit has sent a FC command or when a prequalifying test is being performed. During this time, the controller uses the ESS reference system, presented in *Figure 48*, which is designed to provide the controller with a power reference for which the power of the chiller is supposed to be corrected to.

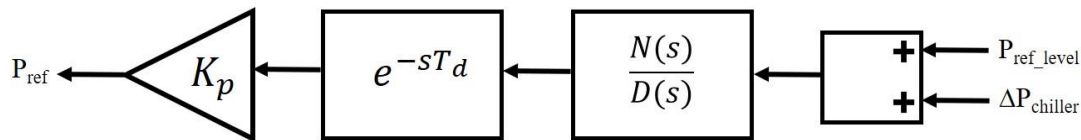


Figure 48: The ESS reference system model used to correct the power of the chillers.

ESS reference system

The power reference is designed to represent a balancing resource which performs just adequately in order to qualify as a balancing resource. By adjusting the deviation of the chiller power with the ESS, such that that the chillers just reach the minimum requirements of a balancing resource, i.e. the reference, the chillers should be capable of qualifying as a balancing resource themselves. The minimum requirements of a balancing resource are defined by SvK. When performing primary FC under normal circumstances, the requirements are set by the FCR-N market regulations and the requirements of the market's prequalifying test. The most obvious requirements are that a resource contributing to FC must respond with 63 % of their regulating power within 60 s of a step change. Also, it shall have reached a stationary, value with a maximum error of $\pm 10\%$ of the regulating power, within 180 s. There are however no detailed requirements that define what should happen before the point at 60 s and in between the point at 60 s and the point at 180 s. Consequently, if one were to study the accepted step responses of a system, there would be infinitely many possible systems as long as they meet the mentioned requirements. An example of this is presented in *Figure 49*. Furthermore, other system responses such as the bare minimum, defined by the blue line, or an instant step from 0 % to 100 % could also be argued to be acceptable according to SvK's requirements. One factor that is not considered in this instance is what happens after 180 s. According to SvK, they set further requirements of repeatability and endurance of the balancing resource. These two factors will not however be considered in this thesis.

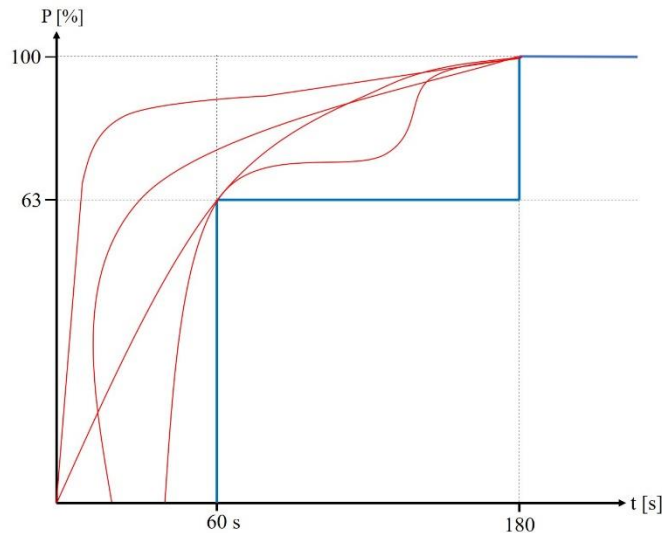


Figure 49: Examples of system step responses capable of passing the requirements of SvK for FCR-N.

With this said, the bare minimum requirements would be defined by the blue line in *Figure 49*. However, adjusting the chiller system response to match the characteristics of the blue line will not be an efficient solution simply due to the fact that the chiller system model already would perform better than the bare minimum requirements, if the irregular controls of the chiller were neglected. If the chiller system model only was represented by the first order transfer function, its step response would perform adequately in regard to the bare minimum. This can be proved by comparing the step response in *Figure 39* to the minimum requirements in *Figure 49*. Consequently, it would be reasonable to only adjust the power of the chillers with the ESS in a way that the net power corresponds to the response of the chiller system model, without irregular control behavior. This way, if no irregular controls are impacting the chiller performance, since the set-point corresponds to a linear or stepwise operating point, the ESS will not have to perform any corrections since the chillers already are performing adequately. A simple illustration of this is shown in *Figure 50* where the correcting power from the ESS is presented as (P_{error}), also shown in *Figure 48*. The ESS reference system model is presented in *Figure 48*, where the parameters are configured to match the chiller model's transfer function.

It can be seen how the activation of one chiller, where the activation sequence does not even take the full 180 s, results in what would be a failed system response. By having the ESS adjust for the error so that the actual power follows the reference, this system response would have passed. Furthermore, when regarding this step response test, it can be noticed that the ESS would have been activated unnecessarily since it surpasses the

minimum requirements. However, if this would have been a true test of the chillers tracking performance on FCR-N, the adjustment of the ESS would be minimal. This is due to the fact that it only would adjust the net power to a reference system, which in a system characteristics point of view, is the closest in response to the actual chiller system model's response. Thus, the ESS reference system model is based on the system model of the chiller, without activation and deactivation sequences.

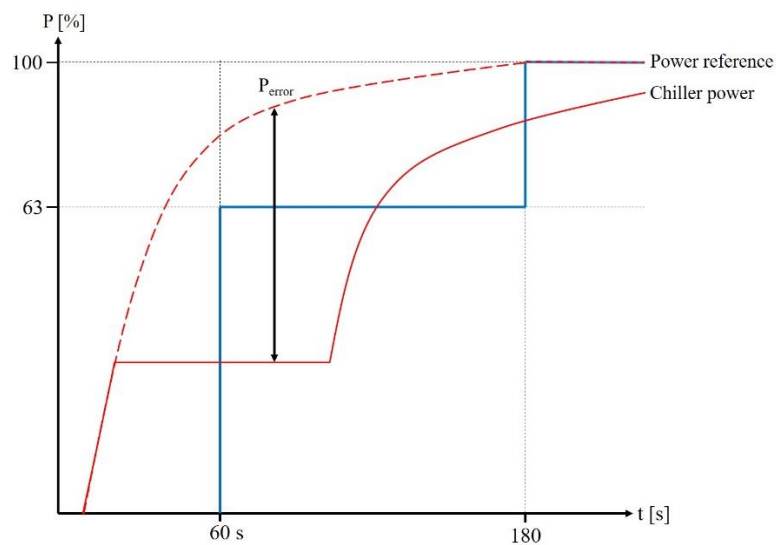


Figure 50: Illustration of the ESS reference system adjusting for the activation of a chiller.

This function is implemented by using the ESS reference system model, which outputs a normalized value corresponding to any value between negative and positive one. This value is then multiplied with the chiller bid size for that current hour, which is sent from the scheduling unit if FC is scheduled for that hour. The resulting value is the power, which together with the reference power level for that hour, will constitute the net balancing power, as illustrated in Figure 6 where blue represents the reference power level and red is power difference from the ESS reference system model.

ESS charging controller

The ESS charging controller is implemented to maintain the ESS SOC at 50 %. The reference of 50 % is chosen since it is assumed that power grid frequency deviations are equal in capacity and number in both directions. Thus, when performing FC, the ESS should charge and discharge an equal number of times, requiring equal capacity to charge and discharge. The charging controller continuously measures the SOC of the ESS. This value is then compared to the corresponding value in a one-dimensional look-up table which translates the SOC into a signal representing the normalized power, which the ESS is to be charged with. The normalized value is then multiplied by the rated power of the ESS charging controller. The look-up table is presented in *Figure 51*. It can be seen that the look-up table data-points implement a linear relationship between the SOC and the charging power. As a contrast, this could be implemented using a simple on-off relationship, or on-off with hysteresis. However, in order to minimize ESS degradation, it is important to minimize the charging power of the ESS. This is done by limiting the charging power to lower values whenever the need for charging is low, i.e. when the SOC deviation is small. Consequently, a linear SOC to charging power relationship is beneficial over a simple on-off relationship. It can however be argued that a logarithmic relationship, with lower power for lower deviations in SOC is even better. However, when dealing with this reasoning, the required charging power in order to maintain the correct SOC, also has to be considered. Consequently, a simplification has been made where the SOC to charging power relationship is implemented linearly.

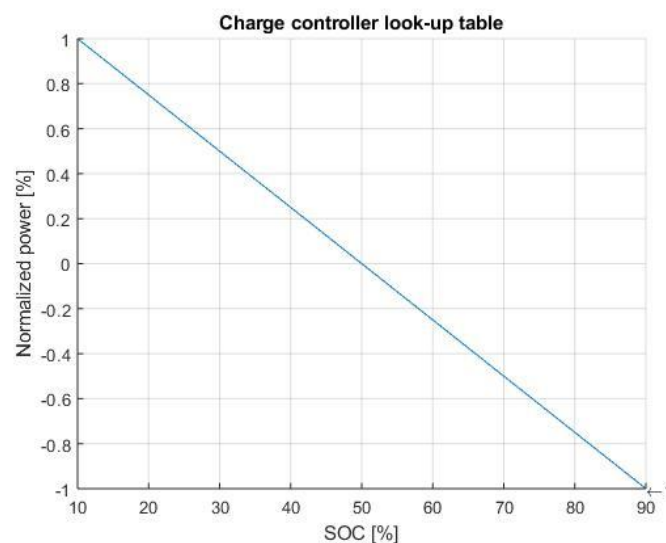


Figure 51: ESS charging controller look-up table for SOC-power calculations.

The required rated power of the charging controller is determined both by the capacity of the ESS but also how much the ESS is being used. With a small capacity, a given charge or discharge event will have a larger SOC deviation than what it would have had for a larger capacity. Consequently, a smaller ESS will also require a larger rated power of the charging controller in order to restore the SOC quicker to a desirable value. Due to this, it is important to define the ESS capacity before defining the rated power of the charging controller. However, in order to define the ESS capacity, the rated power of the ESS itself has to be defined. This is simply due to the fact that a larger rated power of the ESS can lead to faster charging or discharging of the ESS.

In order to define the required power, the prequalifying test for FCR-N was simulated. This was done for an ESS with zero capacity and zero power, resulting in only the DRRs performing the test. The chillers thus ran without assistance from the ESS resulting in a deviation from the ESS reference system. The deviation, or error, was measured and used as a basis to size the ESS rated power. The largest error was used as a basis for the rated power, where the rated power of the ESS was dimensioned to fully compensate for the error. Following this, the ESS capacity was to be determined. Rather than sizing the ESS after the prequalifying test, the ESS size was determined by running a simulation where FC was performed during an arbitrary week in June 2018 where large activation of chillers occurred. By running the simulation with a very large capacity and studying the SOC deviations for that ESS, the utilized capacity for that simulation was used to determine the ESS capacity. The resulting power and capacity for the ESS was determined to be 340 kW and 100 kWh respectively. The SOC upper and lower bounds, were determined as 90 % and 10 %. This rather high level was set this way based on the fact that during the simulation to determine the capacity, it was noticed how the entire battery capacity was utilized seldomly. Consequently, the impacts of large SOC deviations on degradation would remain small since they were few, whilst maintaining a rather large usable capacity.

The most important part of how the charging controller is implemented however, is the strategy to segment the battery power into two parts, where one part is reserved for the charging controller and the other for normal ESS operation. The system boundaries for the balancing resource can be defined in such a way that the balancing resource is defined as including only a part of the rated power of the actual battery. The remaining part of the

battery, outside the system boundaries, is used by the charge controller to regulate the battery SOC. In practice, this allows for a charging strategy that is independent of the current delivered power of the battery. So that if the battery was for instance, to deliver 100 kW of power to balance the grid and the charge controller needed to charge the battery with 20 kW of power, the net power would only be 80 kW. However, due to the way that the system boundaries are defined, the part of the battery that constitutes a balancing resource, still delivers 100 kW as required. Consequently, the actual battery rated power would be defined as the sum of the powers of the balancing resource battery and the charge controller, as illustrated in *Figure 52*.

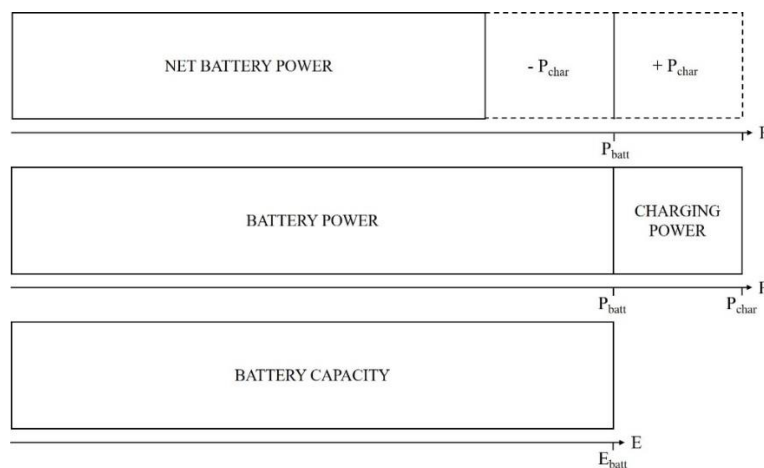


Figure 52: Segmentation of battery power to house charge controller.

This type of strategy might seem to be controversial since the charging power actually creates a deviation from the desired set-point value. However, the benefit of such a system is that the ESS, if the charging controller parameters are well defined, can participate more consecutive hours on FCR-N since it never has to interrupt operation to restore SoC to a nominal value. According to SvK this strategy is acceptable during circumstances where the following two requirements are met by the balancing resource:

- The resource shall manage to maintain within “the blue area”, as presented in *Figure 4*, for an arbitrary constant power grid frequency, irrespectable of how the ESS’s SoC changes.
- The endurance of the resource should in the “worst case” scenario be considerably longer than an hour. Exactly how long is not specified.

The impact of these requirements has been analyzed deductively and it has been determined that the system would meet the requirements.

The charge controller's rated power was still to be determined, despite having determined both the capacity and the rated power of the balancing resource battery. By setting an arbitrary value for the rated power of the charge controller and running the same simulation as earlier, the rated power of the charge controller was gradually adjusted. By starting with a high value, where the SOC was maintained within the boundaries and then lowering the rated power to a low value where the bounds were not maintained a gap was created which contained the power of which the SOC just could be maintained within the bounds. Then a new power value was chosen in the middle of the gap. If the power was too low, the next power would be the middle of the gap above, and if the power was too high, the next power would be the middle of the gap below. This process was repeated until the change of power between each iteration was negligibly small. The resulting power level was then chosen as the rated power of the ESS charge controller and corresponded to about 22 % of the ESS's rated power, i.e. 75 kW. The resulting power of the ESS, including the required power of the charge controller, is approximately 420 kW. However, the only rated power that will be considered further is the power corresponding to the balancing resource of 340 kW.

4.3.6 Regulation controller model

The regulation controller is one of the central control functions when performing FC. The regulation controller is responsible for measuring the grid frequency, doing any necessary analysis or modification to the frequency signal and then outputting a power balancing power signal to any balancing resources, based on the current power grid frequency deviation. The regulation controller is implemented in Simulink and is presented in *Figure 53*. Here the model is represented by a filter, a saturation block, limiting the boundaries of the signal, and a linear power block as presented in *Figure 4*.

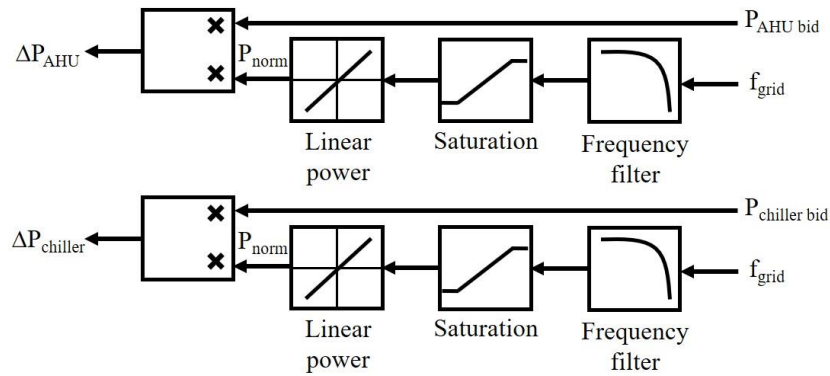


Figure 53: Simulink model of the regulation controller.

To the furthest right, the power grid frequency data is imported with a resolution of 0.1 s. The signal then passes through the low-pass filter with the specified time constants. The signal is then limited to specific boundaries in the saturation block. The resulting value is then passed into the linear power block which translates the filtered frequency signal to a normalized power value. By then multiplying this value with the balancing power bid, the actual demanded balancing power is achieved.

The first component receiving the frequency signal is a filter. The filter is configured as a low-pass filter that dampens all frequency components that are too high. This is done primarily in order to reduce the wear and tear of the balancing resources. The secondary reason to pre-filter the signal is to remove any frequency components that are too high for the assets to be able to respond to. When determining the filter time-constant, both the wear and tear of the resources, as well as the responsiveness of the resources has to be considered. Since the wear and tear of machine components has not been modeled in this thesis, the appropriate cut-off frequency for the low pass filters was estimated based on literature. This cut-off frequency was considered in the model simply due to the fact that, as for the AHU and chiller transfer functions, the low pass filter will introduce further delays in the system.

In order to avoid wear of fan motors in AHUs the cutoff-frequency is supposed to be set to about 1/8 Hz [73]. With (1) it is shown that it corresponds to a filter time-constant of about 1.27 s. Regarding the chiller, the appropriate filter time constant to avoid wear of the compressor, is unknown. Due to this, it is assumed that the corresponding value for chillers is the same as for AHUs. Considering the responsiveness of the assets however, it was shown that all frequencies higher than 0.02 Hz and 0.01 Hz for the AHU and the chiller respectively, are dampened by their natural low-pass characteristics. Adjusting the filter time constant thereafter, results in removing frequency components that the

resources otherwise could not respond to. These frequencies correspond to the time constants of about 8 s and 16 s, respectively. Since these time constants are larger than the time constant of 1.27 s, set to avoid wear of the resources, the low pass filters will mostly filter out its corresponding frequencies, making filtering with that time constant unnecessary. Thus, the larger time constants are used in the model. The low pass filter is modeled as a first-order transfer function and will therefore not have as large of an impact on frequencies just above the cutoff frequency as a higher order filter would have. However, since the filter time constant still is based on simple reasoning and the correct filter time constant might differ, the first order filter was found to be acceptable in this implementation, especially considering that it eases eventual PI-control. An example of the regulation signal, before and after filtering is presented in *Figure 54*.

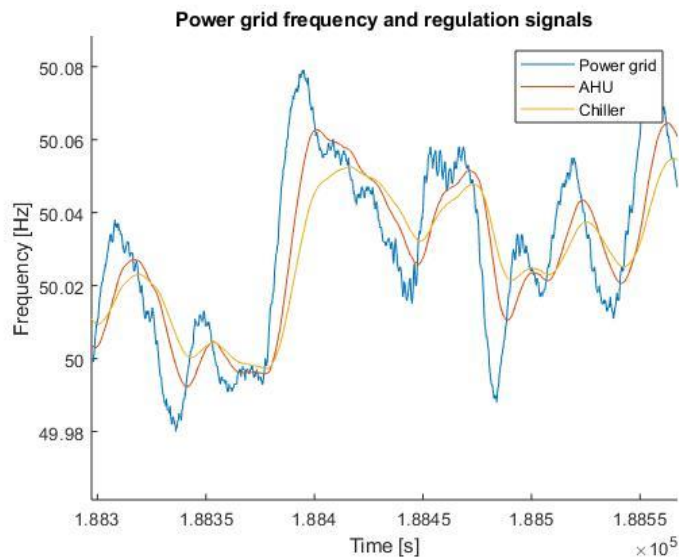


Figure 54: Power grid frequency signal and filtered regulation signals.

The filtered power grid frequency signal, or rather the regulation signal, is then passed through a limiter block which limits the amplitude of the signal to a lower bound of 49.9 Hz and an upper bound of 50.1, adjusted after the balancing market FCR-N. The regulation signal is then sent into a one-dimensional look-up table that translates the current grid frequency into a normalized power value, based on the graph presented in *Figure 55*. This normalized value is then multiplied with the respective bid for each asset during that hour, provided by the scheduling unit. The regulation controller then sends the resulting power offset signal to the DRRs, of which follow the offset signal if FC is scheduled.

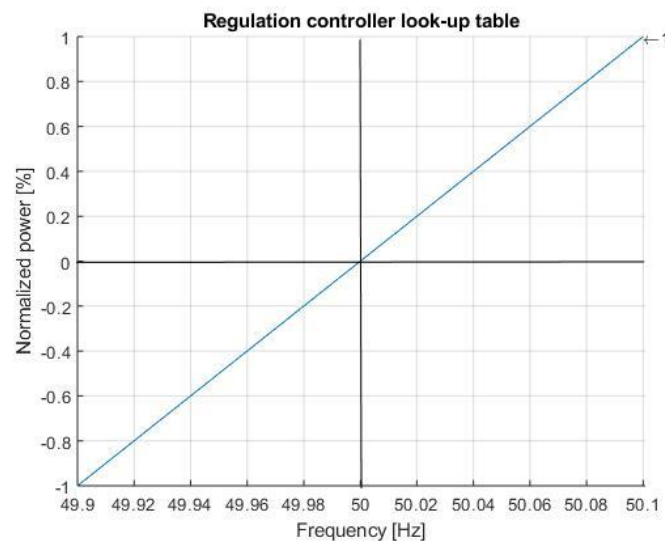


Figure 55: Regulation controller's frequency to normalized power look-up table.

4.3.7 Scheduling unit model

The scheduling unit is modeled as two separate components, of which one is implemented in Simulink and another is implemented in MATLAB. Originally, both were implemented in Simulink and were made to run simultaneously during the simulation. However, since the scheduling unit performs many calculations, this implementation proved to be too demanding on the system. Due to this, the scheduling unit was split into two parts, where the most demanding part instead was implemented in MATLAB, to run before the simulation, effectively splitting the load in half. This first part is the part of the scheduling unit that performs the actual scheduling in the VPP. The other part simply reads the current slot in the schedule during the simulation, and outputs command to the assets in the VPP portfolio, depending on what is scheduled for that time slot.

The scheduling unit is implemented in such a way that it either schedules FC on all assets, or it does not schedule anything, meaning that normal operation will commence. Basically, the scheduling unit will only have to determine whether FC is possible during any given hour, and in the case that it is, it will also have to determine what capacity that is available. If this were a real implementation, the scheduling unit also would contain the necessary logic to place bids on the FC markets.

The scheduling unit constantly checks the current simulation time, which translates into the actual historical time for which the simulation is run. Since bids are to be placed on FC markets, which occurs, at the latest either 15:00 two days ahead, or 18:00 one day ahead of the delivery day, the scheduling unit will have to have decided by then, for the entire day, whether to participate or not, and in that case, with what capacity. Consequently, the scheduling unit will have to by then have calculated the available capacity for FC. This is done by creating a load corridor. The point of the load corridor is to calculate the controllability of the load during any given time point. This is done by determining the limiting lower and upper bounds that will hinder the DRRs from reaching a load that is lower or higher than the respective bound. The upper and lower bounds thus create a “corridor” that the DR load can be within.

Load corridor

When regarding the AHUs and the chillers as DRRs, their respective bounds have to be analyzed. Both the AHUs and the chillers will obviously have lower bounds consisting of zero load, i.e. when the machines are turned off. These bounds will always remain the same and are therefore static. Moreover, the AHUs also have lower bounds consisting of their minimum power draw when the VFDs are set to their lowest speed of 20 Hz. Again, this bound is also static. The chillers however, depending on whether their operating scheme is sequential or parallel, will have different lower bounds. In parallel operation, the lower bound will consist of the total idle power of all machines, whereas for sequential it will only consist of the idle power level for one machine, if not zero load since that machine could be turned off. Beyond these two lower bounds, there could be many other bounds set by limiting factors in the HVAC system or the indoor climate, regulated by tenant contracts at Våla. These will however, not be covered in further detail in this thesis. With the same reasoning, two upper bounds were concluded. These

consisted of the rated power of the AHUs and the chillers respectively, but also, the configured upper VFD limiters. These were although not available for this thesis and have consequently been excluded.

One upper bound proved to be common for the AHUs and the chillers. This bound was constituted by the subscribed power level and the peak load in the energy contract with the DSO. The bound implies increased costs if the subscribed power level is exceeded or if the peak load is increased. However, due to the fact that Väla has managed to keep the peak load under the subscribed power level for 2017 and 2018, only the peak load will be considered as a limiting factor. Since the peak load level is determined month-wise for the winter months, November to March, but also annually for the entire year, the scheduling unit checks which of the current limits that are valid and which one of them that is the lowest. This is done by determining the current month, if it is a winter month, the highest load during that month and during the entire year are compared. The smallest of the two will make up the limiting power level for that month. Otherwise, if the current month is not a winter month, only the annually highest power level will be the limiting factor. In practice, this process could not have been performed since it is based on a completely accurate forecast for the entire year, or based on historical data for the previous year, and assumptions that peak loads do not vary from year to year.

The scheduling unit then calculates the upper bound from the maximum allowed increased total load at Väla, using the load data presented in *Figure 20*, and splits it accordingly amongst the DRR's. If the bound is a limiting factor, the AHUs will be prioritized over the chillers in order to improve responsiveness and to decrease ESS load.

The last bound included in the model is very simple. Since both DRRs, i.e. the AHUs and the chillers, have defined operating times, they will be shut off outside these hours. Consequently, the model calculates a dynamic upper bound which it sets to zero for the AHUs and the chillers respectively, whenever they are supposed to be shut off. The upper bound of zero will force the controllability of the DRRs to zero. The operating hours are configured differently for each AHU. Consequently, the average starting and stopping time for weekdays and weekends respectively, has been calculated and implemented in the model. An illustration of a load corridor is presented in *Figure 56*.

Bid determination

The scheduling unit uses the load corridor with the bounds presented above in order to determine the available capacity in power that can be used for FC for each hour, one or two days ahead. Normally, since there is no inherent way to know one or two days ahead, what the load will be during any given hour, some kind of forecasting method would have been implemented. However, due to constraints in this thesis, no forecasting method was implemented. Instead the model builds upon a completely accurate forecast of the load, which simply has been implemented as historical data. Furthermore, since the forecast is assumed to be completely accurate, there will be no difference for the scheduling unit when calculating the bid one or two days ahead. If a forecast error would have been present, it should have resulted in a larger error two days ahead, and a smaller error one day ahead, which would have affected the bid size since the possible error would have been compensated for.

Since the forecast is completely accurate, all scheduling is performed one day ahead since there will be no impact on whether it is performed one or two days ahead. Consequently, the scheduling unit will at 18:00 in the corresponding simulation time, calculate the available capacity for FC for each hour during the day ahead. This is done by comparing the forecasted load with the lowest of the upper bounds and highest of the lower bounds and choosing the lowest of the margins to each bound. This process is done for both the AHU and the chiller model. This is done as shown in (16), where (P_{upper}) and (P_{lower}) are vectors containing the values of the respective boundaries. Since the price components of the bid are neglected in this thesis, it is simply assumed that all bids are accepted, and that FC is performed whenever capacity is available.

$$P_{capacity} = \min (P_{forecast} - \max(P_{lower}), \min(P_{upper}) - P_{forecast}) \quad (16)$$

The capacity for the AHU and the chillers is then added together and compared to the upper bound consisting of the subscribed power level, also by taking Väla's total forecasted load into consideration. If the total capacity is too large, the capacity is decreased in order to not exceed the boundary. Again, the AHU capacity is prioritized over the chillers, meaning that the chillers' capacity is the first to be reduced. Once this is done, the total capacity is rounded down to the nearest multiple of 100 kW. If the result

of this is larger than the minimum bid size of 100 kW, the scheduling unit schedules the bid for each DRR during the hour for which it has been calculated. Otherwise, nothing will be scheduled and the DRR will operate normally. A more detailed example of this process is presented in *Figure 56* where the smallest of the blue and the red area determines the bidding capacity for one DRR. The dotted line represents a possible bound for the forecasted power, which consists of a forecasting error, which also has to be considered in a future implementation. This bound would not however be implemented as an upper or a lower bound, but rather a dynamic middle bound. Consequently, the blue and red stacks in the figure would never meet. Instead they would be limited by the most limiting part of the middle bound during each hour. During the specific hours and values presented in *Figure 56*, only during the hour 07:00 – 08:00 the power will be determined by the red area.

The rest of the scheduling unit is based in Simulink. Here the scheduling unit reads from a matrix which contains the scheduling information with a minute's resolution. The scheduling unit outputs the current time slot's data which contains the current operation mode, normal or FC, and the respective bid for each DRR. These values are then output to the rest of the Simulink components which respond accordingly.

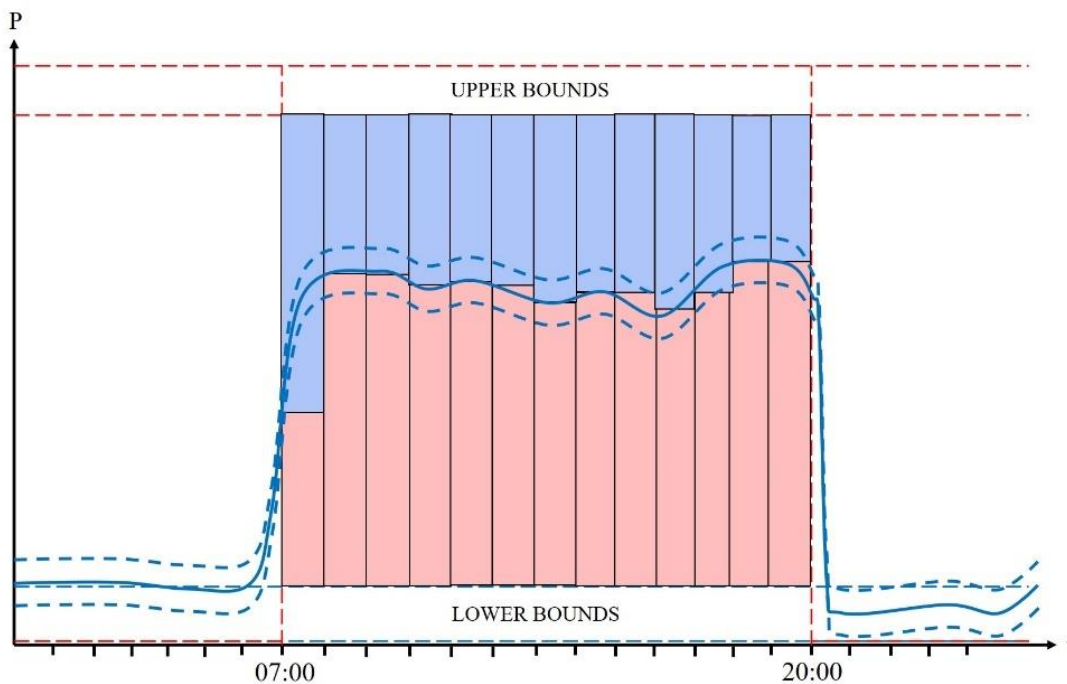


Figure 56: Illustration of how the load corridor and the forecasted load can determine bidding capacity.

4.4 Simulation

The simulations performed in this thesis have all been formulated in order to answer the question formulation in an appropriate way. Consequently, the simulations have been developed in order to provide a sufficient basis for analysis whilst providing reliable grounds for discussion. The simulations can all be categorized in three main categories, of which the first one is solely implemented to verify the function of the model. The second and the third simulation categories have been used to achieve the results needed in order to answer the question formulation and to keep the results and discussion within the scope of the thesis. The first category of simulations has been presented throughout the method chapter in conjunction with its respective model. Consequently, only the second and the third of the three simulation categories will be presented in further detail.

4.4.1 Prequalifying test

The prequalifying test is modeled in both MATLAB and in Simulink. It is based on the actual prequalifying test provided and developed by SvK. The goal while implementing the model for the test was to verify the performance of the DRR and the ESS to perform FC. In order to give a fair representation of the test, both the responsiveness and the endurance of the resource is to be tested. However, since factors such as indoor climate and physical fatigue of HVAC components, which both affect their endurance, have not been modeled due to delimitations in this thesis, the endurance of the FC resource will not be tested in the prequalifying test. Due to this, the endurance part of the test has been excluded from the model in order to enhance the presentation of the results. Left, is a test formulated only to verify the responsiveness of the assets.

The main component of the prequalifying test model is the frequency sequence generator, or rather the step change generator. It creates a signal representing the grid frequency signal which is constituted by a sequence of frequency deviation values that create step changes with an amplitude of + 50 % and \pm 100 % of 0.1 Hz. These are then sent to the DRRs which are scheduled to perform FC. Their response to the signal is then used as a basis for the results. In order to determine whether they perform adequately, the minimum requirements have to be defined. As presented earlier in theory, the minimum requirements are defined by *Table 4*, where requirements for the first 180 s after a step

change are defined. After 180 s following a step change, the system should reach a stationary value where the requirements change an error corresponding to $\pm 10\%$ of the step's power level. These requirements have been implemented in MATLAB and Simulink.

The step-sequence with the corresponding boundaries are presented in *Figure 57*. The yellow line is the frequency reference signal, the blue dotted lines are the upper and lower stationary bounds and the blue line is the boundary defined as the minimum requirement system. The DRR system response has to maintain above the blue line when a positive step is sent and under the blue line when a negative step is sent. Furthermore, it has to maintain within the stationary bounds within 180 s after a step change. By measuring the deviation from these bounds, i.e. the error, conclusions regarding qualifying performance can be drawn. This test is performed both with and without the ESS implemented and for varying bid sizes in order to highlight their impact on performance.

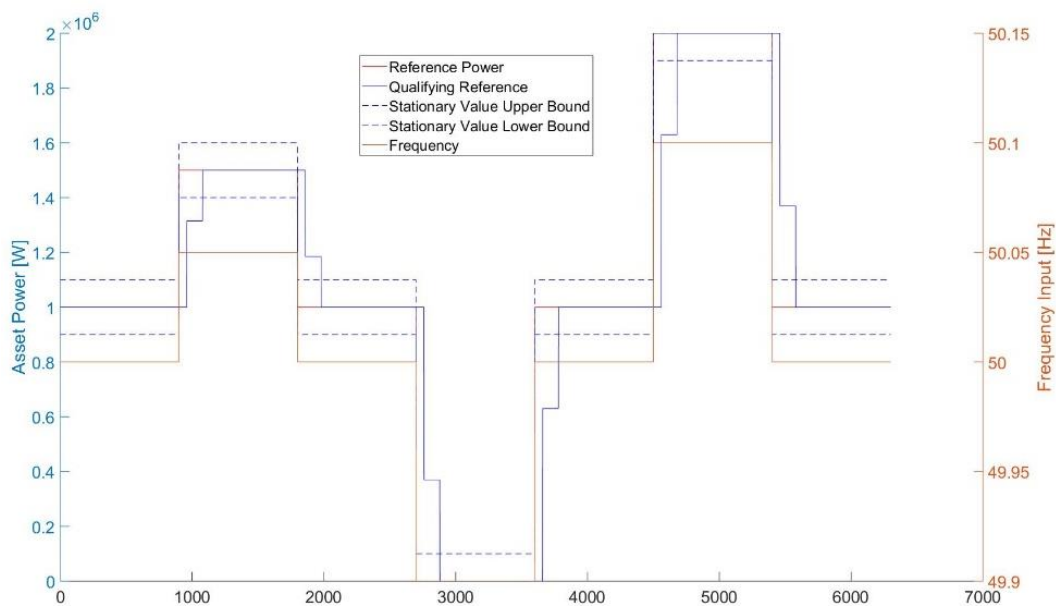


Figure 57: Prequalifying test sequence with upper and lower stationary bounds, minimum requirement bound, frequency reference signal and a reference power signal with optimal response.

The variations on parameter settings are presented in *Table 9*. The first simulation is run in order to present the system response without using ESS compensation. The second will contrast the first simulation by presenting how the system works with ESS. Both simulations will use the maximum regulation capacity for both DRRs. In the third simulation the response of the system without any AHU will be tested. Lastly, the system will be tested with a total regulation capacity corresponding to half of the maximum capacity. The ESS rated power in the table includes the required power of the charging controller, where the charging controller has reserved 21.75 % of the rated power.

Simulation Number	Chiller regulation capacity	AHU regulation capacity	ESS rated power	ESS capacity
1	600 kW	400 kW	0 kW	0 kW
2	600 kW	400 kW	420 kW	100 kWh
3	600 kW	0 kW	420 kW	100 kWh
4	0 kW	400 kW	420 kW	100 kWh
4	300 kW	200 kW	420 kW	100 kWh

Table 9: Summary of prequalifying test simulation parameter configurations.

4.4.2 Frequency containment

The prequalifying test is important in order to determine whether the DRRs have a possibility of performing adequately on FCR-N. However, the test does not test the prerequisites for the entire VPP to act as a balancing resource. In order to verify its performance, it is important to implement a test that truly requires the dispatch of both the regulation controller and the scheduling unit, and then to see how the DRRs perform with consideration to the overall VPP operations.

Naturally, an appropriate way to do this is to perform a real-world test, or at least a simulation thereof. If real historical data of the power grid frequency was used to verify the regulation controller, it would give an indication of how it would have performed in the real world. The same reasoning applies for the scheduling unit, which only can be tested in this way, since the algorithm is based on a forecasted value or a historical value.

Furthermore, the performance of both these components will impact the DRRs' ability to perform FC. Additionally, an actual regulation signal will have a significantly different impact on FC performance than what the prequalifying test signal has. Consequently, in order to achieve a nuanced result, a test of FC performance should be performed.

The FC test is performed solely on historical data for 2018. The test is only performed one week at a time due to the fact that the high resolution of the data and the detailed model is demanding on the computer. In order to create nuanced results, it is important to run the simulation during time periods that provide different prerequisites for the VPP to provide FC. Factors such as the availability of DRRs is known to vary throughout the year. The cooling need of the chillers is next to none during the winter half of the year, whereas in the summer, the cooling need is very large. Including variations of this factor will contribute to an overall more nuanced result. Furthermore, variations in annual and monthly subscription power levels also vary throughout the year resulting in what could be occasionally reduced FC capacity.

In order to provide the basis for an analysis, the FC test is performed for four different weeks spread out during the year. One week during the middle of the winter, one during the middle of the summer, and the other two weeks placed at the middle of spring and at fall. These variations will capture differences in DRR availability, power grid frequency signals and FC capacities. During these simulations the tracking performance of the DRRs, the utilization of the ESS and the availability of DR for FC, will be studied. The time periods that are simulated in each simulation are presented in *Table 10*.

Simulation Number	Start date	End date
1	January 1 st	January 8 th
2	April 2 nd	April 9 th
3	July 2 nd	July 9 th
4	September 3 rd	September 3 rd

Table 10: Summary of frequency containment simulation dates.

In order to determine the tracking performance of DRRs, the deviation from the regulation signal will be of no interest. Due to varying delays and gains the systems representing the regulation signal and the DRRs will have very different responses to the grid frequency signal, whilst both being acceptable system responses when considering their prequalifying test performances. Thus, the DRR tracking performance has to be defined after its own system parameters, given that it passes the prequalifying test and is allowed to perform FC. Consequently, upper and lower bounds have been defined based on the system characteristics of the DRRs. Since each DRR has a different system models, the upper bounds were defined as a 10 % deviation from the largest system response of the two. The same method was used for defining the lower bound, but instead it used -10 % of the smallest system response. This way, upper and lower tracking bounds could be defined, in order to give an indication of the DRRs' tracking performance. It is important to note that there is no true definitions from SvK that define the tracking performance of a resource when performing FC. Thus, the defined boundaries will only be used as an indication of how the DRRs perform.

5. Results

In this chapter the overall results of the thesis will be presented. This is done by first presenting the results of the simulations performed of the prequalifying test and secondly by presenting the results of the simulations performed of the frequency containment tests. The results are analyzed for each simulation and are further summarized at the end.

5.1 Prequalifying test

The results of the prequalifying tests are presented in the figures below. The blue line represents the minimum requirement reference. The dotted blue lines represent the stationary bounds. The red line represents the reference of the optimal response and the dotted red line is the actual power. Each step in the test is run for 15 minutes, where the first 15 minutes are to ensure stable operation before the actual test commences. Thus, the first 15 minutes will not be considered in the results. The ESS rated power is included the reserved power for the charge controller. Any referencing to a specific number of a step change refers to the numbers presented in *Figure 8*. Some results are excluded from the figures such as error that are constant throughout the simulation or results that are the same as a previous simulation. These are however mentioned below.

5.1.1 Simulation 1

Chiller regulation capacity	AHU regulation capacity	ESS rated power	ESS capacity
600 kW	400 kW	0 kW	0 kW

Table 11: Configuration for prequalifying test simulation 1 without ESS.

During the first step the actual power of the DRRs initially remain within the allowed boundaries, i.e. above the qualifying reference. However, when a new chiller activates to accommodate for the increased reference, it can be seen that the actual power falls behind the qualifying reference and remains so until it reaches its stationary value. During the second step, which is of the same amplitude, but in the opposite direction, the actual power remains within the qualifying reference, indicating a faster deactivation than activation of chillers. The same characteristics are presented in the positive and negative step changes respectively, with the only difference being that the larger steps result in larger errors. The errors for each step are presented in *Figure 59*. The largest determining errors occur during the fourth and fifth step for the positive flank and correspond to 253 kW. Furthermore, smaller errors also occur just before the 60 s mark after each positive flank, where the larger flanks again, have larger errors. Regarding qualification, it is clear that this configuration would not be able to qualify simply due to the poor responsiveness during positive flanks. As expected, the model does not prove to have any problems with endurance. In *Figure 60* it is clear how the AHU seems to perform sufficiently and how the chillers deactivation, but mostly activation sequence causes large disturbances.

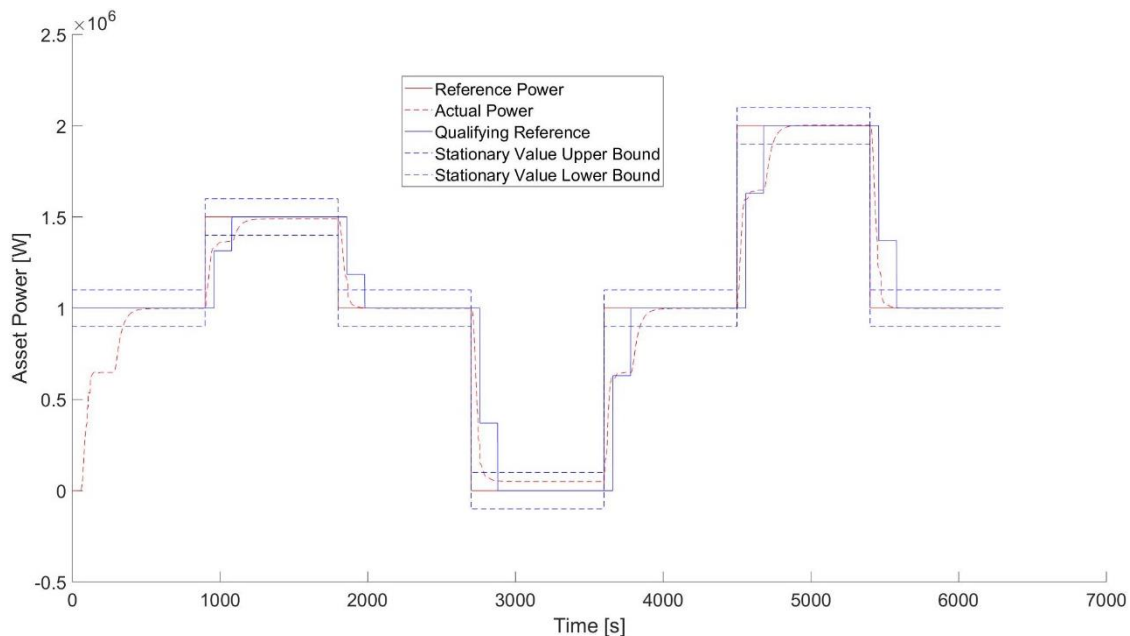


Figure 58: Prequalifying test without ESS.

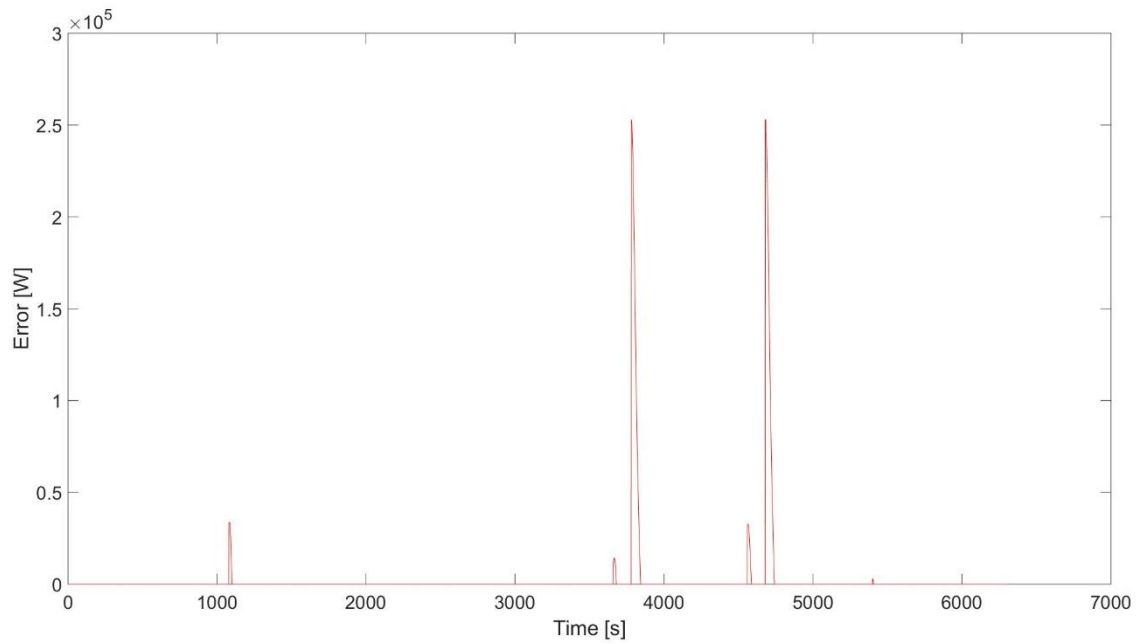


Figure 59: Error in prequalifying test without ESS.

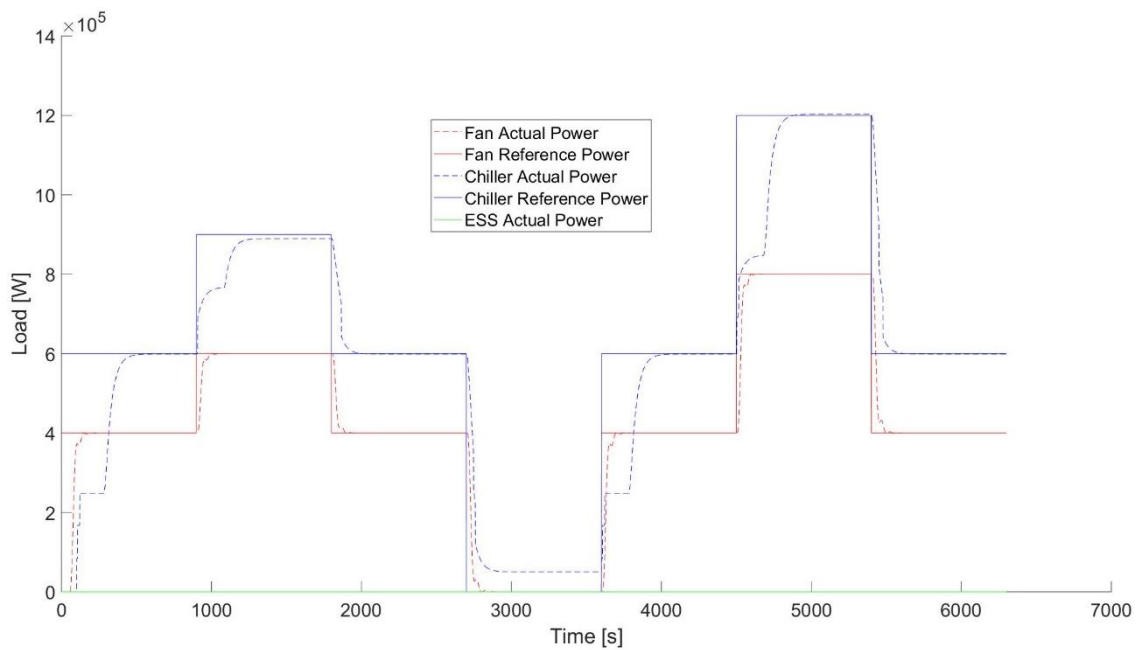


Figure 60: Prequalifying test without ESS with separated DRRs.

5.1.2 Simulation 2

Chiller regulation capacity	AHU regulation capacity	ESS rated power	ESS capacity
600 kW	400 kW	420 kW	100 kWh

Table 12: Configuration for prequalifying test simulation 2 with ESS.

After the ESS has been implemented, it compensates for the chiller error and the system responsiveness greatly improves. When studying *Figure 61* it is apparent that the system's step response is within the boundaries and would qualify. When studying the error of the test, it is confirmed since the error is zero throughout the test and is thus not presented. Additionally, it is shown in *Figure 62* that the ESS activates and both charges and discharges when needed. Lastly, when studying *Figure 63* it is apparent that the SOC remains within the boundaries and in general does not have a large deviation. The largest deviation occurs the fifth step, which also is the largest step where the chiller activation sequence has the largest impact. The SOC does although return quickly towards its nominal value which indicates that the charging controller is working correctly. In summary, the test indicates that the system would pass prequalifying.

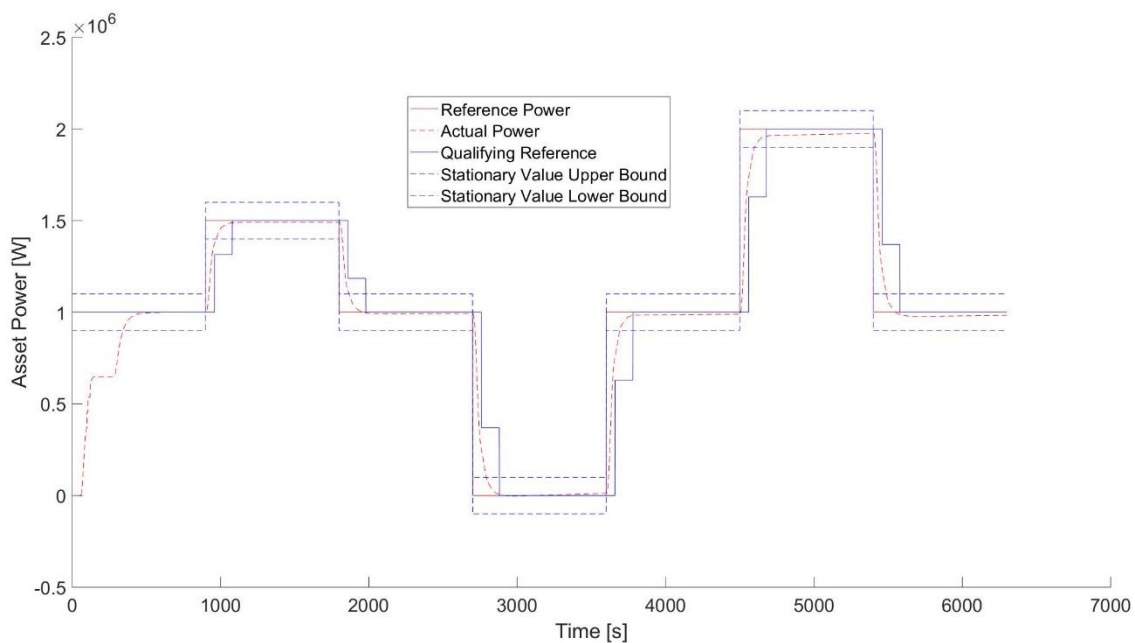


Figure 61: Prequalifying test with ESS.

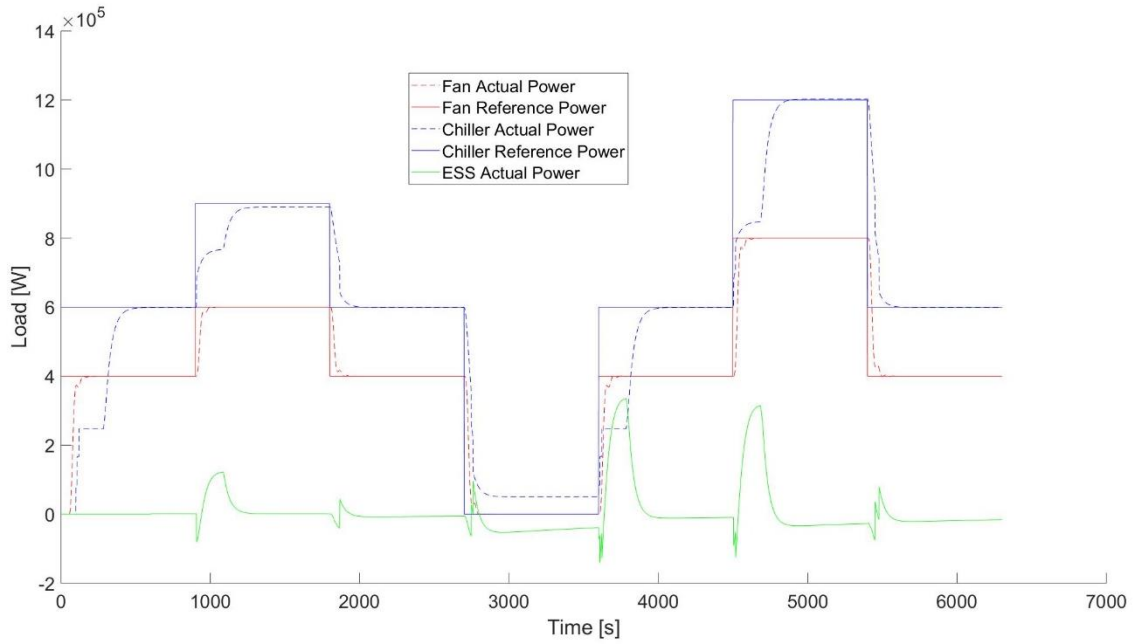


Figure 62: Prequalifying test with ESS with separated DRRs.

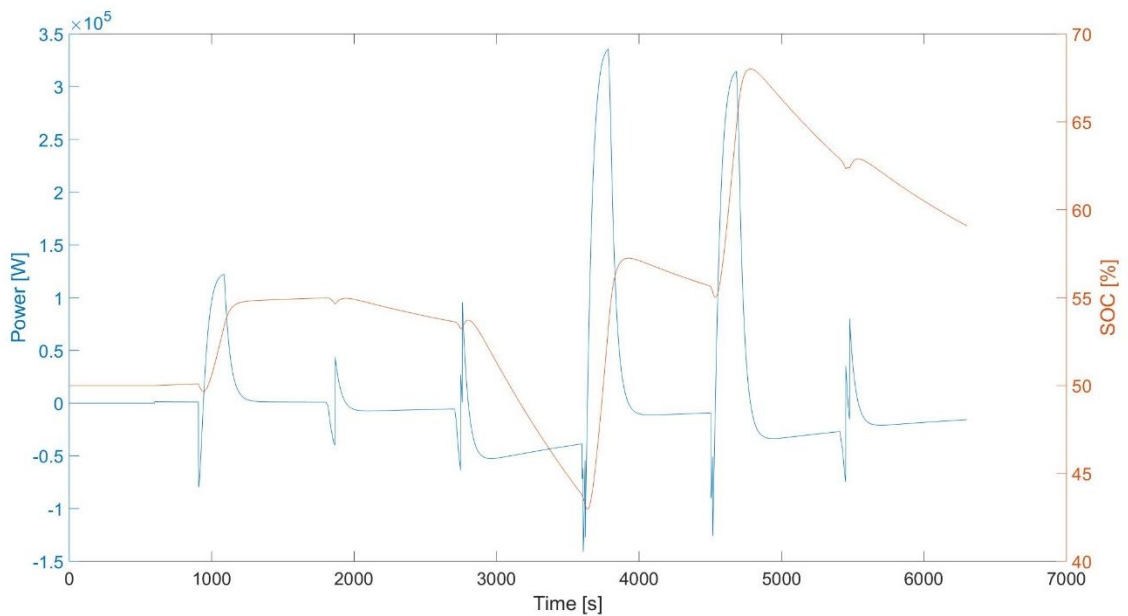


Figure 63: SOC and power for prequalifying test with ESS. The ESS is considered a load in the simulation. Thus, a positive power indicates the charging of the ESS. The power includes the asset power as well as charging power.

5.1.3 Simulation 3

Chiller regulation capacity	AHU regulation capacity	ESS rated power	ESS capacity
600 kW	0 kW	420 kW	100 kWh

Table 13: Configuration for prequalifying test simulation 3 without AHU.

Since the prerequisites for the chillers and the ESS in this simulation are the same as for the previous simulation, the ESS power and SOC have not changed and will thus be excluded from the results in this simulation. When studying *Figure 64* it would seem as if the chillers with ESS correction manages to pass the prequalifying test. Errors do however occur, which are shown in *Figure 65*. When studying the errors in further detail, it is noticed that the largest error is small in relation to the balancing power. The error occurs 63 s after the start of the step change which means that the chillers by a small margin of 3 s will fail the prequalifying test. Thus, the results indicate that the chillers have a responsiveness that is too low when performing FC on their own, even when compensating for errors with the ESS. Some errors occur outside the largest visible error. These occur in the same instance as the large one but is generally much smaller. It is however important to note that these errors occur for this specific control configuration. Alternative control configurations, for instance using the ESS as primary control and chillers as secondary, could still prove to have sufficient responsiveness to pass the test. Additionally, when studying *Figure 64*, the deviations caused by the ESS charging power become apparent in the 3rd and 5th step. These are in practicality deviations from the desired set-point value but are in line with SvK's requirements of the charging strategy.

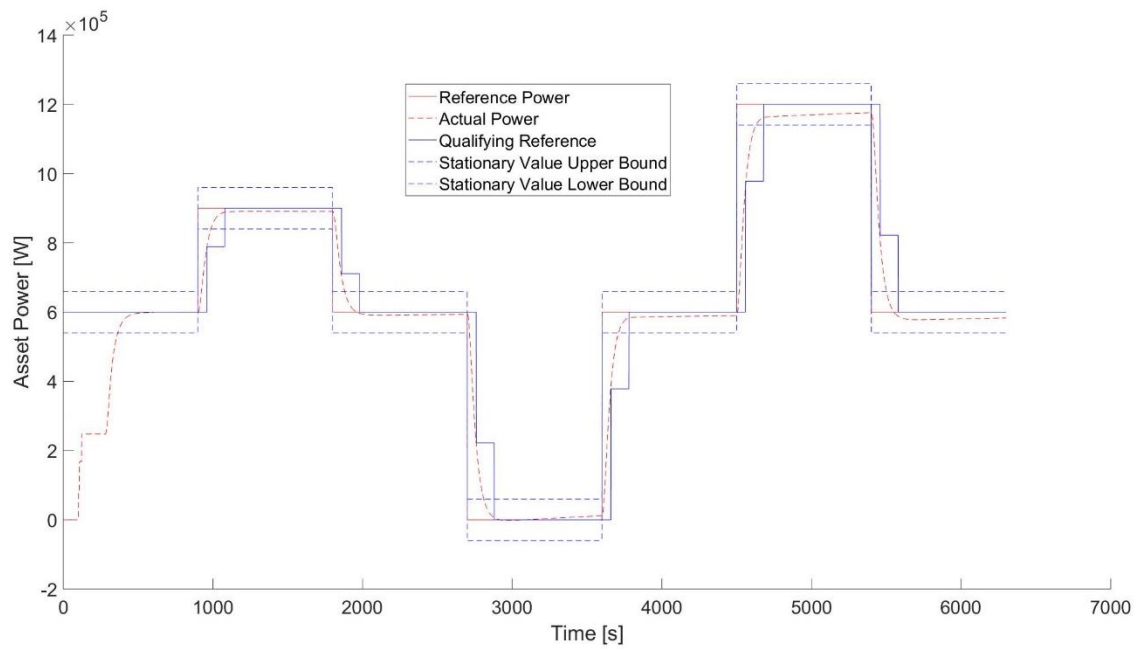


Figure 64: Prequalifying test without AHU capacity.

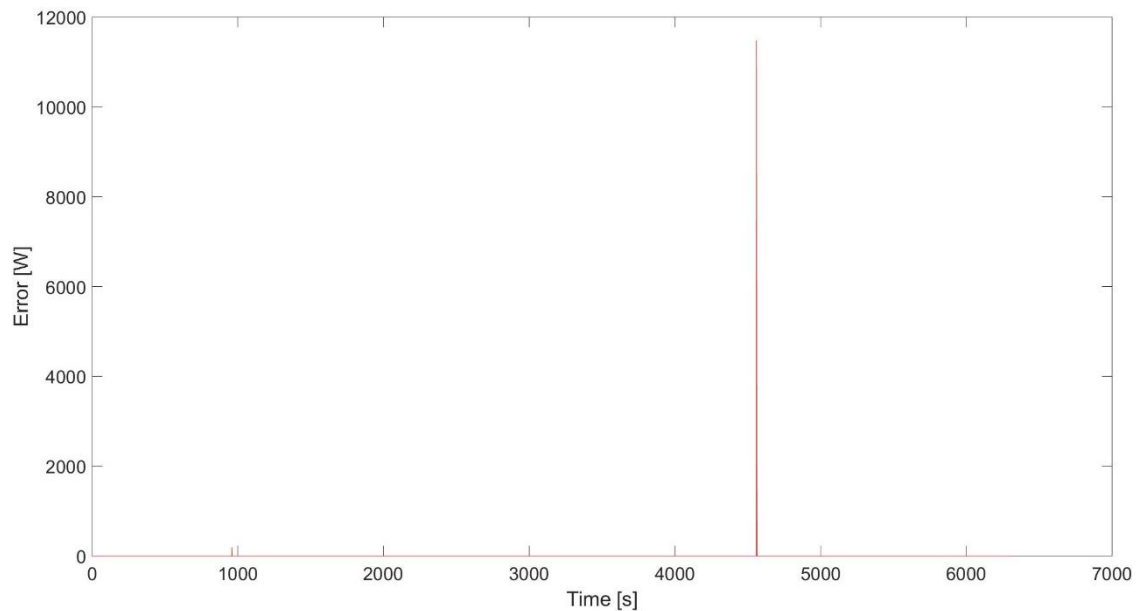


Figure 65: Error in prequalifying test without AHU capacity.

5.1.4 Simulation 4

Chiller regulation capacity	AHU regulation capacity	ESS rated power	ESS capacity
0 kW	400 kW	0 kW	0 kWh

Table 14: Configuration of prequalifying test simulation 4 without chiller and ESS.

The results of simulation 4 which are shown in *Figure 66*, are as expected. Without the chillers and the ESS, the responsiveness is improved, and the AHUs manages to pass the prequalifying test with a good margin. This simulation, there is no error since the AHU manages to pass all requirements. Again, the responsiveness could possibly have been improved by including the ESS in this control configuration but is excluded from the thesis due to delimitations.

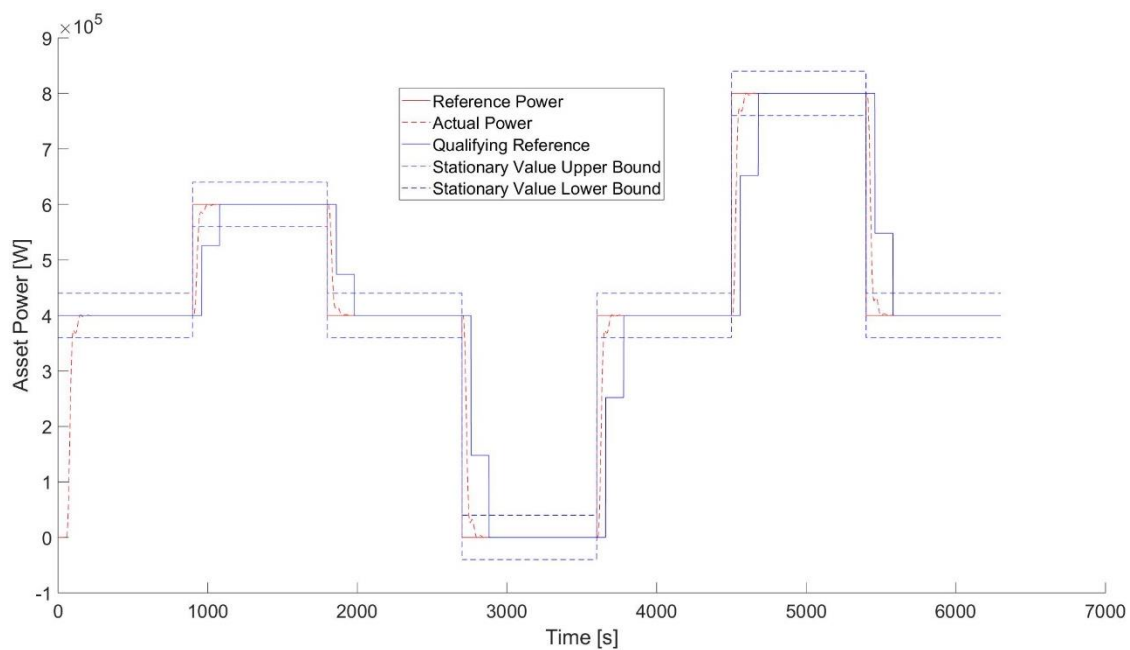


Figure 66: Prequalifying test without chiller and ESS.

5.1.5 Simulation 5

Chiller regulation capacity	AHU regulation capacity	ESS rated power	ESS capacity
300 kW	200 kW	420 kW	100 kWh

Table 15: Configuration for prequalifying test simulation 5 with half capacity.

The last of the five simulations shows that even for lower capacities the system manages to pass the prequalifying test, as shown in *Figure 67*. The errors are the same times as for the second simulation but of lower magnitude since the overall capacity is also smaller. Due to this, the errors are not presented. The SOC which is presented in *Figure 68*, has similar deviations as in the second simulation despite the chiller capacity being smaller. Again, the charging controller manages to maintain the SOC within bounds.

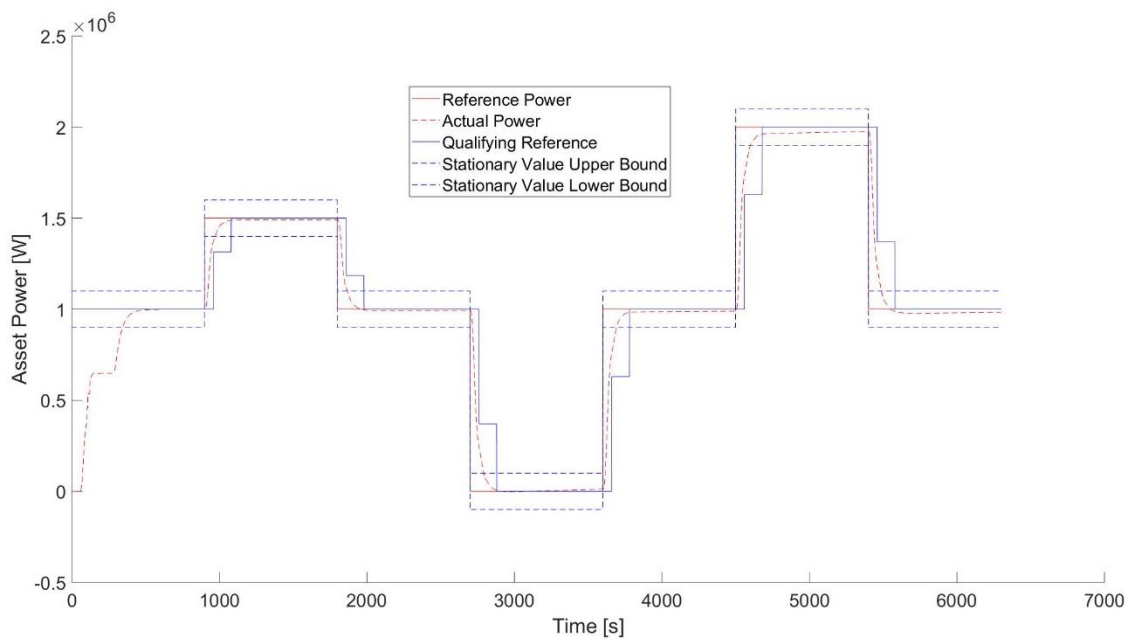


Figure 67: Prequalifying test with half of maximum capacity.

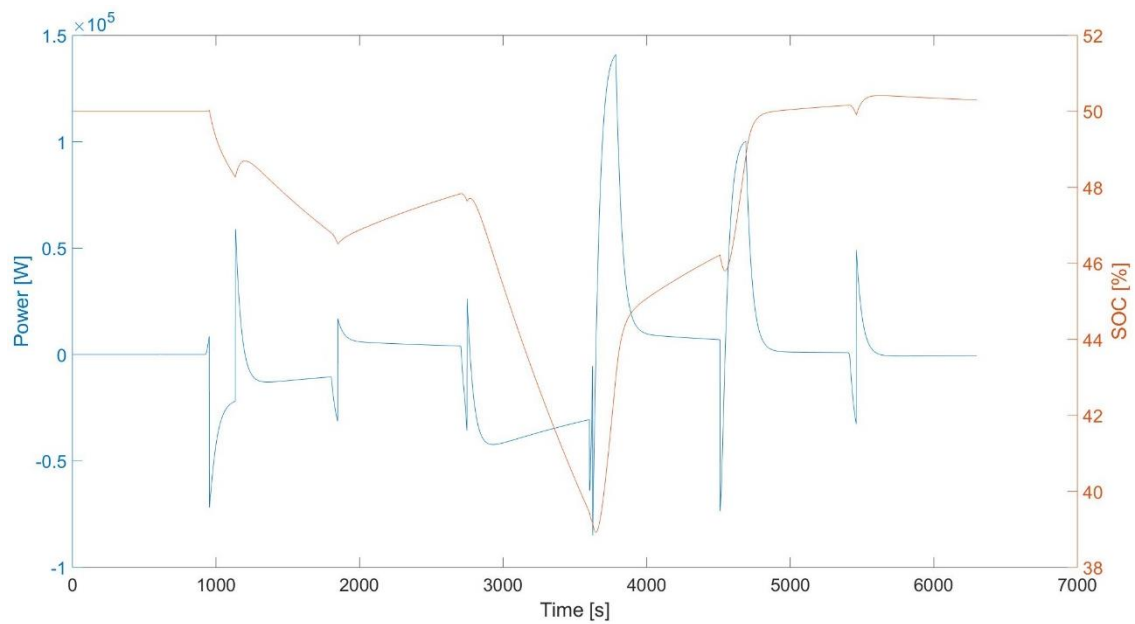


Figure 68: SOC and charging power for prequalifying test with half of maximum capacity. The ESS is considered a load in the simulation. Thus, a positive power indicates the charging of the ESS. The power includes the asset power as well as charging power.

5.2 Frequency containment

The results of the simulations run for the FC tests are presented in the figures below. The scheduled available capacity for FC, as determined by the scheduling unit, and the tracking performance for the DRRs are presented for each simulation. All simulations are based on actual historical data from the respective simulation period as presented in *Table 10*. In the figures of scheduled capacity, the stacks represent capacity available for FC during each hour at FCR-N. The blue stacks represent AHU capacity, red is chiller capacity, yellow is the capacity loss due to rounding capacity down to nearest bid size and purple is also chiller capacity loss due to rounding down. In the FC figures, the red is the actual power of DRRs with the respective upper and lower bounds in dotted red lines. Furthermore, a green line is presented which represents the historical load in 15 min resolution. This signal can also be used to derive the power reference level.

5.2.1 Simulation 1

Simulation Number	Start date	End date
1	January 1 st	January 8 th

Table 16: Frequency containment simulation 1 start and end dates.

As shown in *Figure 69* the scheduling unit manages to determine the capacity available for FC. Since the simulation is run for the middle of the winter, the chillers are not operating and will thus not contribute with power to FCR-N during this time. Due to this, the only DRRs that will contribute to FC are the AHUs. Their maximal capacity during this time is 200 kW with almost as many hours at 100 kW capacity. During some hours, almost 100 kW of capacity is lost due to rounding down to the nearest bid size, meaning that with just a small increase in power the bid capacity could have increased by 100 kW. Other hours the loss remains considerable in regard to capacity. Additionally, the scheduling unit manages to schedule FC during 6-8 hours per day, where most times, the hours are concentrated towards opening hours.

When comparing the scheduled capacity to the actual operation, as presented in *Figure 70*, it is clear that the DRRs perform FC when scheduled to do so. Furthermore, it can be seen that only day 2 to day 7 in each week has been scheduled. This is simply due to the fact that FCR-N scheduling is being performed one day in advance and thus, the first simulated day cannot be scheduled. Additionally, it can be seen in *Figure 71*, that during an arbitrary hour when performing FC that the tracking performance seems to be good. The power reference remains close to the filtered power grid frequency. Moreover, the SOC is not presented for this simulation since the chillers are not scheduled for FC-N and thus the ESS will not be activated.

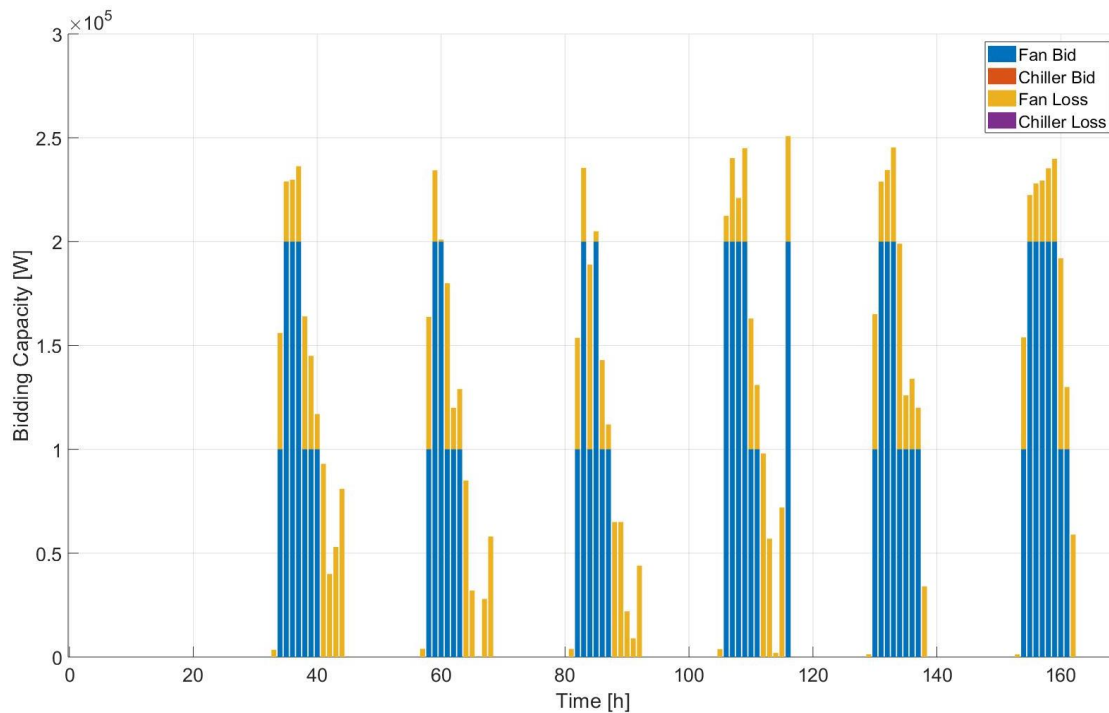


Figure 69: Available capacity for FC as determined by scheduling unit for Jan 1st to Jan 7th.

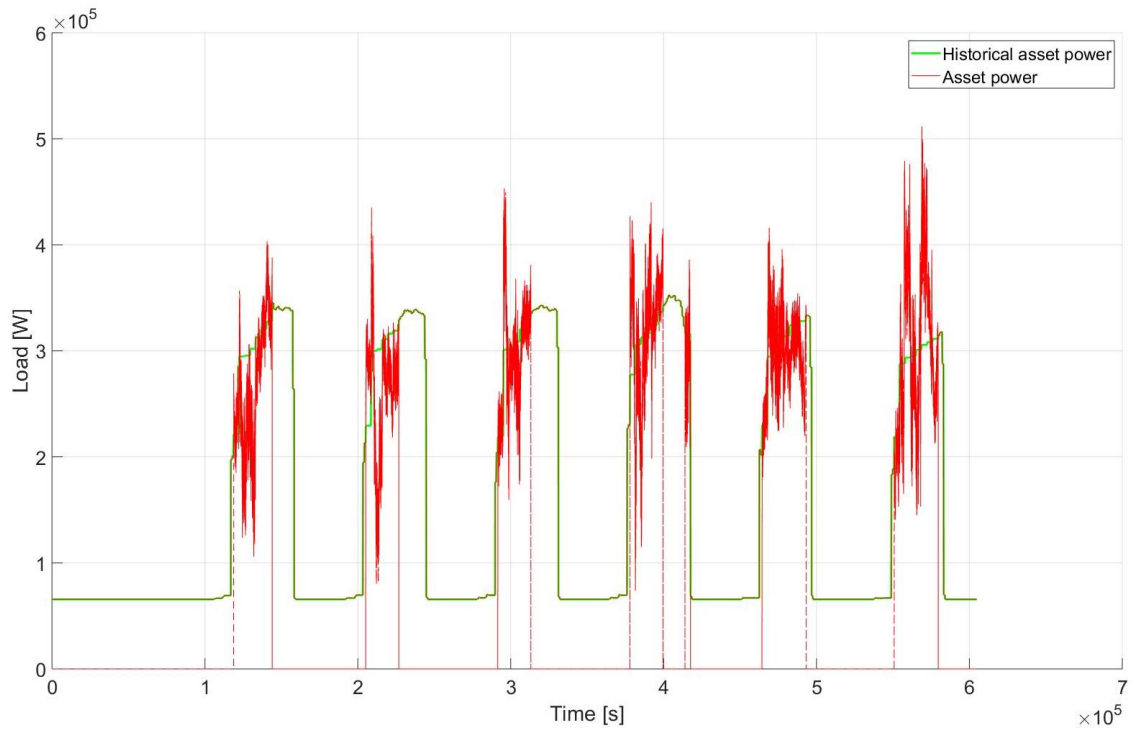


Figure 70: Power of assets during FC and normal operation during Jan 1st to Jan 8th.

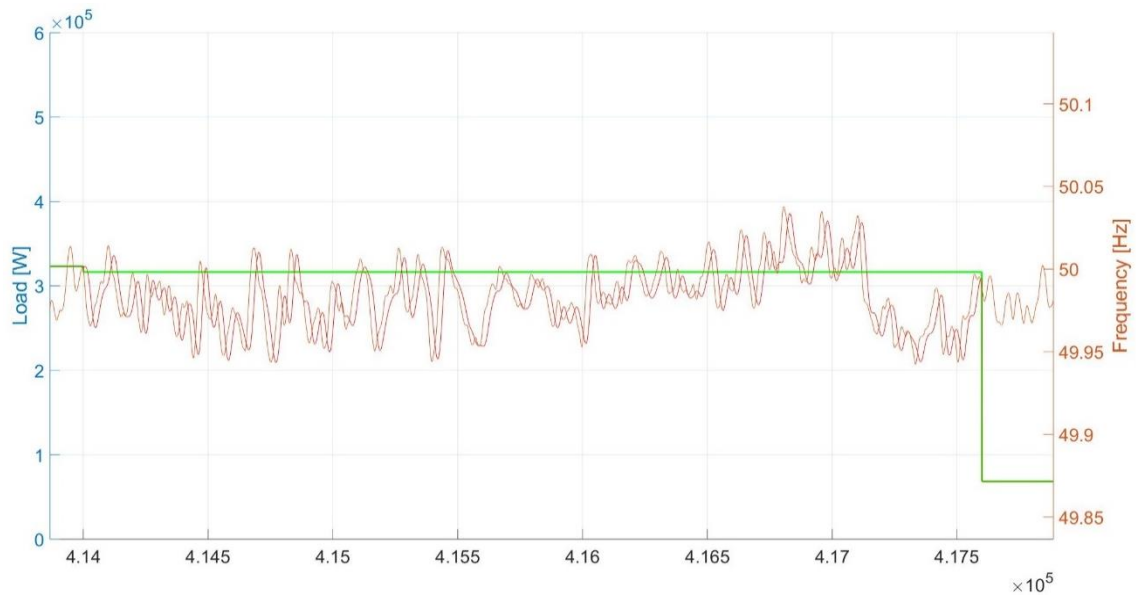


Figure 71: Power of DRRs during one hour of FC operation Jan 5th.

5.2.2 Simulation 2

Simulation Number	Start date	End date
2	April 2 nd	April 9 th

Table 17: Frequency containment simulation 2 start and end dates.

In *Figure 72* it is shown that for most hours only the AHUs are scheduled. However, some hours and days the capacity increases and the chillers also provide capacity for FC. However, they never provide a capacity of 100 kW themselves, meaning that they are reliant of the AHUs in order to participate. Additionally, the chillers manage to provide with sufficient extra capacity in order to increase the bid size during some hours. In general, capacity is available during longer periods of the day during this simulation than in the previous. The largest supplied capacity during this period is equal to 400 kW.

In *Figure 73*, the DRR power is as expected, and when viewing closer in *Figure 74* it seems as if the tracking performance still is good as even with the chillers included the system manages to track the filtered power grid frequency. Additionally, when studying hours when chillers have been scheduled, it can be noticed that no chiller activation or deactivation sequences can be detected, indicating that no activation or deactivation sequences occur, or that the ESS manages to compensate for the chillers efficiently. As shown in *Figure 75*, the ESS SOC only has small deviations meaning that the ESS only experiences little use during small scheduled chiller capacities.

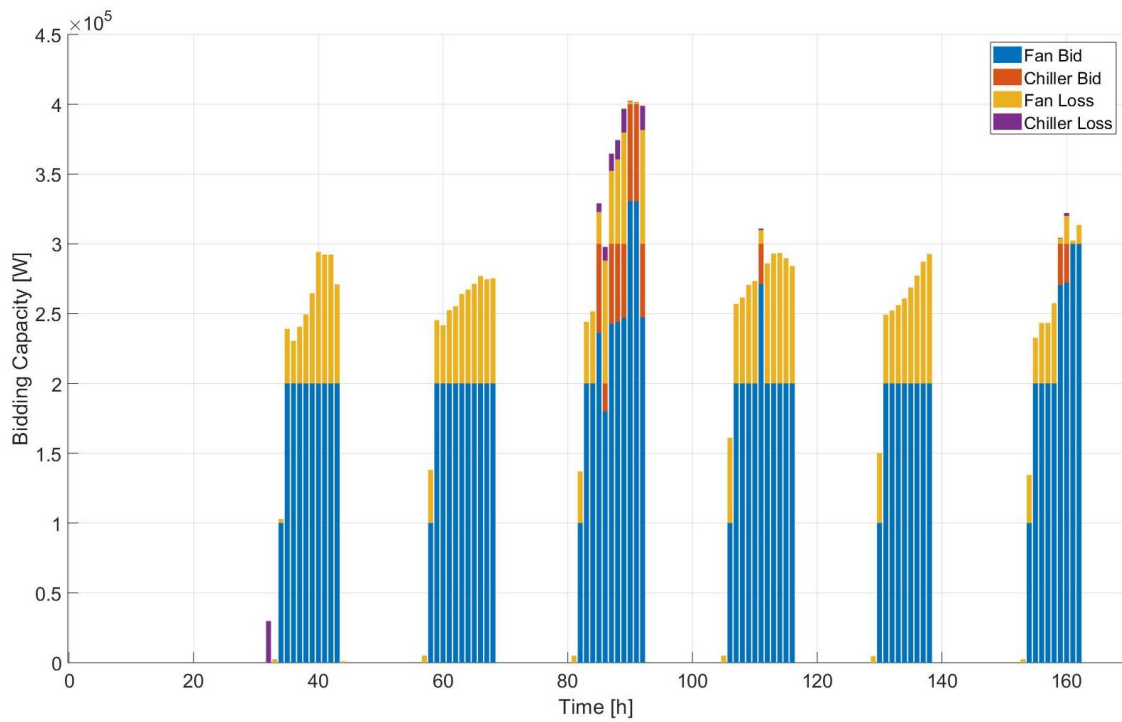


Figure 72: Available capacity for FC as determined by scheduling unit for Apr 2nd to Apr 9th.

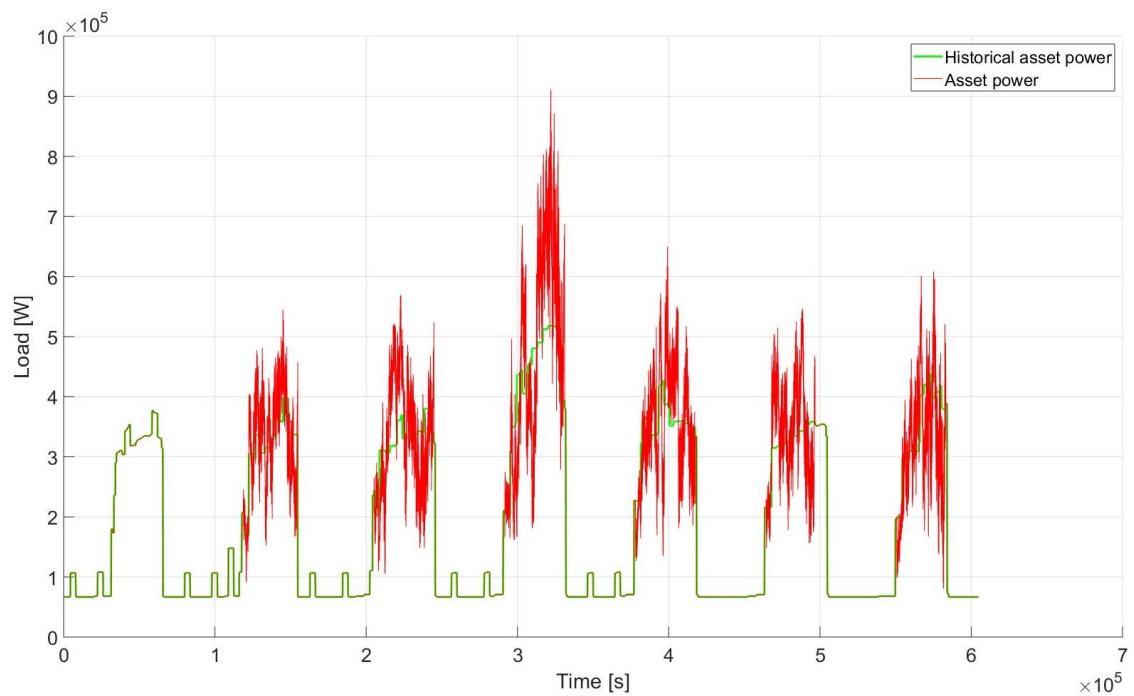


Figure 73: Power of DRR during FC and normal operation during Apr 2nd to Apr 9th.

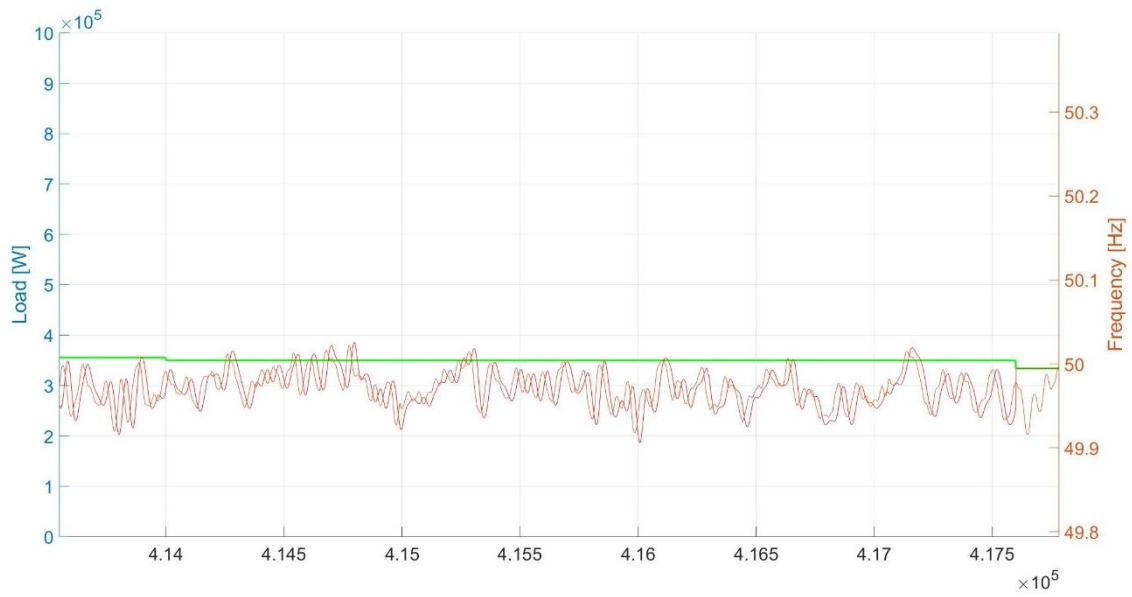


Figure 74: Power of DRRs during one hour of FC operation Apr 5th. Red line corresponds to power of the DRRs tracking the orange filtered power grid frequency signal.

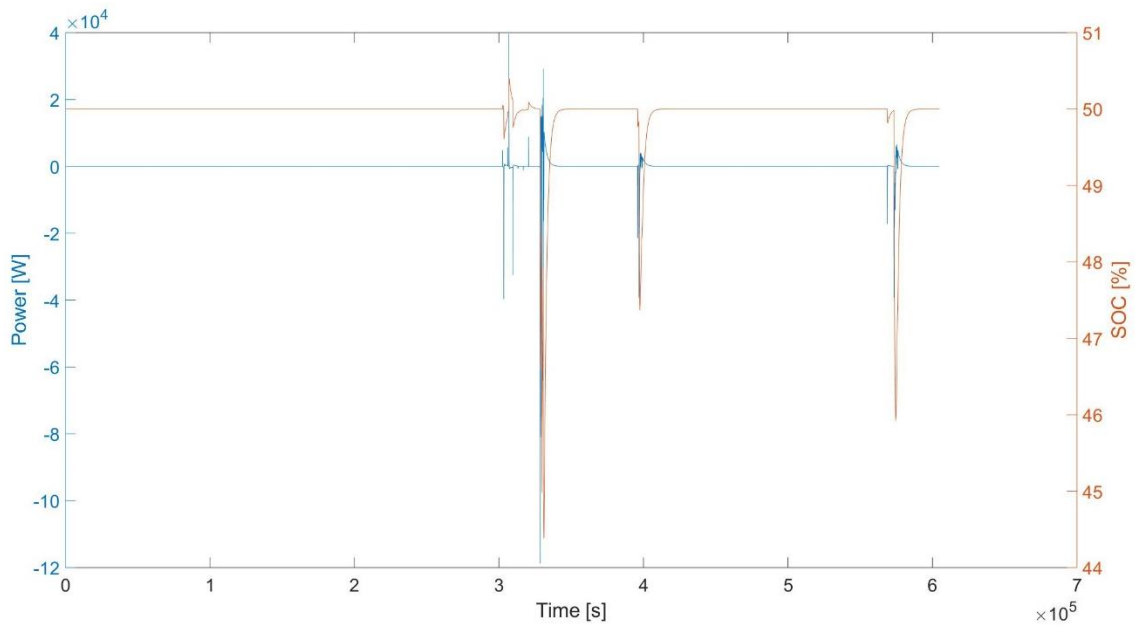


Figure 75: SOC and power of ESS during FC and normal operation during Apr 2nd to Apr 9th.

5.2.3 Simulation 3

Simulation Number	Start date	End date
3	July 2 nd	July 9 th

Table 18: Frequency containment simulation 3 start and end dates.

In *Figure 76* the scheduled capacities for simulation 3 are shown. It is clear that the overall available capacity increases significantly due to a large increase of chiller capacity. This confirms that the chillers have the largest capacity during the summer when cooling need is the largest. The chillers manage to contribute with 600 kW of power meanwhile the AHUs contribute with about 300 kW. The maximum total capacity is 900 kW, a considerable amount larger than the maximum for the previous simulations. Furthermore, in relation to the total capacity, the losses due to rounding down to the nearest bid are smaller than for previous simulations, but still similar considering actual capacity.

In *Figure 78* it is shown that the tracking performance of the DRRs remains good, even when a large amount of chiller capacity is used. Only a few outliers occur during the start and at the end of the balancing hour when the power reference level changes and the system adjusts to the change. When performing FC with large chiller capacity it is obvious that the balancing power which constantly increases and decreases with large variation, will lead to many chiller activation and deactivations which will have to be compensated for. By tracking the number of activation and deactivation sequences of chillers manually in the model, it was shown that about 6-10 sequences occurred during an arbitrary hour. This is problematic when considering the increased wear and tear of the chillers. Despite this the ESS manages to compensate the chillers whilst maintaining a DoD smaller than 15 % from its reference SOC of 50 %, as shown in *Figure 79*. The ESS utilization seems to be large when studying the power curve of the ESS. However, *Figure 79* presents the variations for an entire week. When studying the variations in closer detail it is apparent that they are not as frequently occurring as it might first seem.

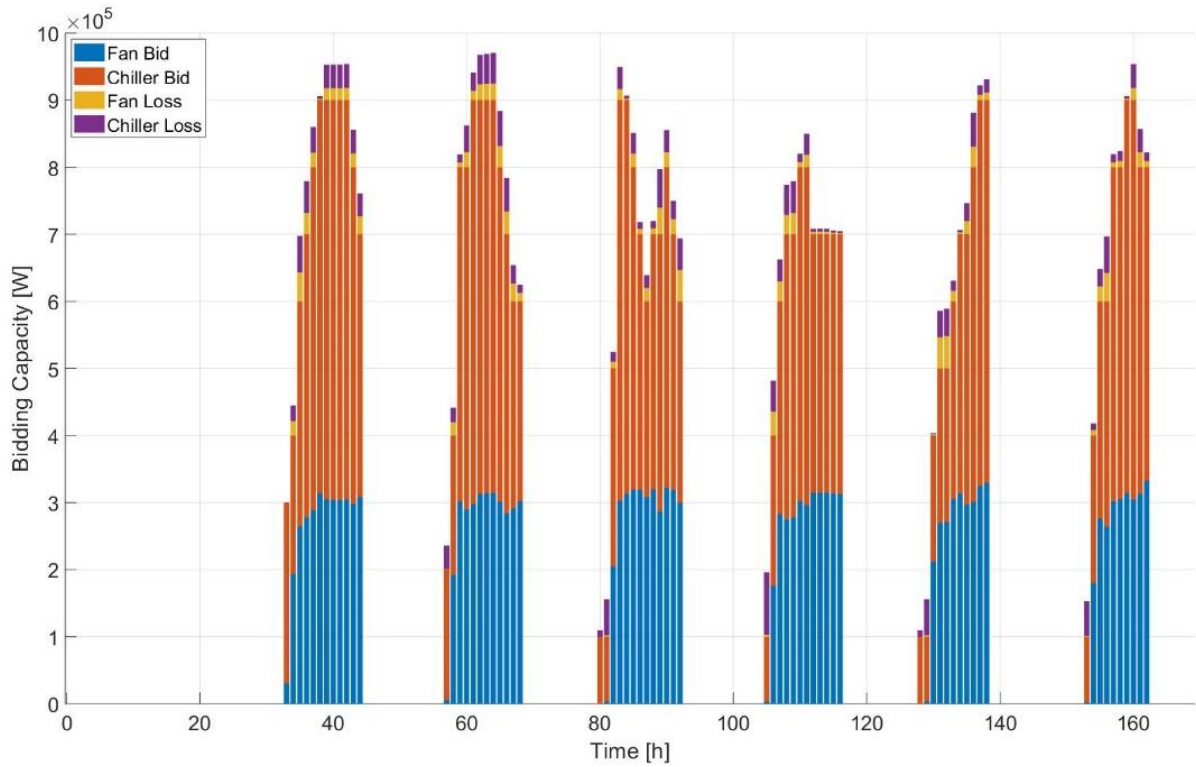


Figure 76: Available capacity for FC as determined by scheduling unit for Jul 2nd to Jul 9th.

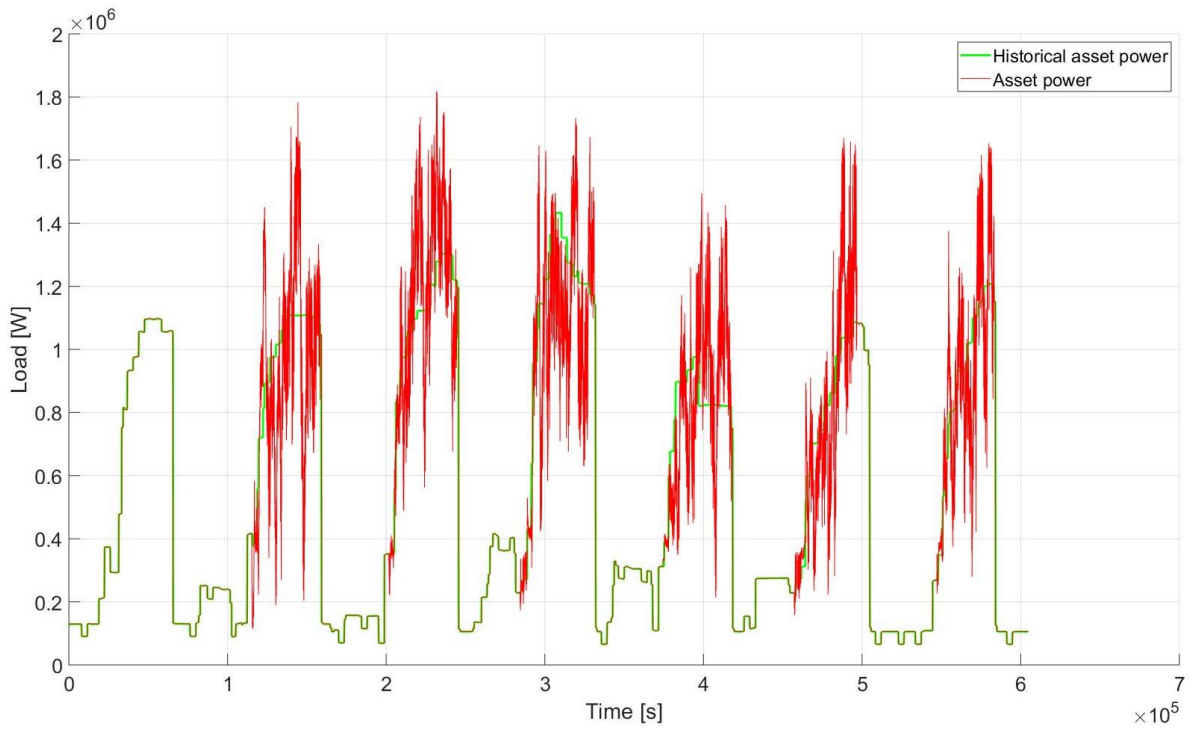


Figure 77: Power of DRR during FC and normal operation during Jul 2nd to Jul 9th.

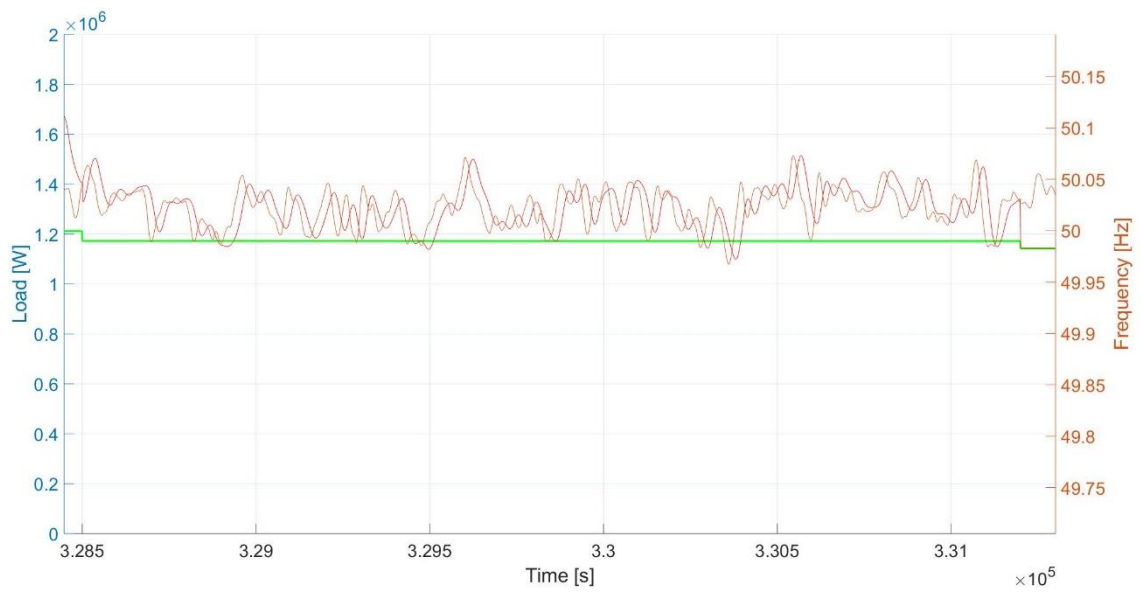


Figure 78: Power of DRRs during one arbitrary hour of FC operation during Jul 2nd to Jul 9th.

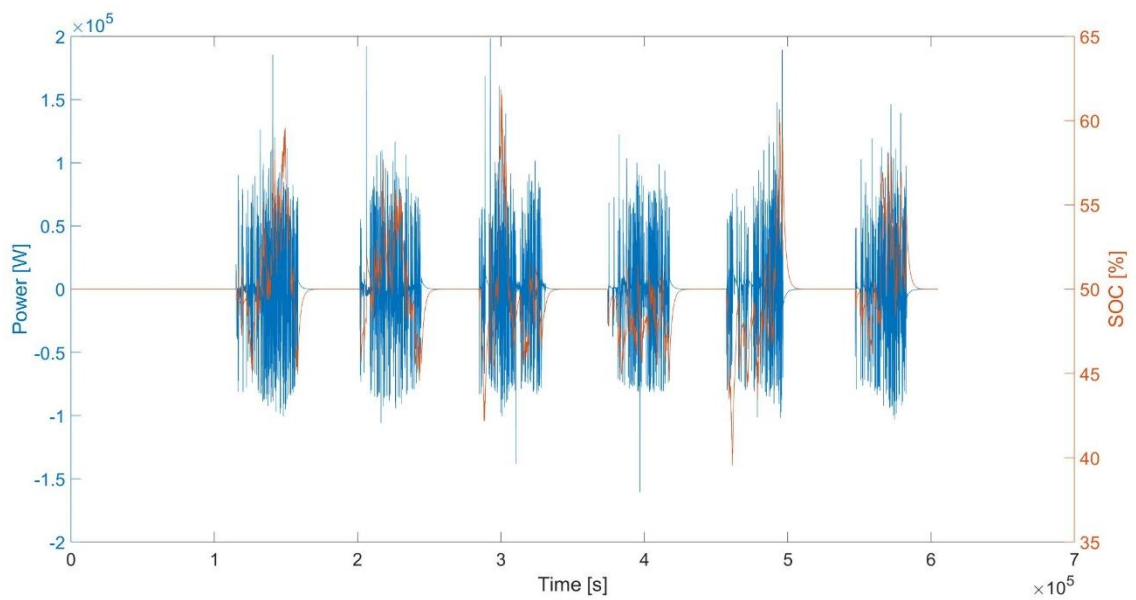


Figure 79: SOC and charging power of ESS during FC and normal operation during Jul 2nd to Jul 9th.

5.2.4 Simulation 4

Simulation Number	Start date	End date
4	October 1 st	October 8 th

Table 19: Frequency containment simulation 4 start and end dates.

As shown in *Figure 80*, the available capacity decreases from simulation 3. The capacity contributed by chillers is at largest just above 200 kW. The scheduling of chillers occurs during three consecutive days, suggesting a higher outdoor temperature during that period. The AHUs contribute with 200 kW most hours with the exception for the first hour each morning when the capacity is lower and also for some hours mid-day when their capacity is slightly increased due to chiller scheduling.

As expected, the tracking performance still seems to remain good as presented in *Figure 82*. There are no apparent outliers except for when the power reference level changes at the end of the hour. Furthermore, as shown in *Figure 83*, the SoC does not seem to have any large deviations since the largest corresponds to a DoD of about 11 %. Additionally, the utilization of the ESS in general seems to be quite low due to few variations in SoC. This is common for all simulations where the chiller capacity is low in relation to its overall rated power. This implies that there is a possibility to schedule the capacity of the ESS separately in order to increase the capacity on FCR-N or to increase system responsiveness.

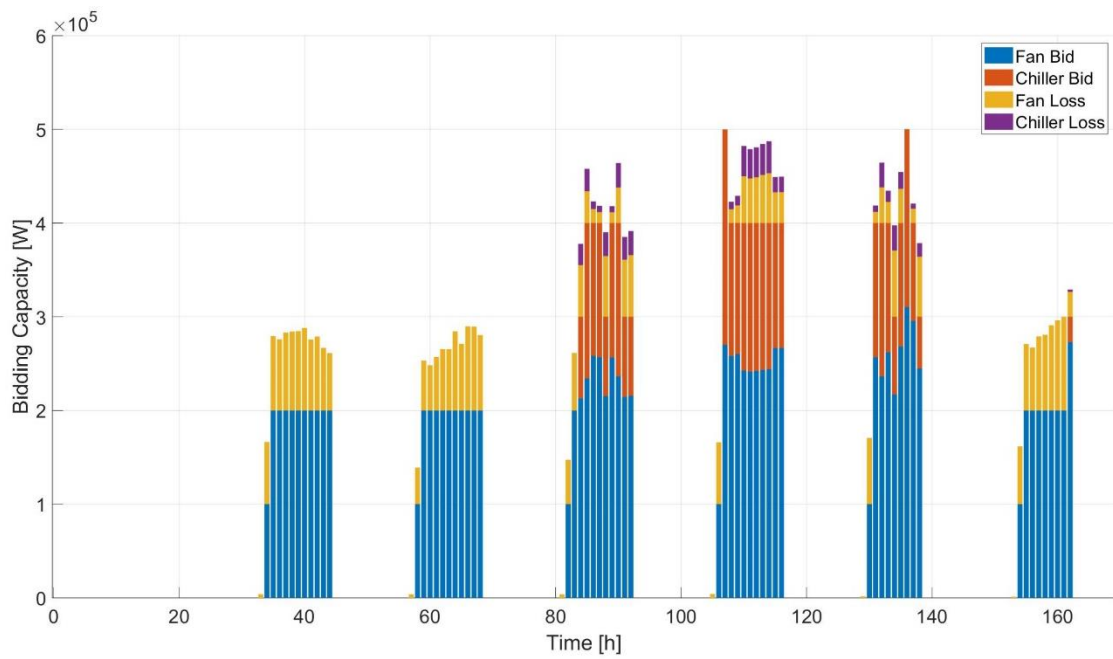


Figure 80: Available capacity for FC as determined by scheduling unit for Oct 1st to Oct 8th.

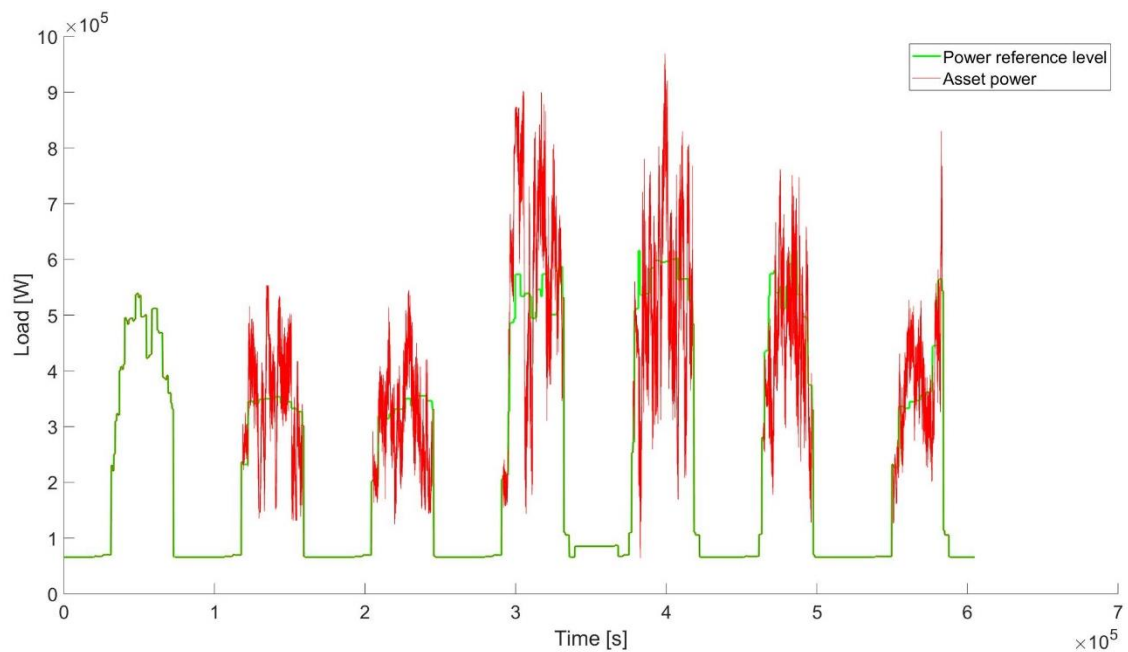


Figure 81: Power of DRR during FC and normal operation during Oct 1st to Oct 8th.

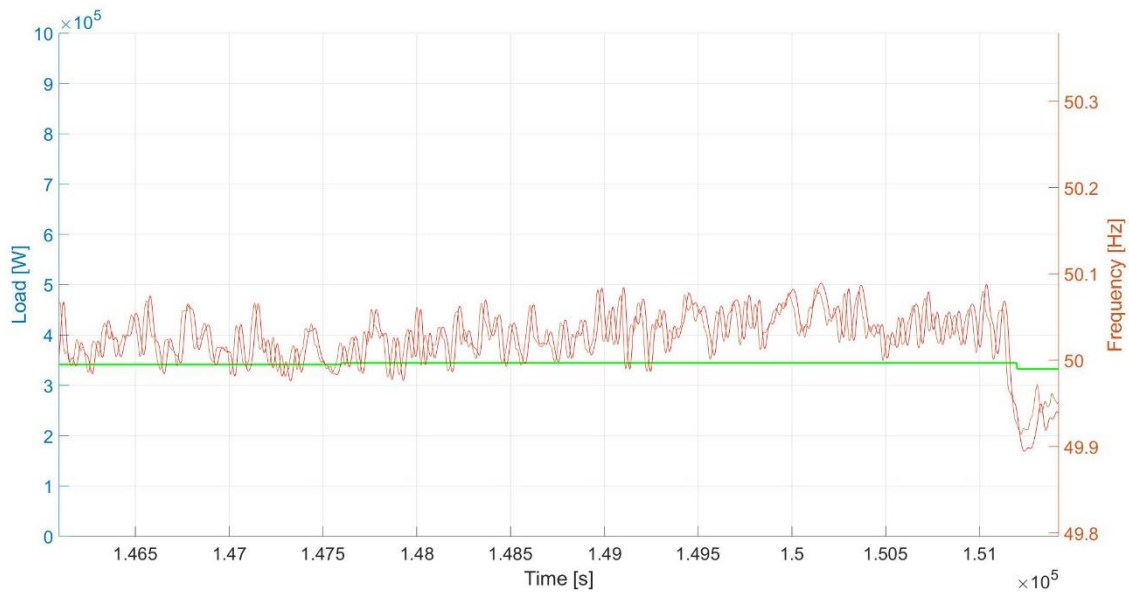


Figure 82: Power of DRRs during one hour of FC operation Oct 1st to Oct 8th.

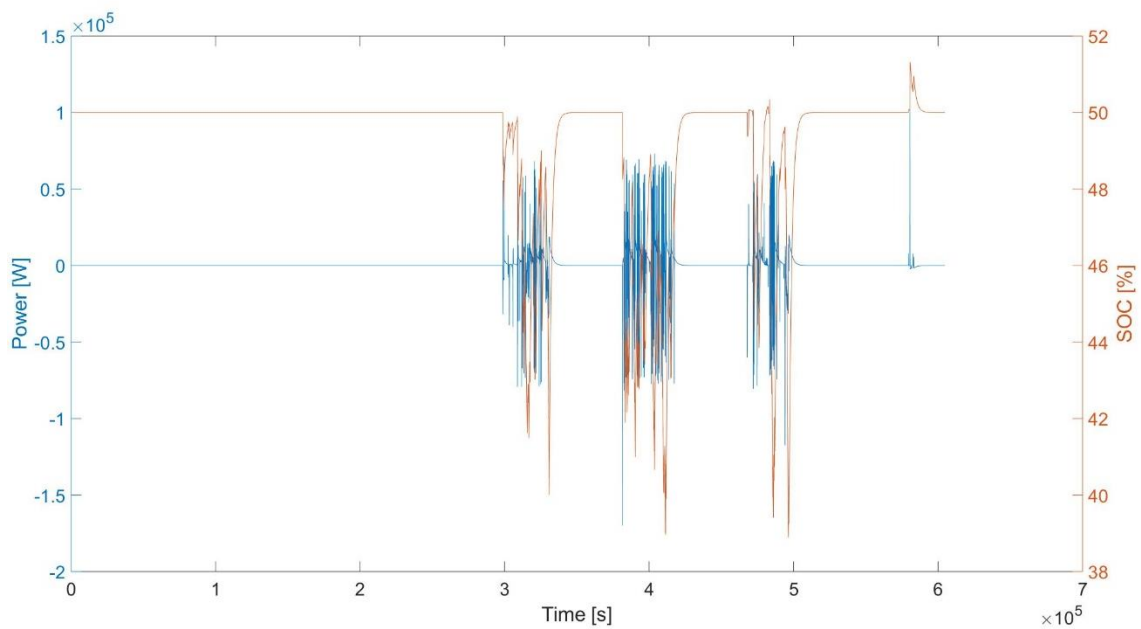


Figure 83: SOC and charging power of ESS during FC and normal operation during Oct 1st to Oct 8th.

5.3 Results summary

5.3.1 Prequalifying test

Simulation	Peak balancing error	Peak DoD	Peak ESS power	Peak ESS charging power
1	253 kW	0 %	0 kW	0 kW
2	0 kW	18 %	342 kW	33 kW
3	11.5 kW	18 %	342 kW	33 kW
4	0 kW	0 %	0 kW	0 kW
5	0 kW	11 %	128 kW	21 kW

Table 20: A summary of results from the prequalifying tests. The DoD uses 50 % SoC as reference.

As can be concluded from *Table 20* when studying the peak balancing error, the system without the support of the ESS does not manage to perform adequately, due to the poor chiller responsiveness. However, when the system is supported by an ESS the performance is adequate and it passes the prequalifying test in regard to system responsiveness. Additionally, despite having a large power contributed by the chillers, the ESS manages to keep a small DoD deviation from 50 % SoC. The power at this moment, when the DoD is the largest, corresponds to rated power of the ESS. Since this only occurs momentarily without any balancing error, it indicates that the battery is correctly dimensioned to pass the prequalifying test. Furthermore, the results show that without AHUs contributing with power, the chillers will fail the test marginally. This indicates that the chiller time constant of 40 s, which also is used in the ESS reference system is too slow. The AHUs, as a difference from the chillers, manage to perform adequately on their own. The ESS degradation caused by the prequalifying test would seem to be small as indicated by the small DoD and the fact that the utilization is low considering the rather short length of the test.

- The chillers combined with the ESS cannot pass the prequalifying test without the support of AHUs, based on the estimated chiller time constant.
- AHUs manage to pass the prequalifying test without the support of chillers combined with ESS.
- The prequalifying test will have a low impact on ESS SoH with consideration of the DoD and charging power.

5.3.2 Frequency containment

Simulation	Max AHU bid	Max chiller bid	Peak balancing deviation	Peak DoD
1	200 kW	0 kW	- 72 %	0 %
2	300 kW	70 kW	- 79 %	13 %
3	333 kW	602 kW	+ 82 %	12 %
4	300 kW	0 kW	+ 81 %	0 %

Table 21: A summary of results from the frequency containment simulation. The DoD uses 50 % SoC as reference. Peak balancing deviation is the largest relative power deviation from historical values.

As can be seen in *Table 21*, the AHUs available capacity increases during the summer months of the year, as indicated by the AHU capacity of simulation 1. This also applies for the chillers which drastically increase the available capacity during simulation 3. Since the chillers only are active for about half the year, this means that the ESS is only utilized during that time. Consequently, the ESS could provide extra capacity whenever the chillers are not scheduled, or whenever the scheduled capacity of the chillers is so small that no activation or deactivation sequence of the chillers occurs. Furthermore, it was shown that the largest deviations relative to the historical asset power is about $\pm 70 - 80$ %. This means that for any given hour during the simulated periods, when performing FC, the balancing power would increase or decrease the total power to the corresponding values, from the power reference level. Furthermore, it is important to note that the ESS experiences relatively small DoDs during all simulations. The largest possible DoD is 40 %, with a 50 % SoC as reference and considering the boundaries of 90 % and 10 % SoC, it means that a about 17 % DoD is underutilized during the simulated periods. Consequently, it is indicated that the ESS utilization is very low.

- The chillers are only utilized during the summer half of the year with an increasing capacity for warmer months, whereas the AHUs have about the same capacity all year, with only about 100 kW lower during some winter months.
- ESS utilization most times is very low, even when considering hours with large chiller capacity scheduled.
- The balancing power is oftentimes very large in relation to the power reference level resulting in large deviations from historical values.

6. Discussion

In this chapter the results of the thesis will be discussed. Initially, the reliability of the sources, methods and results will be highlighted in order to understand their impact. Further, the results from the prequalifying tests and the frequency containment simulations are analyzed. Lastly, appropriate future work on the subject will be suggested, both to improve the methods and results in this thesis, but also future work in order to contribute to new understanding in the field.

6.1 Reliability

6.1.1 Chiller time constant estimation

One of the most obvious liabilities in this thesis is the chiller time constant. Since the responsiveness of chillers today was, in accordance with literature, determined to be too poor due to the proprietary integrated control logic of the chillers, it was important to improve this parameter. According to the manufacturers of the chillers, this could be done by reviewing the control software and by installing VFDs. Since the increased responsiveness, which was vital for the application of FC, required reviewed software and new hardware, which has not been installed, this proved that system identification could not be performed experimentally. Consequently, the system had to be estimated based on sources, which in this case was the manufacturers themselves who approximated the time constant to 40 s. This value also cohered to the time constant which was extracted from the step response test of another chiller of about the same rated power. Given these two sources the time constant of the system model was set to 40 s.

Since the manufacturers estimation of the time constant also was not based on experimental results nor was based on calculated values, it is hard to determine whether this is a reliable source or not. Given that the manufacturer has some degree of expertise, the value should be more or less accurate, with a variability in the scale of ± 10 s. A larger error would indicate that the estimation is not made by an expert, and a smaller error would possibly require great knowledge of such systems or be based on calculated values.

Consequently, when viewing the performance of the chillers in FC, it is important to consider this possible error when estimating the time constant. A larger value would decrease performance and a smaller value would increase performance. Furthermore, the measured time constant from the step response test performed in literature also can not be considered to be completely accurate, despite cohering with the value estimated by the chiller manufacturers. This due to the fact that the chiller on which the test was performed was not of exactly the same size, was not of the same manufacturer and probably did not even have the same control logic. However, since the source cohered with the manufacturer's estimations, it does show that the time constant value, at least, is in the scale of 40 s. Despite this, the possible error of the time-constant value has to be considered.

6.1.2 Approximated load data

Beyond the possible error contributed by the time constant estimation, another error could be caused by the way that the AHU load data was calculated. In the method it was presented that the data corresponding to the VFD output speed set-point only was available for both the supply and exhaust fan for 14 AHUs. This was then, together with the rated power of each fan, used to calculate the historical load data for the 14 AHUs. However, since a representation for the historical load of all AHUs was needed, this data was extrapolated to include the remaining 21 AHUs. This was done by calculating the AHU load relative to the rated power of all 14 AHU and then by multiplying with the rated power of all 35 AHUs. Due to this approximation, the load characteristics was assumed to be the same for all AHUs.

Considering that the operating hours for all AHUs are more or less the same and that the total load curve of Väla is relatively consistent, it was assumed that the error caused by this extrapolation would be rather small. Furthermore, when considering that all capacities of the bids placed on FCR-N were rounded down to the nearest multiple of 100 kW, the impact of the error caused by extrapolation was assumed to be negligible. However, it is important to note that the bid estimation system thus only is applicable for an aggregated amount of assets and not individual AHUs, which would have required individual accurate historical load data.

6.1.3 Single system identification

A third possible liability in this thesis is how system identification was performed on the chillers. The system identification process required an active power measurement of the supply and exhaust fan during a step change in the VFD output speed signal. This measurement would ideally, be performed for both the supply and exhaust fan of each AHU at Väla. This would result in the step response test being performed a total of 70 times in order to be able to model each AHU at Väla. Furthermore, it can be discussed how accurately a single test can be when performing system identification of an AHU. Possibly, the test should be performed for varying prerequisites, where factors such as the pressure, temperature and humidity should be taken into consideration when performing system identification.

However, due to constrains which were presented in *AHU system identification*, the test could only be performed once for a single fan. This means that the result of the step response test only truly represented the characteristics of the fan which was measured. Consequently, the only choice was to assume that the system identified would sufficiently describe the characteristics of all other fans as well. Due to this, the resulting transfer function from the system identification process was normalized in order to be applicable for any AHU's rated power. The possible error of this estimation is hard to determine. The time-constant of a fan could be argued to be dependent on the inertia of the fan and thus its size. This would imply that larger fans would have longer time constants due to larger inertias. Consequently, this would mean that the fan which the system model is based on, which is large considering its rated power of 37 kW, in reality would have a time constant larger than that of the other fans. However, since larger AHUs, and thus larger fans, also have larger electric motors, the impact of the increased inertia should be counteracted by the increased power of the motor. With this reasoning, the time-constant should be the same for most fans, given that the ratio between its inertia and rated power is approximately the same for all fans. Thus, the error should be small. However, this is to be verified by performing more system identification test in the other AHUs.

6.2 Results

6.2.1 Chiller performance

The results of the prequalifying test prove that with the chosen sequential operating scheme of the chillers, where activation and deactivation of chillers occur during FC in a sequential fashion, the chillers are not capable of qualifying as balancing resources due to their long activation times. The activation sequence will, depending on the oil circulation in the compressor, take anywhere from 30 s to 180 s. Since this characteristic is not included in the model, where all activation sequences take 180 s to perform, the performance of the chillers could in reality be better than presented in this thesis. However, when considering the results of simulation 3, which was performed without a capacity contributed by the AHUs, it was shown that the responsiveness of the chillers was too poor, even with compensation from the ESS. Consequently, this implies that even with a shortened activation time of 30 s, the system does not perform adequately. The reason for this is the ESS reference system which has the time-constant of 40 s, which together with any other delays from filters, will prove to have too poor responsiveness. By adjusting the time constant of the ESS reference system or the filters to be faster, the chillers could pass the prequalifying test, given a larger power and capacity of the ESS. This would however cause problems regarding the chiller compensation during FC operations. Thus, it would be more suitable to decrease the delays of the filter and thus accept more high-frequency components in the power grid frequency signal. It is also noteworthy that some estimations of the chiller time-constant was lower than 40 s, possibly indicating that chillers could perform equally to AHUs.

Due to the possibly large error in the estimation of the chiller system time constant, the chillers could prove to perform sufficiently in regard to their responsiveness and thus, no adjustment of filters or ESS reference system would be needed. However, considering a possibly larger time constant, this would imply even worse chiller responsiveness, possibly to a degree where the responsiveness could not be adjusted for by the ESS reference system or by filter parameters. Therefore, it is important to perform system identification on a reviewed version of the chillers in order to verify their estimated performance in the model. If the time-constant would prove to be too large, the chillers could instead possibly be used for secondary or tertiary frequency regulation.

When studying the number of activations and deactivations of chillers during the FC simulations the results indicate that for most simulations there is an appropriate occurrence. It is further shown that the occurrence of these sequences is proportional against the overall capacity of the chillers that participate on FCR-N, where an increased capacity leads to an increased number of activations. This is simply due to the fact that the larger capacity includes more power levels in the power band corresponding to chiller activation. However, the number of activations is logically also proportionate against the number of frequency oscillations, and their respective amplitude, around the power levels corresponding to a chiller activation. Since the number of activations in general is low, it indicates that the implemented filter is configured appropriately. However, in FC simulation 3 when a high chiller capacity was utilized, it was deduced that there was an increased occurrence of activation and deactivation sequences. This suggests a need for a slightly larger hysteresis band than 20 % of a chillers rated power. Although, another implementation of a hysteresis function could be studied, where instead of using the signal amplitude as a determining factor, a delay could be implemented where the hysteresis changes only occurred if the signal persisted above the threshold for a certain amount of time. This would decrease the number of unnecessary activation sequences where they were followed by a deactivation shortly after. This activation logic is only relevant though if sequential operation is implemented.

6.2.2 ESS performance

When studying the results of simulation 1 and simulation 2 of the prequalifying test, the differences of using the ESS in order to compensate for the chillers are obvious. The ESS manages to improve their performance considerably, to a point where the operation of only chillers and the ESS, without the assistance of AHUs, just marginally fail the prequalifying test. This failure is however, caused by the large time constant of the ESS reference system and would in reality be adjusted after performing true system identification of the chillers in an experimental manner. Due to this, the responsiveness of the combined chiller and ESS will not be regarded as an error, but rather a result of the delimitations which had to be made. An alternative way to increase the responsiveness of the chillers would be to decrease the time constant of their frequency filter. The filter time constant was chosen on the basis of the time constant of the chiller

system transfer function. However, the filter time constant does not necessarily need to be that large. The exact implications of the filter parametrization need to be studied in a more detailed manner where the balance between responsiveness, degradation and overall performance would be optimized. Optionally, another way to increase responsiveness would be to research alternative control methods. One method that possibly could offer larger responsiveness would be to use the ESS as a primary balancing resource and to control the chillers as a secondary resources. This would use the resources in a more suitable way where the full responsiveness of the ESS could be utilized and the slower chillers would take the larger part of the base load.

A factor to consider when determining the ESS performance is the utilization when performing FC. The results proved that the simulated time periods never resulted in a full utilization of the ESS capacity where the largest DoD was 18 %, giving an unused margin of 22 % in either direction. Just studying these results, it would indicate that the capacity of the ESS is too large and thus, that it is incorrectly dimensioned. However, considering that the capacity was determined by performing a simulation of FC for an arbitrarily chosen week during the summer, and that during that time point a DoD of 40 % was reached, thus fully utilizing the battery capacity, it would imply that the ESS is not over dimensioned. This does although illuminate a potential problem with the method used to determine the ESS capacity. Since the periods used in the FC simulations had a significantly smaller impact on ESS utilization than the period used to size the ESS, it indicates that that different periods could have large variations in ESS utilization. Consequently, the period used in order to determine the required ESS capacity, might not be the period with the highest utilization and thus, the ESS might in practice require an even larger capacity than 100 kWh. This highlights the problem of performing the simulations on a weekly basis instead of an annual basis where the information in historical data between the selected simulated periods, is lost. Consequently, in order to accurately determine the required battery capacity, the simulation should be performed for an entire year, and possibly, also for several years in order to account for annual variations. Alternatively, the battery could be sized after the largest possible error which could be derived by performing a step response where activation of all chillers was included. This could however, lead to a significantly under-utilized ESS during most times of the year. The rated power of the ESS however, was

correctly dimensioned since it only was determined by the minimum requirement of the prequalifying test.

Further considering an ESS with a rated power of 420 kW and a capacity of 100 kWh, or possibly more as previously mentioned, it is important to discuss whether the implementation of such an ESS would be an efficient solution in order to qualify the chillers. To determine this, the operating scheme of the chillers has to be considered. The advantage of the sequential operation scheme was that the overall chiller capacity was increased, since no power was lost to idle operation of all chillers. However, as a difference from the parallel operation scheme, where all operation occurred above the idle power level when all chillers already are activated and no ESS compensation is needed, the sequential operation scheme requires an ESS to compensate for the error of chiller activation during operation. Consequently, the use of the ESS has to be motivated by a sufficient increase of chiller capacity. Considering that the sequential operation scheme can increase the available capacity by up to 246 kW from the parallel operation scheme, as presented in *Chiller operation scheme*, a required ESS power of 420 kW and 100 kWh seems rather large. Furthermore, when considering that the availability of chillers proved to be rather low for most times of the year where an increased power seldomly came to use, it would indicate that the sequential operation scheme, which requires an ESS of that specification is unnecessary. This reasoning however, becomes problematic when considering that the ESS could be scheduled for FC as well, whenever the chillers do not require the ESS's full capacity. This would motivate the use of the ESS and thus also the sequential operation scheme of the chillers. In order to determine which solution is best, a cost-based analysis of both implementations would have to be performed where the cost and the income of both solutions would be considered.

A part of this cost-based analysis is to consider the degradation of the ESS caused by its operating scheme. Regarding the utilization of the battery capacity, it is apparent that the cyclic degradation of the ESS caused by large DoDs does not constitute a problem since the DoD in general is quite small. Consequently, this implies that the degradation caused by large charging powers is quite small when considering the rated power of the ESS. Furthermore, due to the charging strategy of the ESS, the net power of the ESS will in actuality be smaller than the power contributing to chiller compensation. Thus,

the degradation will be even smaller. However, it is important to consider that due to the specification of the suggested ESS, the C-rate is rather high with a value of about four, implying that the cyclic degradation already is higher than that of a battery with lower C-rate. However, due to the fact that the number of cycles is rather small since the ESS only is operational once the chillers activate, the cyclic degradation should be quite small despite this. Furthermore, should the calendric degradation also be small due to a SoC which mostly remains at 50 % and assuming an appropriate temperature.

6.2.3 AHU performance

In the prequalifying tests, especially in simulation 1 and in simulation 4, it is apparent that the performance of the AHUs is sufficient in order to perform FC. The responsiveness surpasses the minimum requirements with a margin. It is noticeable when the AHUs are combined with the chiller systems that the AHU compensates the chillers for their insufficient performance. Furthermore, since the chillers do not manage to perform adequately on their own, it suggests that the AHUs should always be scheduled in combination with the chiller or should be scheduled on their own. However, without available capacity from the AHUs, the chillers should not be scheduled. Given the fact that the AHU can pass the prequalifying test with a margin, the possibilities of using filtering techniques that decrease the wear and tear whilst increasing the time delay of the system is possible. Furthermore, since the control method in this thesis is built on the fan speed offset method, which is the fastest of the three control methods presented in 2.7.4 *Control systems*, this implies that there could be a margin to implement a slower method such as the supply pressure/mass flow offset method, if it proves to be more economically viable. This way, some of the control systems downstream of the AHU, could be circumvented, easing the installation and configuration of a DR system, dispatching AHUs.

6.2.4 Scheduling unit performance

Studying the FC tests, it seems as if the scheduling unit performs adequately. But determining this is quite complex and uncertain. From the chiller and AHU load data presented earlier, it would seem as if the capacity increases during the summer months when the ventilation and cooling need increases. This conforms with the results where there is a clear increase in chiller capacity and a small increase in AHU capacity during the summer half of the year.

The impact of the implemented boundaries of the load corridor used for bid estimation are unknown, but do not seem to be a considerable limiting factor since both the AHUs and the chiller come close to their respective maximum capacities of 400 kW and 600 kW respectively. However, the boundaries miss to include several factors which could prove to be vital when determining the available capacity.

Firstly, it is important to note that throughout the FC simulations, it was noticed that the balancing power relative to the power reference level, or rather the historical load, was very large. In many instances the balancing power increased or decreased the power from its historical value by about 70 – 80 %. When considering that the HVAC system reduces its load momentarily to 20 % of its historical value, it sounds quite drastic in regard to the impact on indoor climate. However, when considering the fan affinity laws in (3) to (5), it is apparent that despite having potential decrease of power corresponding to 80 % of the AHUs' historical load, this would only correspond to about a 50 % decrease of air flow, due to the cubic relation between power and air flow. Given this, it can be argued that the impact on the indoor climate would be smaller. Additionally, since these large deviations from historical load mostly occurred during short periods of time, the impact on indoor climate would be even smaller. Despite this, the indoor climate implies a potentially decisive boundary which should be considered by the scheduling unit when determining available DR capacity of the HVAC system. In order to implement this as a boundary however, the parameters affecting the indoor climate, if varying, would have to be forecasted. This could for instance include the number of visitors at Väla, the outdoor temperature, solar irradiance and more.

Secondly, the boundaries in this thesis were solely based on the experimentally tested boundaries for the AHUs and the sourced boundaries for the chillers. Since the system

identification process only was performed on one AHU, this means that the boundaries solely are based on the boundaries of that AHU. Boundaries from more AHUs could not be taken into consideration since these boundaries are explicitly unknown and have to be determined by experimentally testing the upper and lower boundaries. Additionally, since the boundaries were based on one specific AHU, the effects of interconnected AHUs, which are common at Väla, are unknown. Consequently, in order to accurately determine the available capacity of each AHU, the bounds of each AHU has to be experimentally verified. If this was to be performed for this thesis, the overall capacity would be expected to decrease or remain the same since the boundaries of the AHU which acted as a basis for the system identification process, had rather small boundaries. The boundaries of the chillers are rather unknown and have to be examined further. Factors such as refrigerant temperatures and capacities of downstream components such as pumps and cooling towers are unknown, but also have to be considered.

Thirdly, one boundary to take into further consideration is the boundary determined by the power subscription. In this thesis, the boundary is implemented with a completely accurate forecast of the load which in practice would not be possible. Instead, this would have to be either based on historical values, or it would have to be incrementally increased for each day if the maximum where the load was higher than any previous day. The new value would then be a benchmark for following days, when the capacity is to be estimated. Alternatively, if the income generated by participation on FCR-N could justify an increased power subscription cost, the boundary could be neglected. However, considering the increasing capacity shortage of the distribution grid, this solution should be implemented sparsely.

Lastly, one boundary which was neglected in this thesis is the forecasting error. Depending on the amount of parameters which have to be forecasted the impact of the forecasting error will vary. Furthermore, since the forecasting error also varies depending on how far forth data has to be forecasted, a strategy whether to place bids one day ahead or two days ahead has to be considered. The most important parameter to forecast is the load of the asset which is going to contribute to FC. In the case of Väla, this would be implemented for each AHU where some AHUs would contribute with more or less capacity. Beyond forecasting the load of the contributing assets, further parameters for bounds that are dynamic would have to be considered. These could include the indoor

climate, power subscription fee, PV generation and more. The impact of the forecasting error has to be determined specifically for each parameter and for each forecasting method implemented.

Considering all the mentioned bounds which have not been included in this thesis, but that could make up a limiting factor in regard to the available capacity, it is reasonable that the actual available capacity is smaller than that presented in this thesis. Consequently, the capacity presented here should possibly be interpreted as an exaggerated value. However, the trends presented in the results should still be valid.

6.2.5 Overall performance

Considering the entirety of the result, it is seen that the prerequisites for a VPP to perform primary FC, by dispatching the assets of a commercial building are good, in consideration to available capacity, performance and the implemented control system. The proposed VPP manages to qualify to FCR-N, given the configuration and parameters used in this thesis. However, determining how well the VPP performs FC is problematic due to the unclear requirements set by SvK. As presented in *4.4.2 Frequency containment*, upper and lower boundaries were defined with the basis of the qualified system. Since these boundaries do not represent the possible systems that would perform adequately, but rather are defined after an acceptable deviation from the AHU and chiller systems, a deviation outside these boundaries does not necessarily mean that the performance is poor. Due to this problematic definition set by SvK it can only be assumed that if the assets pass prequalifying, they would perform FC adequately. With this reasoning, and by studying the characteristics of the results when performing FC, it would be suggested that the overall ability of the VPP to perform FC is good.

Studying the characteristics of the DRRs, i.e. the AHUs and the chillers, it is obvious that the responsiveness of the AHUs is good. The chillers however, based on their estimated time-constant could only be considered to have fair responsiveness. However, since this parameter is subject to a possibly large variation, the responsiveness could prove to be as good as the AHUs but could also be worse than what it is estimated to. If this is the case, the chillers most likely would not be suitable for primary FC but could perhaps instead qualify as resources for secondary or tertiary regulation, or load shedding. Moreover, all assets have rather high sheddability since their lower boundaries have proven to be both low and few. Furthermore, since the AHUs inherently can be controlled by the BMS, only with smaller adjustments to the software, they present a high controllability whereas the chillers currently do not present as high. However, with a review of their control logic and by installing VFDs this can be improved greatly. With this in consideration, the AHUs seem to be well suited for FCR whereas the chillers could possibly be well suited depending on their actual time constant and the used control logic.

7. Conclusion

In this chapter the conclusions of this thesis are presented. By summarizing the results and the main points of the discussion, the general outcome of the thesis method is settled. Furthermore, by answering the question formulation the scope of this thesis will be covered.

The scope of this thesis was to study the ability for a VPP to contribute to balancing of the power system by performing primary frequency regulation. This was to be done by determining whether the implemented VPP could qualify as balancing resource and by studying how well the commercial building of the case study could be used for FC. Furthermore, the inherent assets of the commercial building were to be analyzed in regard to their sheddability, controllability and responsiveness. Moreover, the scope was also to study how the VPP could be implemented to provide increased flexibility to the Swedish power system.

The proposed way of implementing the VPP with the regulation controller and the scheduling unit, showed that the overall control scheme worked in regard to the scheduling and regulation process. The scheduled capacity of the assets was large in relation to their historical load but did take the main boundaries and power levels into consideration. This scheduling process was determined to have potential for further development to include forecasting errors, consideration of the indoor climate and scheduling of the ESS as well. The proposed assets and their corresponding control system proved to be a viable implementation. The fan speed offset method presented great responsiveness to a point where another slower, easier to implement, method likely could have been chosen. The chillers with the parallel activation and sequential operation scheme were also viable given the assistance of an ESS. The control system implemented for the ESS functioned as planned but did prove to struggle whenever solely chillers were scheduled, suggesting a factor to take into consideration in the scheduling unit.

Studying the assets of the commercial building used in the case study, it was shown that the AHUs proved to be a viable balancing resource to include in the VPP portfolio. The use of the chillers also proved to be viable given the suggested control system.

However, the possibilities of using parallel operation of chillers has not been neglected and should still be considered as a possible viable method of controlling the chillers.

More important although, is the estimated time-constant used in this thesis which will have to be verified experimentally, through a system identification process. The AHU and the chillers were chosen due to their high sheddability, were most parts of the loads can be shed, and their high controllability, through the integration with the BMS. The responsiveness of the AHU was confirmed via a system identification process and the responsiveness of the chillers was estimated based on several sources. Other possible assets were neglected due to the failure in consideration to one of these aspects.

With this said, it is concluded that a VPP utilizing the commercial building in the case study does have the prerequisites in order to perform primary FC. It manages to qualify as a balancing resource on the market FCR-N, given the configuration in this thesis. Moreover, the VPP manages to perform FC in what is determined to be an adequate way.

8. Future work

In this chapter different subjects for future work suggested in order to forward the work on the thesis topic. These are chosen to achieve a more nuanced and complete study in the area. Following this, some ending remarks with an outlook on the future of virtual power plants, demand response and frequency containment is presented.

8.1 Thesis expansion

In order to highlight the possibilities for future work in the thesis's topic, several areas will be presented. These areas have partly been raised due to the delimitations in this thesis where their respective impact has to be determined. Additionally, the results and discussion in this thesis has resulted in new topics which would be interesting to study in order to complement the results in this thesis.

8.1.1 Chiller time constant

Suggestively, the first future work to perform would be to verify the system time constant of the chillers. By using accurate models with a physical representation, the time constant could be simulated and verified with the reviewed control logic and with installed VFDs. Alternatively, if this alteration was made to the existing chillers, a system identification procedure could be performed in the same manner as performed for the AHUs. Depending on the results of the step response tests, it could prove that the chillers are more or less suitable for primary FC and possibly should be utilized for another purpose. The application of HVAC loads for demand response purposes is a relatively new area which describes why the chillers might not be suitable with their inherently slow control logic. However, this is something that might change with future implementations of large electrical loads where demand response compatibility could be a requirement thus, removing the necessity to retrofit hardware and to reprogram control logic.

8.1.2 Forecasting system

Further on, a forecasting system of relevant parameters should be implemented. These parameters will at minimum include the load of each DRR but could be expanded to include parameters needed for determination of dynamic bounds in the scheduling unit. The accuracy of the forecasts could have a large impact on how the control logic of the VPP and will thus have to be considered. Additionally, the VPP operator will have to take the requirements of each market into consideration when configuring the forecasting system. When performing submetering on FCR-N for instance, it could be required to forecast the load on an asset basis for each sub-metered component instead of forecasting the load at the point of connection to the grid which otherwise would have been typical for these types of applications. Furthermore, if the VPP was implemented to perform on a multiple of markets, generating more value streams, the forecasting system could also be implemented to forecast market pricing, enabling more educated decision making in income-based optimization of VPP operation.

8.1.3 Indoor climate

The impact of FC on the indoor climate could prove to be one of the largest limitations in regard to the available DR capacity VPP. Either by performing experiments on smaller secluded climate zones in the building or by simulating the impact in a thermal model of the building, using the scheduled capacities and the corresponding balancing power in this thesis, the impact on the indoor climate could be estimated and related to the scheduled capacity, possibly as a dynamic bound in the scheduling unit. However, if this indoor climate was to be fully considered in the operation of the VPP, it would be required to forecast the parameters that are possibly affecting the indoor climate. Parameters such as outdoor temperature, humidity, solar irradiation and number of visitors could prove to become vital to forecast and to use as inputs in a thermal model of the site. Alternatively, experiments of typical FC operation could be used as a basis in order to determine static boundaries. Static boundaries would be easier to implement whilst still taking the indoor climate into consideration when determining the overall flexibility, making them a possible to a full forecasted thermal model.

8.1.4 ESS scheduling

Additional future work that can be performed is to develop an algorithm to determine when and how much capacity of the ESS to schedule. Since the ESS utilization proved to be low both throughout the year and throughout the day, since it only operated during daytime when the chillers are active, the ESS provides unused capacity available for FC. Considering that the ESS has very high responsiveness, it could prove to be suitable for a niche market with higher requirements of responsiveness, such as FFR. Additionally, there are some periods where just small incremental increases of capacity would increase the overall bid capacity on FCR-N. In many cases the ESS could possibly increase the bid size whilst still being able to support the sequential operation of the chillers, increasing the efficiency of the dispatch of VPP assets.

8.1.5 Parallel chiller operation

In this thesis the sequential operating scheme of chillers was implemented in order to increase the DR capacity available. However, if the chillers prove to have sufficient responsiveness after performing system identification, a parallel operation scheme should be considered as a viable option to sequential operation, where there possibly would be no need for ESS compensation. Currently, the legislation around demand response resources on FCR-N and the charging strategy used by the ESS is unclear. Since the use of demand response and energy storage on Swedish markets is still new, it is expected that a lot of the legislation will change. The requirements for DRRs will probably be required to be specified further and the charging strategy will probably not be allowed in the long term due to a risk of causing increased imbalances. Due to this, a sounder approach of dispatching DR, and in this case chillers, is appropriate to ensure that the solution is operable even long term.

8.2 Thesis outlook

This thesis has expanded on the concept of VPPs dispatching commercial building DR for FC purposes. As presented earlier in *3.5 Context of case study* the VPP implemented in this thesis is simple in its current implementation, but still manages to address one central problem in the Swedish power system: the increasing imbalance caused by decreased system inertia and an increased share of renewable generation which is growing and expected to continue to grow. However, one single commercial building with a peak capacity on FCR-N of 900 kW will not be sufficient in order to balance the grid. But by increasing the capacity by aggregating more commercial building's DRRs, the capacity could increase to correspond to a considerable amount of the overall Swedish balancing power. In the same manner, a single building will not be able to solve the problems of capacity limitations in the power grid, caused by the ongoing urbanization and electrification. However, if several other buildings also were aggregated into the VPP portfolio, the overall impact could be large enough to make a considerable difference. The possibilities of aggregation makes the VPP an interesting scalable solution capable of offering impactful capacities to both ancillary and flexibility markets. In this sense, the implementation in this thesis, where only one commercial building is aggregated, does not do the VPP technology justice in regard to what potential impact it could have, when more capacity is aggregated.

Moreover, the VPP only dispatches an ESS and DRRs, which possibly is as simple as the VPP can be in regard to heterogeneity. What has become apparent during the end of this thesis and thus has not been included, is that Väla also has a backup generator, increasing the possibility for a heterogenous dispatch of resources, especially when including on-site PV-generation. When controlling all resources in conjunction, the VPP could possibly be capable of performing a multiple of services beyond only primary FC. These services could include trading on energy markets with PV-generation, voltage regulation with the ESS and the fans in AHUs, participation in secondary and tertiary reserves, black-start capability with the ESS and the genset, and possibly more. What is important to note about this is that all services are offered by existing resources with the only exception of the ESS. However, in the future when electrification of vehicles has come further, the ESS could potentially be replaced by V2G solutions which would make the entire VPP built upon existing assets, making efficient use of available resources.

With this picture in mind, a simple commercial building such as Väla Centrum can become a very interesting asset in the power system. It can both create new revenue streams for players such as system integrators, aggregators and the site owners which offer their resources, as well as it can help overcoming the barriers of the modern power system. Which in the long term will be supporting our transition into a sustainable future. Moreover, not only commercial buildings such as shopping centres are the only assets which can be included into the VPP portfolio. Considering the vast variation of commercial buildings or assets such as hospitals, data centres, offices, warehouses, garages and more, it is obvious that there are even larger possibilities than what has become apparent in this thesis. And it is important to keep this in mind. It is not always necessary to invest in new resources as we always have done. In some cases, it might be better to look at what we already have and to ask what more we could do with it. And this is what the VPP is all about. Not necessarily about inventing new ways to solve existing problems, but rather to find new ways to create more with less. Only by approaching the problems of the power system with this resource efficient mindset, by using intelligent control and by aggregating existing resources, these hurdles can be overcome in a truly sustainable way.

Bibliography

- [1] Prime Minister's Office; Ministry of the Environment, *Framework agreement between the Swedish Social Democratic Party, the Moderate Party, the Swedish Green Party, the Centre Party and the Christian Democrats*, 2016.
- [2] European Parliament, "Energy policy: general principles," 2019. [Online]. Available: <http://www.europarl.europa.eu/factsheets/en/sheet/68/energy-policy-general-principles>. [Accessed 10 09 2019].
- [3] Energimyndigheten, "Energiläget 2018," 2018.
- [4] IEA, "World Energy Outlook 2017," International Energy Agency, 2017.
- [5] Svenska Kraftnät, "Svenska Kraftnäts Systemutvecklingsplan 2018-2027," 2017.
- [6] Swedish Smart Grid, "swedishsmartgrid.se," 2019. [Online]. Available: <http://www.swedishsmartgrid.se/varfor-smarta-elnet/>. [Accessed 10 09 2019].
- [7] Swedish Smart Grid, "swedishsmartgrid.se," 2019. [Online]. Available: <http://www.swedishsmartgrid.se/varfor-smarta-elnet/smarta-elnet--entillvaxtbransch/teknikomraden-inom-smarta-elnet/>. [Accessed 10 09 2019].
- [8] Swedish Smart Grid, "swedishsmartgrid.se," 2019. [Online]. Available: <http://swedishsmartgrid.se/smarta-nat-i-sverige/fler-projekt-i-branschen/>. [Accessed 10 09 2019].
- [9] Next-Kraftwerke, "next-kraftwerke.com," 2019. [Online]. Available: <https://www.next-kraftwerke.com/knowledge/derms>. [Använd 10 09 2019].
- [10] D. Manerba, S. Rinaldi och M. Pasetti, *A Virtual Power Plant Architecture for the Demand-Side Management of Smart Prosumers*, 2018.
- [11] Svenska Kraftnät, *Svenska Kraftnäts Systemutvecklingsplan 2018-2027*, 2017, pp. 37 - 49.
- [12] Svenska Kraftnät, *Svenska Kraftnäts Systemutvecklingsplan 2018-2027*, 2017, pp. 21 - 26.
- [13] Svenska Kraftnät, *Svenska Kraftnäts Systemutvecklingsplan 2018-2027*, 2017, pp. 11 - 15.
- [14] Svenska Kraftnät, "svk.se," 2019. [Online]. Available: <https://www.svk.se/om-oss/verksamhet/?id=865>. [Använd 10 09 2019].
- [15] EU ETS, "emissions-euets.com," 2019. [Online]. Available: <https://www.emissions-euets.com/internal-electricity-market-glossary/622-transmission-system-operators-tsos>. [Använd 10 09 2019].
- [16] Svenska Kraftnät, "svk.se," 2019. [Online]. Available: <https://www.svk.se/drift-av-stamnatet/drift-och-marknad/balans-i-natet/>. [Använd 10 09 2019].
- [17] EU ETS, "emissions-euets.com," 2019. [Online]. Available: <https://www.emissions-euets.com/-balance-responsible-parties-brp>. [Använd 10 09 2019].

- [18] Svenska Kraftnät, "svk.se," 2019. [Online]. Available: <https://www.svk.se/aktorsportalen/elmarknad/balansansvar/> . [Använd 11 09 2019].
- [19] Svenska Kraftnät, *Svenska Kraftnäts Systemutvecklingsplan 2018-2027*, 2017.
- [20] EU ETS, "emissions-euets.com," 2019. [Online]. Available: <https://www.emissions-euets.com/-balancing-service-provider-bsp>. [Använd 10 09 2019].
- [21] Svenska Kraftnät, *Svenska Kraftnäts Systemutvecklingsplan 2018 - 2027*, 2017, pp. 7 - 10.
- [22] EU ETS, "emissions-euets.com," 2019. [Online]. Available: <https://www.emissions-euets.com/internal-electricity-market-glossary/623-distribution-system-operators-dsos>. [Använd 10 09 2019].
- [23] Swedish Smart Grid, "swedishsmartgrid.se," 2019. [Online]. Available: <http://www.swedishsmartgrid.se/aktuellt/nyheter/sa-kan-aggregatorer-verka-pa-den-svenska-marknaden/>. [Använd 10 09 2019].
- [24] EU ETS, "emissions-euets.com," 2019. [Online]. Available: <https://www.emissions-euets.com/internal-electricity-market-glossary/855-demand-side-response-aggregator-dsr-aggregator>. [Använd 10 09 2019].
- [25] Swedish Smart Grid, "swedishsmartgrid.se," 2019. [Online]. Available: http://www.swedishsmartgrid.se/globalassets/publikationer/aggregatorer_pa_den_svenska_elmarknaden.pdf . [Använd 10 09 2019].
- [26] Svenska Kraftnät, "svk.se," 2019. [Online]. Available: <https://www.svk.se/siteassets/aktorsportalen/elmarknad/information-om-reserver/reservmarknader.pdf>. [Använd 10 09 2019].
- [27] M. Amelin, "kth.se," 2019. [Online]. Available: <https://www.kth.se/social/upload/52e0c925f2765446480bda2b/L5-L6.pdf>. [Använd 10 09 2019].
- [28] L. Saarinen, "The Frequency of the Frequency," Uppsala, 2016.
- [29] W. Yang, P. Norrlund, L. Saarinen, J. Yang, W. Zeng och U. Lundin, "Wear Reduction for Hydropower Turbines Considering Frequency Quality of Power Systems: A Study on Controller Filters," 2016.
- [30] Svenska Kraftnät, "svk.se," 2018. [Online]. Available: <https://www.svk.se/contentassets/d40f9124238743228577c310291cbf53/regler-for-upphandling-och-rapportering-av-frc-n-och-fcr-d.pdf>. [Använd 10 09 2019].
- [31] Svenska Kraftnät, "svk.se," 2018. [Online]. Available: <https://www.svk.se/siteassets/aktorsportalen/elmarknad/balansansvar/dokument/balansansvarsavtal/8-regeldokument-fcr---forbrukning-v1-andringar-inkluderade.pdf>. [Använd 10 09 2019].
- [32] B. Rideout, T. Sahin och D. Shereck, "Implementation of a virtual power plant: The integrated load management system," i *The 2014 2nd International Conference on Systems and Informatics (ICSAI 2014) Systems and Informatics (ICSAI), 2014 2nd International Conference* , 2014.
- [33] Svenska Kraftnät, *Testprogram för leverans av FCR-N*, 2018.

- [34] C. Andersson och M. Lindberg, *Autotuning of a PID-controller*, Lund, 2004.
- [35] G. Hauser och K. Grandall, "Smart Grid Is a Lot More than Just "Technology";", *Smart Grid: Integrating Renewable, Distributed & Efficient Energy*, 2012.
- [36] N. Good, K. Ellis och P. Mancarella, *Review and classification of barriers and enablers of demand response in the smart grid*, 2017.
- [37] Svenska Kraftnät, *Svenska Kraftnäts Systemutvecklingsplan 2018 - 2027*, 2017, pp. 50 - 62.
- [38] Energiföretagen, *Ny rapport: Trånga elnät allvarligt hinder för tillväxt*, 2018.
- [39] M. Tuballa och M. Abundo, *A review of the development of Smart Grid technologies*, 2016.
- [40] D. Ton och M. Smith, *The U.S. Department of Energy's Microgrid Initiative*, 2012.
- [41] H. Saboori, M. Mohammadi and R. Taghe, *Virtual Power Plant (VPP), Definition, Concept, Components and Types*, 2011.
- [42] L. Li, S. Ghavidel, J. Aghaei, T. Yu och J. Zhu, *A Review on the Virtual Power Plant: Components and Operation Systems*, 2018.
- [43] U.S Department of Energy, *Distribution Automation: Results from the Smart Grid Investment Grant Program*, 2016.
- [44] FENIX, "fenix-project.org," 2019. [Online]. Available: <http://www.fenix-project.org/>. [Använd 10 19 2019].
- [45] D. Pudjianto, C. Ramsay och G. Strbac, *Virtual power plant and system integration of distributed energy resources*, 2007.
- [46] C. Ziegler, A. Richter, I. Hauer och M. Wolter, *Technical Integration of Virtual Power Plants enhanced by Energy Storages into German System*, Magdeburg, 2018.
- [47] C. Dong, X. Ai, S. Guo, K. Wang, Y. Liu och L. Li, *A study on short-term trading and optimal operation strategy for virtual power plant*, 2015.
- [48] J. Yu, Y. Jiao, X. Wang, J. Cao och S. Fei, *Bi-level optimal dispatch in the Virtual Power Plant considering uncertain agents number*, 2015.
- [49] P. Moutis och N. Hatziargyiou, *Decision trees aided scheduling for firm power capacity provision by virtual power plants*, 2014.
- [50] M. Pasetti, S. Rinaldi och D. Manerbra, *A Virtual Power Plant Architecture for the Demand-Side Management of Smart Prosumers*, 2018.
- [51] Svenska Kraftnät, Fortum, *Slutrapport pilotprojekt Flexibla hushåll*, 2016.
- [52] H. Xin, D. Gan, N. Li, H. Li och C. Dai, *Virtual power plant-based distributed control strategy for multiple distributed generators*, 2013.
- [53] F. Heimgaertner, U. Ziegler, B. Thomas och M. Menth, *A Distributed Control Architecture for a Loosely Coupled Virtual Power Plant*, 2018.
- [54] M. Yazdanian och A. Mehrizi-Sani, *Distributed Control Techniques in Microgrids*, 2014.
- [55] H. Morais, M. Cardoso, L. Castanheira och Z. Vale, *A Decision-Support Simulation Tool for Virtual Power Producers*, 2005.

- [56] A. Rufer, *Energy Storage Systems and Components*, 2018.
- [57] R. Huggins, *Energy Storage*, 2010.
- [58] L. Munuera, "iea.org," 2019. [Online]. Available: <https://www.iea.org/tcep/energyintegration/energystorage/>. [Använd 10 09 2019].
- [59] T. Chen, T. Hsieh, N. Yang, J. Yang och C. Liao, *Evaluation of advantages of an energy storage system using recycled EV batteries*, 2013.
- [60] MIT Electric Vehicle Team, "web.mit.edu," [Online]. Available: https://web.mit.edu/evt/summary_battery_specifications.pdf. [Använd 10 09 2019].
- [61] R. Yallamilli, L. Vedula och M. Mishra, *Cost Savings Oriented Microgrid Control Strategy Considering Battery Degradation*, 2018.
- [62] CoordiNet, *Market and regulatory analysis: Analysis of current market and regulatory framework in the involved areas*, 2019.
- [63] L. Wagner, *Overview of Energy Storage Technologies*, 2014.
- [64] L. Agarwal, W. Peng och L. Goel, *Probabilistic Estimation of Aggregated Power Capacity of EVs for Vehicle-to-Grid Application*, 2014.
- [65] Q. Zhang och J. Li, *Demand Response in Electricity Markets*., 2007.
- [66] Council of European Regulators , *Flexibility Use at Distribution Level*, 2018.
- [67] Y. Wu och K. Tang, *Frequency Support by Demand Response – Review and Analysis*, 2018.
- [68] D. J. Olsen, *Grid Integration of Aggregated Demand Response, Part 1: Load Availability Profiles and Constraints for the Western Interconnection*, 2014.
- [69] O. Ma, N. Alkadi, P. Cappers, P. Denholm, J. Dudley, S. Goli, M. Hummon, S. Kiliccote, J. MacDonald, J. Matson, D. Olsen, C. Rose, D. M. Sohn, M. Starke, B. Kirby och M. O'Malley, *Demand Response for Ancillary Services*, 2013.
- [70] S. Basnet och W. Jewell, *Predictive Analytics to Estimate Level of Residential Participation in Residential Demand Response Program*, 2018.
- [71] M. Starke, D. Letto, N. Alkadi, R. George, B. Johnson, K. Dowling och S. Khan, *Demand-Side Response from Industrial Loads*, 2013.
- [72] R. Tang, S. Wang och C. Yan, *A direct load control strategy of centralized air-conditioning systems for building fast demand response to urgent requests of smart grids*, 2018.
- [73] H. Hao, Y. Lin, A. Kowli, P. Barooah och S. Meyn, *Ancillary Service to the Grid Through Control of Fans in Commercial Building HVAC Systems*, 2014.
- [74] J. Yang, Q. Zheng, J. Zhao, X. Guo och C. Gao, *Control strategy of virtual power plant participating in the system frequency regulation service*, 2017.
- [75] M. Brandemuehl, "ceae.colorado.edu," 2019. [Online]. Available: <http://ceae.colorado.edu/~brandem/aren3050/docs/HVACDesignOverview.pdf>. [Använd 10 09 2019].
- [76] F. Qureshi och C. Jones, *Hierarchical control of building HVAC system for ancillary services*, 2018.

- [77] I. Beil, I. Hiskens och S. Backhaus, *Frequency Regulation From Commercial Building HVAC Demand Response*, 2016.
- [78] H. Hao, Y. Lin, A. Kowli, P. Barooah och S. Meyn, *Ancillary Service to the Grid Through Control of Fans in Commercial Building HVAC Systems*, 2014.
- [79] P.-A. Su, *Demonstration of HVAC chiller control for power grid frequency regulation*, 2015.
- [80] Väla Centrum, "vala.se," [Online]. Available: <https://www.vala.se/Om-vala/CSR>. [Använd 10 09 2019].

Appendices

Appendix A – Air handling unit specifications

AHU	Total rated power	Supply fan rated power	Exhaust fan rated power	Weekday active hours	Weekend active hours
FTX 10	33.5 kW	18.5 kW	15 kW	09:00 - 20:00	09:00 - 18:00
FTX 12	26 kW	15 kW	11 kW	09:15 - 20:00	09:15 - 18:00
FTX 14	5.64 kW	2.82 kW	2.82 kW	07:00 - 17:00	Off
FTX 15	< 1 kW	< 1 kW	< 1 kW	00:00 - 23:59	00:00 - 23:59
FTX 25	3.7 kW	1.85 kW	1.85 kW	05:30 - 20:00	05:30 - 18:00
FTX 32	32 kW	18 kW	15 kW	08:30 - 20:00	08:30 - 18:00
FTX 33	32 kW	18 kW	15 kW	09:00 - 20:00	09:00 - 18:00
FTX 34	32 kW	18 kW	15 kW	09:00 - 20:00	09:00 - 18:00
FTX 35	32 kW	18 kW	15 kW	09:00 - 20:00	09:00 - 18:00
FTX 36	32 kW	18 kW	15 kW	08:30 - 20:00	08:30 - 18:00
FTX 37	32 kW	18 kW	15 kW	08:30 - 20:00	08:30 - 18:00
FTX 38	32 kW	18 kW	15 kW	08:30 - 20:00	08:30 - 18:00
FTX 39	52 kW	30 kW	22 kW	09:15 - 20:00	09:15 - 18:00
FTX 40	52 kW	30 kW	22 kW	09:15 - 20:00	09:15 - 18:00
FTX 41	52 kW	30 kW	22 kW	08:30 - 20:00	08:30 - 18:00
FTX 42	52 kW	30 kW	22 kW	08:30 - 20:00	08:30 - 18:00
FTX 43	2.2 kW	1.1 kW	1.1 kW	10:00 - 20:00	10:00 - 18:00
FTX 44	1.5 kW	0.75 kW	0.75 kW	09:30 - 20:00	09:30 - 18:00
TA 01	10.5 kW	7.5 kW	3 kW	09:00 - 20:00	09:00 - 18:00
TA 02	18.5 kW	11 kW	7.5 kW	09:15 - 20:00	09:15 - 18:00
TA 03	18.5 kW	11 kW	7.5 kW	09:15 - 20:00	09:15 - 18:00
TA 04	15.6 kW	11 kW	4.6 kW	08:15 - 20:00	10:00 - 18:00
TA 05	18.5 kW	11 kW	7.5 kW	09:15 - 20:00	09:15 - 18:00
TA 06	18.5 kW	11 kW	7.5 kW	09:15 - 20:00	09:15 - 18:00
TA 08	18.5 kW	11 kW	7.5 kW	09:30 - 20:00	09:30 - 18:00
TA 09	18.5 kW	11 kW	7.5 kW	00:00 - 23:59	00:00 - 23:59
TA 11	29.5 kW	18.5 kW	11 kW	09:15 - 20:00	09:15 - 18:00
TA 17	29.5 kW	18.5 kW	11 kW	07:00 - 20:00	07:00 - 18:00
TA 18	30 kW	NaN	NaN	07:00 - 20:00	07:00 - 18:00
TA 19	30 kW	NaN	NaN	07:00 - 20:00	07:00 - 18:00
TA 20	30 kW	NaN	NaN	07:00 - 20:00	07:00 - 18:00
TA 22	30 kW	NaN	NaN	07:00 - 20:00	07:00 - 18:00
TA 23	30 kW	NaN	NaN	07:00 - 20:00	07:00 - 18:00
TA 26	10.5 kW	7.5 kW	3 kW	09:00 - 20:00	09:45 - 20:00
TA 28	67 kW	37 kW	30 kW	09:00 - 20:00	09:00 - 18:00

Table 22: Specification of power and active hours of air handling units at Väla.

Note from the author:

Unfortunately, the amount of MATLAB code and Simulink modeling made in this master thesis is too much to be presented in a comprehensive and transparent way. The number of pages that would have been required to present all the code and model would be inappropriate to include considering the already long report and is thus not included in the appendices. However, it is still important to remain transparent with what has been done in this thesis. Due to this, feel free to contact the author at *elt14vpe@student.lu.se* in case any references from the code or the model is wanted.

